UNIVERSITY OF CALIFORNIA,
IRVINE

Semiclassical Theory of Fermions

DISSERTATION

submitted in partial satisfaction of the requirements
for the degree of

DOCTOR OF PHILOSOPHY

in Chemistry

by

Raphael Florentino Ribeiro

Dissertation Committee:
Kieron Burke, Chair
Filipp Furche
Vladimir A. Mandelshtam

2016

TABLE OF CONTENTS

LIST OF FIGURES

LIST OF TABLES

ACKNOWLEDGMENTS

It was an honor for me to be supervised by Professor Kieron Burke. His support and belief were instrumental to the completion of this thesis. I am fortunate to have been mentored by someone who respects individualities and genuinely cares about the scientific and personal development of his students. His enthusiasm and unending stream of suggestions have propelled the research here presented and for that I am grateful.

I would like also to express gratitude towards direct collaborators Attila Cangi, Donghyung Lee, Peter Elliott and Zhenfei Liu. Previous work of the first three on semiclassical approximations for many-particle systems provided guidance for the developments presented in Chapters 2-4. Zhenfei's detailed feedbacks were conducive to the main results of Chapter 5.

I was happy to have been part of the highly active theoretical chemistry group at UCI. It was a privilege to be exposed to a plethora of different branches and points of view on theoretical chemistry.

The UCI Chemistry Department staff has made life simpler. In particular, Jenny Du, Jaime Albano, Tenley Dunn and Kerry Kick have provided immense help. I am similarly thankful to the UCI International Center where I always found quick solutions to any urgent issues.

Burke group members, Guo Chen and Prasoon Saurabh have provided useful feedback and comic relief over these four years. From them I learned much.

I here acknowledge my parents, Rosa Florentino Ribeiro and Jose Orlando Ribeiro for having transmitted me the passion for knowledge, truth and discovery. For all of my life they have been examples of resilience, openness and integrity. That I am here today is a consequence of their deepest values.

I would also like to thank my brother, Gustavo, sister, Andressa and parents-in-law Mario and Maria Silene. I am glad to have your presence in my life. It is also good to be reminded sometimes that there exists an external world.

Vinicius, Fernanda, Arthur and Paula have provided those moments of distraction which I desperately needed even when I did not think so. I will miss the parties.

Finally, it is impossible for me to think about life in general without my spouse Ana Paula. She has been a constant source of happiness and balance. Her gentleness, patience and strong will have inspired me every step of the way.

The research described in chapters 2-4 was supported by the National Science Foundation under grant numbers CHE-1112442 and CHE-1464795, while the work shown in chapter 5 was funded by the Department of Energy (DE-FG02-08ER46496). I am thankful to the UCI Regents' Dissertation Fellowship and the Miguel Velez Scholarship for partial funding.

I acknowledge the American Physical Society and the American Institute of Physics for copyright permissions.

- Sections 2.3, 3.2-3.5 contain edited portions of material published in Ribeiro, R. F., Burke, K. "Uniform semiclassical approximations for one-dimensional fermionic systems" *arXiv:1510.05676, submitted to J. Math. Phys.* and Ribeiro, R. F., Lee, D., Cangi, A., Elliott, P., Burke, K. "Corrections to Thomas-Fermi densities at turning points and beyond" *Phys. Rev. Lett.*, 2015, **114**, 050401.

- Chapter 4 contains data and text from Ribeiro, R. F., Burke K. "Leading corrections to local approximations II (with turning points)" *in prep.*.

- Sections 5.2, 5.3, 5.5 and 5.7 include results which will be found in Ribeiro, R. F., Liu, Z., Bergfield, J. P., Stafford, C. A., Burke, K. "Hard-wall quantum transport calculations: Thinking inside the box" *in prep.*

The research reported in this thesis was exclusively performed by the author under the supervision of Professor Kieron Burke.

CURRICULUM VITAE

Raphael Florentino Ribeiro

EDUCATION

Doctor of Philosophy in Chemistry **2016**
University of California, Irvine *Irvine, California*

Master of Science in Chemistry **2012**
University of Minnesota, Twin Cities *Minneapolis, Minnesota*

Bachelor of Science in Chemistry **2010**
Universidade Federal de Sao Carlos *Sao Carlos, Brazil*

PUBLICATIONS

- Ribeiro, R. F., Burke K. "Leading corrections to local approximations II (with turning points)" *in prep.*
- Ribeiro, R. F., Liu, Z., Bergfield, J. P., Stafford, C. A., Burke, K. "Hard-wall quantum transport calculations: Thinking inside the box" *in prep.*
- Ribeiro, R. F., Burke, K. "Uniform semiclassical approximations for one-dimensional fermionic systems" *submitted to J. Math. Phys., arXiv:1510.05676*
- Ribeiro, R. F., Lee, D., Cangi, A., Elliott, P., Burke, K. "Corrections to Thomas-Fermi densities at turning points and beyond" *Phys. Rev. Lett.*, 2015, **114**, 050401
- Ribeiro, R. F., Marenich, A. V., Cramer, C. J., Truhlar, D. G. "Use of Solution-Phase Vibrational Frequencies in Continuum Models for the Free Energy of Solvation " *Journal of Physical Chemistry B*, 2011, **115**, 14556-14562
- Ribeiro, R. F., Marenich, A. V., Cramer, C. J., Truhlar, D. G. "The Solvation, Partitioning, Hydrogen Bonding, and Dimerization of Nucleotide Bases: A Multifaceted Challenge for Quantum Chemistry" *Physical Chemistry Chemical Physics*, 2011, **13**, 10908-109222
- Ribeiro, R. F., Marenich, A. V., Cramer, C. J., Truhlar, D. G. "Prediction of SAMPL2 Aqueous Solvation Free Energies and Tautomeric Ratios Using the SM8, SM8AD, and SMD Solvation Models" *Journal of Computer-Aided Molecular Design*, 2010, **24**, 317-333
- Ribeiro, R. F., Marenich, A. V., Cramer, C. J., Truhlar, D. G. "Solvent Dependence of ^{14}N Nuclear Magnetic Resonance Chemical Shielding Constants as a Test of the Accuracy of the Computed Polarization of Solute Electron Densities by the Solvent" *Journal of Chemical Theory and Computation*, 2009, **5**, 2284-2300

INVITED PRESENTATIONS

Uniform asymptotic approximations for fermionic systems **02/2016**
34th Annual Western States Mathematical Physics Meeting, California Institute of Technology, Pasadena, CA

Semiclassical Approximations to Electronic Structure Theory via Density/Potential Functionals **06/2013**
SIAM Conference on Mathematical Aspects of Materials Science (June 2013) Philadelphia, PA

CONTRIBUTED PRESENTATIONS

Uniform Semiclassical Approximations for Many-Particle Systems **03/2014**
American Physics Society March Meeting, Denver, CO

Airy Uniform Approximations to Many-Particle Systems **09/2013**
Workshop on the Semiclassical Origins of Density Functionals at the Institute of Pure and Applied Mathematics, Los Angeles, CA

HONORS, AWARDS AND FELLOWSHIPS

- Regents' Dissertation Fellowship, University of California Irvine, 2015
- Miguel Velez Scholarship Award, University of California Irvine, 2013, 2014, 2015
- Travel Grant Award for the Villa de Leyva Summer School on Geometric, Algebraic and Topological Methods for Quantum Field Theory, 2015
- MCC/NSF Travel Grant Award for the tutorial and workshop: "5th Time-Dependent Density-Functional Theory: Prospects and Applications", 2012
- Phi Kappa Phi, 2011
- GPA Bonus Award, University of Minnesota, 2011
- Graduate School Fellowship, Department of Chemistry, University of Minnesota, 2010

TEACHING/MENTORING EXPERIENCE

Mentored Summer projects of

- Timothy Middlemas (physics undergraduate student at Harvey Mudd College), Summer 2015
- Katrina Ellis (chemistry undergraduate student at Skidmore University), Summer 2014

Teaching Assistant for

- CHEM 252 Density Functional Theory, University of California Irvine, 2013-2014
- CHEM 4021/8021 Computational Chemistry, University of Minnesota Twin Cities, 2011
- CHEM 1021 Principles of Chemistry I, University of Minnesota Twin Cities, 2010-2012

ABSTRACT OF THE DISSERTATION

Semiclassical Theory of Fermions

By

Raphael Florentino Ribeiro

Doctor of Philosophy in Chemistry

University of California, Irvine, 2016

Kieron Burke, Chair

A blend of non-perturbative semiclassical techniques is employed to systematically construct approximations to noninteracting many-fermion systems (coupled to some external potential mimicking the Kohn-Sham potential of density functional theory). In particular, uniform asymptotic approximations are obtained for the particle and kinetic energy density in terms of the external potential acting on the fermions and the Fermi energy. Dominant corrections to the classical limit of quantum mechanics are shown to be captured by the semiclassical approximation everywhere in configuration space. As opposed to previous treatments, no singular behavior arising from inappropriate choice of representation ever arises. Such convenient properties allow us to derive a number of universal limits for the particle density and kinetic and potential energies in the semiclassical limit. Additionally, we study the performance of the semiclassical approximations in a variety of one-dimensional potentials.

In the second part of this thesis, a Dyson-like equation is derived relating the Green's function of an isolated subsystem satisfying Dirichlet boundary conditions with that of an associated infinite coupled system. We explain the relation to the Landauer model and quantum transport. In particular an analytical form for the self-energy operator is obtained for a simple model. The developed framework is illustrated with a semiclassical calculation.

Chapter 1

Introduction and Outline

1.1 Fermionic Ground-State

It has been clear since the early part of the 1900's that a complete understanding of the low-energy microscopic phenomena of chemistry and physics can be obtained only by application of the laws of quantum mechanics. However, it was also obvious then the impossibility of obtaining exact descriptions of physical systems containing a macroscopic, e.g., $O(10^{23})$, number of atoms. In the words of Dirac: "It therefore becomes desirable that approximate practical methods of applying quantum mechanics should be developed, which can lead to an explanation of the main features of complex atomic systems without too much computation". Despite much progress, and almost a century after such words were articulated, they remain appropriate [30].

A large part of theoretical chemistry relies on approximate solutions to the quantum-mechanical partial differential equations to describe molecular structure and dynamics [24, 48, 64]. As is usual in the study of complex physical phenomena, suitable approximations may differ depending on the relevant energy scale and property which is to be probed. In the first

part of this thesis we will only be concerned with the lowest energy phenomena of finite systems. In other words, our main interest will be in the description of the ground-state of a finite sample of fermions coupled to an external potential. This is exactly analogous to the problem of obtaining the infimum of the spectrum of a molecular system in the Born-Oppenheimer approximation, where the nuclei are fixed and the electrons are coupled to the former's electrostatic fields [17]. Relativistic or spin-dependent effects play no role in forthcoming considerations so they will be completely ignored.

A variety of methodologies exist for the investigation of the electronic states of matter. The most popular can be classified into two groups: that of wave function (WF) [48, 96], and density functional theory (DFT) methods [31, 35, 50]. These differ in the central variable whence any other observable can (in principle) be obtained from. The main advantage of a certain branch of wave function-based methods is that there exists a systematic method to improve the accuracy of a given prediction by increasing the size of the approximate Hilbert space. Its most unfavorable drawback concerns the computational cost usually required to obtain results of chemical accuracy (that is, with an approximate error of 1 kcal/mol). For instance, a well-reputed (though non-variational, and with poor accuracy for so-called multireference systems [24]) wave function method is coupled cluster with single and double excitations (CCSD). Its computational cost scales asymptotically as N^6, where N is the number of dimensions of the approximate Hilbert space. Such a cost is prohibitive for systems with more than 20 electrons, and therefore limits the application of CCSD to electronic states including only a small number of particles. Density-functional methods provide a much cheaper alternative. However, while DFT has been rigorously proved to exist, its practical implementation (in the form of Kohn-Sham DFT) requires approximation of the so-called exchange-correlation functional. Useful approximations exist, but there are neither rigorous, nor systematic ways to improve their quality and applicability. This implies that questions loom over the reasons behind the general accuracy of approximate exchange-correlation energy functionals as well as on how to systematically correct for their known flaws [21, 95].

The *modus operandi* of Kohn-Sham DFT (KS-DFT) is similar to that of mean-field theory. In particular, in its pure state formulation, it is conjectured that the particle density $\rho(x)$ of an interacting many-electron system is equal to that of a noninteracting fermionic system coupled to the conventionally denoted Kohn-Sham potential $v_s[\rho]$ [35]. The latter is supposed to include all of the effects of the electron-electron repulsion as well as the electronic coupling to the external potential (e.g., due to the fixed nuclei present in the system), i.e.,

$$v_s[\rho](x) = \int \mathrm{d}^3x' \frac{\rho(x')}{|x - x'|} + v_{\mathrm{xc}}[\rho](x) + v_{\mathrm{ext}}(x), \quad x \in \mathbb{R}^3, \tag{1.1}$$

where $v_{\mathrm{xc}}[\rho]$ is the exchange-correlation potential carrying all of the effects of dynamical and statical electronic correlation, and $v_{\mathrm{ext}}(x)$ is the external potential acting on the electron density. It follows that the orbitals $\{\phi_i(x)\}_{i\in\mathbb{N}}$, of the noninteracting (Kohn-Sham) system satisfy

$$\rho(x) = \sum_{i=1}^{N} |\phi_i(x)|^2, \tag{1.2}$$

$$\left[-\frac{\hbar^2}{2m}\Delta + v_s[\rho](x)\right] \phi_j(x) = \epsilon_j \phi_j(x), \tag{1.3}$$

where ϵ_j corresponds to Kohn-Sham orbital energies, and $\epsilon_j < \epsilon_i,\ \forall\ j < i$. The ground-state was assumed to be non-degenerate for the purposes of this basic discussion, and the spectrum of the Kohn-Sham system was similarly assumed discrete (the foundational theorems of DFT make no such requirement) [35, 50, 65, 66].

There exists no general mathematical proof of existence of a Kohn-Sham system for an arbitrary interacting electron density $n_0(x)$ [35]. However, the many successes of the KS-DFT approach (with approximate exchange-correlation potentials) suggest that at least for a sizable fraction of the electronic ground-states of interest to chemistry the Kohn-Sham

system exists. Thus, the main focus of the field of developmental ground-state DFT is directed at the construction of exchange-correlation functionals $E_{\mathrm{xc}}[\rho]$ [21, 86, 95]. These give rise to the previously mentioned exchange-correlation KS potentials via application of the functional derivative with respect to the particle density,

$$v_{\mathrm{xc}}[\rho] = \frac{\delta E_{\mathrm{xc}}[\rho]}{\delta \rho}. \tag{1.4}$$

Unfortunately, as already mentioned, there is no universal guiding principle for the construction of approximations to $E_{\mathrm{xc}}[\rho]$. The most successful (first-principles) exchange-correlation energy functionals were built by defining a class of functional forms with parameters that are constrained so they satisfy universal exact conditions from the theory of many-body systems [83, 88]. An important example of exact condition satisfied by adequate exchange-correlation functionals is that they reduce in the limit where the system is infinite and homogeneous to that of the homogeneous electron gas [21, 86, 95]. Notwithstanding the simplicity of the discussed strategy, it has an obvious non-uniqueness problem, as there is an infinite number of ways to satisfy a finite number of conditions. As a result, much remains to be learned about optimal strategies for the design of exchange-correlation functionals [95].

Despite its drawbacks, DFT is the most popular approach to the study of molecular electronic structure theory. This is a fruit of its lower computational complexity and general reasonable accuracy (assuming the choice of a well-established approximation to the exchange-correlation energy functional). For example, if an exchange-correlation functional of the form

$$E_{\mathrm{xc}}[\rho] = \int \mathrm{d}^3x \; G\left(\rho, |\nabla \rho|\right), \tag{1.5}$$

(where G is a map from some suitably defined space of particle densities to the real numbers [35]) is employed, the asymptotic cost of a self-consistent Kohn-Sham computation scales as N^3, which is already inferior to that of the mean-field Hartree-Fock method (the cost of the latter scales as N^4 [24]). These factors have allowed electronic structure effects to be included for example in a variety of liquid [72, 76] and solid-state [46] simulations of complex phenomena in chemical biology [3, 16] and material sciences [78, 99]. Nonetheless, there is no question that ground-state DFT would greatly benefit from systematic developments in the subfields of orbital-free i) exchange-correlation, and ii) kinetic energy density functionals [21, 87, 95]. The latter item's importance resides on the fact that the computational bottleneck of most *ab initio* molecular simulations consists of obtaining self-consistent solutions of the Kohn-Sham eqs. 1.3, the main purpose of which is to generate highly-accurate noninteracting kinetic energies. Thus, a simple, accurate, orbital-free kinetic energy density functional would be particularly useful to speed up large-scale *ab initio* simulations of chemical kinetics and thermodynamics in abstruse environments.

It is however, even harder to build useful, i.e., reasonably accurate, orbital-free density functional approximations to the noninteracting kinetic energy than it is for the exchange-correlation energy [31, 105]. Therefore, in spite of their much lower cost (the cost incurred by employing orbital-free density functionals tends to scale linearly with the number of particles of a system [105]), because they provide dismal general accuracy, orbital-free approximations to the kinetic energy density functional are not widely used.

Motivated by the central problems of ground-state Kohn-Sham DFT, in this thesis, we will only be concerned with orbital-free descriptions of noninteracting fermions coupled to generic external potentials. This already presents formidable challenges.

1.2 Semiclassical Mechanics

In the first part of this thesis, semiclassical analysis of quantum mechanics will be the main formalism employed in the construction of accurate, yet simple, descriptions of many-fermion systems. Here we introduce some of its basic ideas.

Semiclassical mechanics has been historically associated to asymptotic expansions of quantum mechanical properties in the limit where $\hbar \to 0^+$ [11, 18, 23]. This is considered a formal limit for two reasons: a) $\hbar$ is a natural constant, so what should be understood as going to zero is a dimensionless quantity involving $\hbar$, and b) the semiclassical limit is generally singular, so it leads to divergent mathematical quantities, the interpretation of which is subtle [11, 61, 110]. To illustrate point a), let $V(x)$ denote a nonconstant, positive smooth function on $\mathbb{R}^3$, and define $p(x, E) = \sqrt{2[E - V(x)]}, E \geq V(x), \ \forall \ x \in \mathbb{R}^3$. Then, the spatial rate of change of the *local* de Broglie wavelength $\lambda(x, E) = \hbar/p(x, E)$ of a quantum particle with energy E provides a particularly useful dimensionless parameter which can be used to measure the relative importance of quantum effects and the breakdown of primitive semiclassical approximations [11, 23]:

$$\delta(x, E) = \left| \frac{\mathrm{d}\lambda(x, E)}{\mathrm{d}x} \right| = \frac{\hbar |\nabla V(x)|}{p^3(x, E)}. \tag{1.6}$$

In particular, for a given $V(x)$, semiclassical analysis shows that certain quantum effects may be neglected when $\delta(x, E) \to 0$ (which is equivalent to $\hbar \to 0^+$ except for x in a set of measure zero which we describe below) [11, 23, 98]. For instance, if $p(x)$ is arbitrarily large, then local quantum oscillations will be of such short wave-length that the uncertainty principle would only allow their resolution by experiments involving arbitrarily high energies. A measurement of any local property would then yield an average expected to conform to that of a classical description. Note that the interchangeability of the $\hbar \to 0^+$ and $\delta(x, E) \to 0^+$ limits breaks down entirely in a small neighborhood containing zeros of $p(x, E)$ (generally

called turning points). This simple consideration begins to reveal certain intricacies of the semiclassical limit, which we discuss in some detail in Chapters 2-4.

In the semiclassical limit, the properties of a system, such as expectation values of observables or probability amplitudes, may be written as a series in powers of $\hbar$ where the zeroth order term is given by the classical limit of the quantum system of interest (here and everywhere else in this thesis assumed to be a pure state). For instance, if $\hat{O}$ is a linear self-adjoint operator on a Hilbert space $\mathcal{H}$, it corresponds to an observable quantity, the expectation value of which on a system with density operator $\hat{\rho}$ is given by

$$O = \mathrm{Tr}\left(\hat{\rho}\hat{O}\right). \tag{1.7}$$

In the semiclassical limit O generally admits the following formal asymptotic expansion,

$$O \sim O_{\mathrm{cl}} + \sum_{n=1}^{\infty} O_n \hbar^{n+\alpha} + O\left(e^{-A/\hbar}\right),\ \alpha \in \mathbb{Q},\ A \in \mathbb{R}^{+}, \tag{1.8}$$

where O_{cl} denotes the classical limit of the observable in question and the remaining terms are corrections due to quantum effects.

While the singular nature of the semiclassical limit imply expansions such as that given by Eq. 1.8 rarely converge, a variety of experiences with both elementary and complex systems indicates that if only the first few terms of an expansion are retained, it generally provides highly-accurate estimates of many quantum mechanical properties, even in regimes which may be considered to be far from classical [9, 11, 18, 23, 34, 49]. A dramatic example is the

simple harmonic oscillator, for which the Schrodinger equation propagator

$$K(q, q', t) = (q, e^{-i\hat{H}t/\hbar}q'),\ t \in \mathbb{R}^+,\ q, q' \in \mathbb{R}, \tag{1.9}$$

is given exactly by semiclassical techniques [38]. This leads to well-known result that primitive (WKB) semiclassical quantization also provides exact energy eigenvalues for this system. While this is an exceptional case, it serves to demonstrate that semiclassical theories can be much more accurate than expected on first thought.

As we shall demonstrate later explicitly for the case of fermions on a line, the appropriate semiclassical approximations to the particle and kinetic energy densities of a fermionic system do not admit global continuous power series expansion of the form shown in Eq. 1.8. This happens generally for quantities which vary in space according to classical phase-space structures which have singularities in isolated points.

Before concluding this section we make a connection to the study of many-electron systems. Notably, the first density functional method, discovered by Thomas and Fermi in the early days of quantum mechanics [37, 101], can be interpreted as the classical limit of a noninteracting fermionic system [18].

1.3 Molecular Transport

In the last part of this thesis we provide a reformulation of a problem related to the field of molecular electronics [97]. The paradigmatic experiment of this interdisciplinary branch of chemistry and physics can be roughly summarized as follows: a molecule with low-lying electronic states, such as 1,4-benzene-dithiol, is coupled (e.g., by adsorption) to metallic

electrodes (also called *leads*) with different electrochemical potentials (e.g., gold wires connected to a battery) and electric current is measured between the latter as a function of initial electrochemical potential difference (also referred to as *bias*). This was the setup of a famous experiment by Reed and Tour [89], though there exists plenty of variations, see e.g., [47]. At low temperatures, distinct phenomena is generally observed, e.g., the absence of any appreciable current below a certain voltage threshold and the occurrence of steps in the *current-voltage* $I(V)$ profile indicating the opening of new channels for molecular electronic conduction [54, 89]. Aside from the various technological advances which might be realized in the future based on this simple idea [75, 97], this class of experiments provide a beautiful view of the molecular electronic spectrum [80, 89].

A theoretical description of the phenomena of molecular transport is complicated by the fact that electric current conduction is intrinsically a complex non-equilibrium process [27]. A complete microscopic description of all components and couplings involved in the single-molecule transport experiment contains much more information than what is generally experimentally probed (e.g., the dynamics of the battery which provides the initial bias). Thus, it is common to assume the effects of external degrees of freedom (e.g., those of the battery which is connected to electrodes) can be accounted for by imposing suitable boundary conditions [26, 27]. The simplest approximations also neglect any process involving energy-momentum relaxation and dephasing. This is acceptable in a variety of cases where the mean free path and coherence length of the system is much larger than that of a typical path traveled by a conduction electron. An additional assumption of a certain class of models is that the molecular junction reaches a steady-state. This allows the application of methods of time-independent scattering theory to the study of quantum transport [26, 27]. It also defines the Landauer model [60], the framework investigated by this thesis.

In the Landauer theory a transmission map $T : \mathbb{R}^+ \to [0, 1]$ contains all of the information required to determine the average electric current I in a molecular circuit under an applied

bias V [26, 27, 60]. In fact, the $I(V)$ curve in the Landauer model is obtained from a simple equation

$$I(V) = \frac{2e^2}{h} \int_{-\infty}^{\infty} \mathrm{d}E \, [f_L(E) - f_R(E)] \, T(E), \tag{1.10}$$

where e denotes the elementary unit of electric charge, h is Planck's constant and $f_{L/R}(E)$ gives the probability that a conducting electron prepared at the left or right leads has energy in the interval $[E, E + dE] \subset \mathbb{R}$. Generally, the free electron gas is assumed to provide a reasonable description of the electrodes (since these are generally metals), so $f_{L/R}(E)$ is the Fermi-Dirac distribution for noninteracting electrons at the temperature of the experiment [26, 27]. The map $T(E)$ determines with what probability electrons will be transmitted to the opposite electrode [26, 27]. It follows that the conducting electrons are described in each lead by a scattering wave function obtained as a linear combination of an incoming plane-wave and an outgoing scattered wave.

A steady-state description includes only the average effects of molecular time-dependent relaxation in the presence of electric current. Thus, the Landauer model can only be employed in cases where electronic correlation is neglected or modeled by a single-particle effective potential. Additionally, the distortion of the molecular environment by the presence of the leads and the passage of a steady current is modeled (in the stationary regime) by a self-energy operator $\hat{\Sigma}$. This satisfies the following operator equation

$$\hat{G}(z) \left[\hat{H}_0 + \hat{\Sigma}(z) - z\hat{1} \right] = \hat{1}, \tag{1.11}$$

where $z \in \mathbb{C} - \{\text{spectrum } [\hat{H}_0 + \hat{\Sigma}(z)]\}$, $\hat{H}_0$ is the Hamiltonian operator for the isolated molecule, and $\hat{G}(z)$ is the Green's function for the time-independent Schrodinger equation

with Hamiltonian $\hat{H} = \hat{H}_0 + \hat{H}_L + \hat{H}_R + \hat{V}$, where $\hat{V}$ includes all of the couplings between degrees of freedom of the molecule and the metallic leads and $\hat{H}_{L/R}$ corresponds to the isolated Hamiltonian for the left and right electrodes. A final assumption is that there is no coupling between the left and right leads, so $(x|\hat{V}|x') = 0$ if x and x' correspond to positions in different electrodes [26, 27].

The physical interpretation of $\hat{\Sigma}(E)$ can be obtained by considering its spectrum: the real part of its eigenvalues provides the shift to molecular electronic energies provoked by the coupling with the electrodes, while their imaginary part determines dissipative effects. They induce a finite lifetime on the coupled states of the molecule and the electrodes [26, 27].

Even within the above model there exists a variety of different treatments which have been pursued in the literature [27]. For instance, the self-energy matrix may be obtained from tight-binding models, which may employ parameters obtained from molecular electronic structure computations performed with open boundary conditions (sometimes the contact regions between the electrodes and the molecule is also included in the description of the latter so that electrode-molecule interface effects are described with improved accuracy). Most of these prescriptions are guided by heuristic principles. The study of the Landauer model in this thesis seeks to systematically construct the self-energy operator from first-principles for a simple model, and perhaps shed light on some of the approaches which are pursued in the literature.

1.4 Outline of Thesis

A variety of analytical techniques involving semiclassical analysis and singular perturbation theory will be employed in this thesis. Therefore, Chapter 2 is dedicated to their discussion. In particular, we provide the basics of the mathematical formalism which is later extensively

employed as well as the physical interpretation of the most important results. Chapter 2 ends with an application of the methods described in the previous sections to the simple case of weakly-perturbed noninteracting fermions satisfying Dirichlet boundary conditions in one-dimension. While this example has been recently studied in the literature with a different methodology [33], the derivation presented here is new, and serves to illustrate the priorly exposed ideas.

Chapter 3 presents a systematic construction of semiclassical approximations to the particle and kinetic energy densities of fermions on a line. This contains novel phenomena such as tunneling which are unseen in the Dirichlet case. In this problem, all of the ideas introduced in Chapter 2 are taken to their limit.

The novel results of the chapter 3 are extensively investigated in chapter 4. Analytical corrections to Thomas-Fermi observables are derived in different configuration space regions, and the numerical behavior of the particle and kinetic energy densities of one-dimensional fermionic systems coupled to different classes of external potentials is explored.

In Chapter 5 we provide a new formulation for a simple model of molecular conductance. A systematic construction of the self-energy operator in real-space is presented as well as the ensuing generalized Dyson equation which follows from it.

In the Epilogue we provide a global discussion of the main results of this thesis including comments on promising future research directions.

Chapter 2

Mathematical Preliminaries

In this chapter we explain the essentials of semiclassical theories of many-fermion systems and the concepts of Poisson duality and uniform asymptotic approximations. We end with the construction of a semiclassical approximation to the density matrix of Dirichlet fermions. This gives a demonstration of the ideas described in the first sections and provides a warm-up exercise to the problem discussed in the next chapter. Our presentation alternates between formal and heuristic. In particular, we aim to expose some of the mathematical subtleties of this work without losing sight of their physical significance.

2.1 Semiclassical Analysis for Many-Fermion Systems

The predictions of classical mechanics are supposed to emerge from the quantum theory in some limit. This is what is expected based on the fact that the former explains the behavior of most macroscopic systems. Semiclassical analysis is concerned with the mathematical investigation of this idea [18, 23, 110]. The non-triviality of the classical-quantum interface is revealed by the simple observation that the states and observables according to each

theory belong to different mathematical arenas: quantum-mechanical (pure) states are rays in the projective Hilbert space, while observables are self-adjoint linear operators; classical-mechanical states are phase space densities and its observables are phase space functions. The quantum and classical theories are qualitatively different (an obvious fact in light of their completely different interpretation). This is not an unprecedented situation in the theoretical description of physical phenomena (as for instance the case of geometric optics arising as a short-wave length limit of wave optics reveals [52]). Nonetheless, there is a myriad of interesting questions which could be asked about the correspondence (or lack thereof) between the mathematical structures governing the quantum and classical theories. In this thesis we focus only on those related to the development of non-perturbative approximations to the quantum-mechanical theory of many-particle systems which are simple, accurate and contain the classical limit as a reference upon which quantum effects are included. As will be seen in chapters 3 and 4 this strategy gives rise to highly accurate description of many-fermion systems in terms of properties of classical phase space orbits.

2.1.1 A First Look at Thomas-Fermi Theory

The classical limit of atomic systems containing many-fermions is as old as quantum mechanics. It was obtained originally by Thomas [101] and Fermi [37]. A quick derivation of its main result for the case of one-dimensional noninteracting fermions coupled to an external potential $v(x)$ can be obtained by employing some simple assumptions: i) quantum states accessible to fermions become in the classical limit equivalent to phase space cells of area $2\pi\hbar$ (this is justified by the old Bohr-Sommerfeld quantization theory), ii) at 0K *all* phase space states with energy lower than the so-called Fermi energy E_F (defined by the number of fermions described by the model, see below) are occupied by a single fermion (due to the Pauli exclusion principle). This implies that within this theory the fermionic particle density

can be written as

$$\rho_{\rm cl}(x, E_F) = \frac{1}{2\pi\hbar}\int_{\mathbb{R}} {\rm d}p\ \theta[E_F - H(x,p)], \tag{2.1}$$

with the normalization,

$$\frac{1}{2\pi\hbar}\int_{\mathbb{R}^2} {\rm d}x{\rm d}p\ \theta[E_F - H(x,p)] = N, \tag{2.2}$$

where $H(x,p) = \frac{p^2}{2m} + v(x)$ is the classical Hamiltonian for a given fermion and $\theta(z)$ is the Heaviside step function [53]. It follows that the classical limit of the one-dimensional noninteracting fermionic particle density is given by

$$\rho_{\rm cl}(x, E_F) = \frac{\sqrt{2[E_F - v(x)]}}{\pi\hbar}\theta[E_F - v(x)]. \tag{2.3}$$

The classical limit of the expectation value of any observable O can also be quickly derived:

$$O_{\rm cl}(N) = \int_{\mathbb{R}^2} {\rm d}x{\rm d}p\ O(x,p)\theta[E_F(N) - H(x,p)]. \tag{2.4}$$

Figure 2.1 compares the classical limit of the quantum-mechanical particle density as predicted by Thomas-Fermi theory to the exact for the case where the confining potential is a harmonic oscillator.

Here one sees the distinctive feature of the classical limit: it can only describe the average/bulk behavior of quantum-mechanical systems. Oscillations arising from quantum interference (see below) and barrier penetration effects are completely absent from Thomas-Fermi theory. In the exceptional harmonic oscillator case, the quantum oscillations and

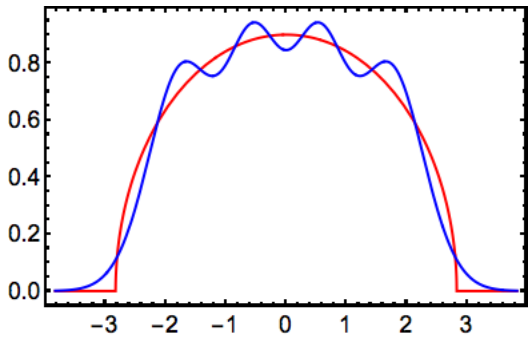

Figure 2.1: Quantum-Mechanical particle density for a system containing 4 noninteracting fermions. Exact results are given in blue, while the classical limit is given in red

tunneling which can be seen from Fig. 2.1 (any region where the Thomas-Fermi particle density vanishes, but not the exact can only be populated in the quantum-mechanical theory) conspire in such a way that the values taken by Thomas-Fermi observables, e.g., the average kinetic and potential energies of the system, match the exact. Obviously, such perfect cancellation does not happen generically, so that if quantum effects are relevant to the description of a particular system, it becomes important to unravel corrections to Thomas-Fermi theory. It is not obvious how these can be obtained from the above construction. In particular, the above derivation does not even provide much insight into how the classical limit emerges from the quantum formalism.

In the next subsection the semiclassical limit of quantum mechanics is discussed from a more general perspective. This will provide the necessary pre-requisites to the study of the semiclassical limit of many-fermion systems which we present in subsection 2.1.3.

2.1.2 Semiclassical Limit with the Feynman Path Integral

There exists a plethora of methods which may be employed to describe the emergence of classical behavior from the fundamental postulates of quantum mechanics. Here we employ the Feynman path integral, for it provides a systematic approach to the semiclassical limit which is transparent and insightful [39, 55]. The discussion is limited to the case of single-

particle quantum mechanics (for the case of many-particle systems see the next subsection).

In the Feynman approach to quantum mechanics, the probability amplitude for a given event to be measured is expressed as a sum over all possible histories of the system between its initial and final states. Each particular history has with it associated a phase, and the event probability is obtained by application of the Born rule. In particular, the quantum-mechanical propagator indicating the probability amplitude for a particle coupled to a smooth external potential $V(x)$, first measured at q to be encountered in q' after time t can be represented by

$$\langle q'|\hat{U}(t)|q\rangle = \sum_{\text{paths } \alpha} \mathrm{d}\mu[x_\alpha] e^{iS_\alpha[q,q',t]/\hbar}, \tag{2.5}$$

where $\hat{U}(t)$ denotes the (retarded) Green's function for the time-dependent Schrodinger equation, $\mathrm{d}\mu[x_\alpha]$ is a measure on the space of histories, and $S_\alpha[q,q',t]$ is the classical action for the history (also commonly denoted by path) x_α satisfying boundary conditions $x_\alpha(0) = q, x_\alpha(t) = q'$, i.e.,

$$S_\alpha[x_\alpha, \dot{x}_\alpha] = \int_0^t \mathrm{d}\tau L[x_\alpha(\tau), \dot{x}_\alpha(\tau)],\ L(x,\dot{x}) = T(x,\dot{x}) - V(x), \tag{2.6}$$

where $\dot{x}(\tau) = \mathrm{d}x(\tau)/\mathrm{d}\tau$, and we assumed for simplicity that the Lagrangian has no explicit time-dependence, and takes the conventional form given above.

Now suppose that the parameters defining the system (e.g., the particle mass) are sufficiently large that a typical path $x_\alpha(\tau)$ gives rise to an action S_α which is much larger than $\hbar$. Then the phase difference of neighboring paths will likely be sufficiently large and uncorrelated that a random neighborhood of paths will be irrelevant to the computation of the quantum-mechanical amplitude. In this case, the dominant contributions to the quantum-mechanical amplitude are given by by the neighborhoods of paths $\{x_{\text{cl}}(\tau)\}$ which extremize the classical

action. They satisfy the Euler-Lagrange equations deriving from the action functional $S[q]$

$$\left.\frac{\delta S[q]}{\delta q}\right|_{x=x_{\mathrm{cl}}} = 0. \tag{2.7}$$

This argument is justified with the observation that paths differing from x_{cl} by a sufficiently small amount give rise to an action which is different from that of the classical path only at second order (in the path difference $\delta x = x - x_{\mathrm{cl}}$). Thus, from a macroscopic point of view only classical paths (and those arbitrarily close to them) contribute to quantum-mechanical probabilities (recall that $\hbar$ is $O\left(10^{-34}\right)$ in SI units, so the condition that the action is large relative to $\hbar$ is satisfied by essentially any macroscopic system).

While the argument given is far from perfect (starting with the notion of a path integral that despite all successes can only be rigorously proved to exist in a very small number of simple cases [98]), it serves two main purposes: i) to show that the study of the classical limit of quantum mechanics can be formally accomplished by assuming that $\hbar$ is a very small quantity, and ii) it demonstrates how corrections to the semiclassical limit maybe concretely derived within the formalism of path integrals. Furthermore, a variation of the argument given here may be employed to extract the semiclassical limit in a variety of other contexts [42, 55, 109].

2.1.3 Semiclassical Scaling for Many-Fermion Systems

The discussion of the previous subsection was limited to the semiclassical limit of particle motion. It is unsurprising much of the points presented there remain valid when more than one particle is present. However, complications can be foreseen from the fact that if $\hbar \to 0$, but the number of particles N is kept fixed, the energy of the highest-occupied state of a

system will become arbitrarily small. This maybe undesirable. Additionally, because the Thomas-Fermi density (Eq. 2.3) only depends indirectly on N through the Fermi energy E_F, the latter seems to be a natural parameter to be kept fixed in the limiting process which takes $\hbar \to 0$ (as opposed to the particle number). This is particularly true if the limit being sought is that where the predictions of Thomas-Fermi theory agree with those of quantum mechanics.

With E_F constant, a variation of $\hbar$ then necessarily implies change in particle number (see Eq. 2.2)]. This modifies the normalization of the Thomas-Fermi particle density, albeit in a simple way, as both E_F and $v(x)$ remain fixed. The simple qualitative argument just given thus determines not only that the semiclassical limit of many-fermion systems should be approached by varying Planck's constant and the particle number, but also in what way this should happen. In particular, it follows from 2.2, that the Fermi energy is invariant under a scaling of $\hbar$ and N, in which $N \to \infty$ and $\hbar \to 0$, but $N\hbar$ remains fixed. This can be further clarified by defining a small parameter $\gamma \in \mathbb{R}^+$ and the scaled particle number and Planck's constant, N_γ and $\hbar_\gamma$, satisfying

$$N_\gamma = \frac{N}{\gamma}, \ \hbar_\gamma = \hbar\gamma. \tag{2.8}$$

The semiclassical limit is now understood to arise when $\gamma \to 0$. A simple explicit illustration of the above ideas is given by the harmonic oscillator. Let its frequency ω be equal to 1. Then, $E_F^\gamma = N^\gamma \hbar^\gamma = N\hbar$ but $E_{N+1\gamma} - E_{N\gamma} = \Delta E_\gamma = \hbar\gamma$. The number of occupied states is $E_{F\gamma}/\Delta E_\gamma = N/\gamma$ as required.

While the discussion of the semiclassical limit above was somewhat heuristic, it finds rigorous justification in the works of Lieb and Simon [67] and of Fournais, Solovej and Lewin [40]. The former showed that Thomas-Fermi theory becomes exact for atomic systems (including molecules and crystals) as the total nuclear charge of the system goes to infinity, while the

latter have recently generalized the Lieb-Simon approach to any class of non-relativistic quantum-mechanical fermionic system, thus proving the universality of the Thomas-Fermi limit for any class of external couplings. In the mathematical literature, the scaling given here is justified by a Lieb-Thirring inequality. This bounds the kinetic energy of a fermionic system in such a way that requires N to scale as $\hbar^{-1/d}$ for the semiclassical limit to be well-defined [40]. Notably, the semiclassical scaling we described above follows from the requirement that all energy components scale with the same power of γ in the limit where $\gamma \to 0$. For the case of interacting systems it follows the mean-field (e.g., Hartree theory) limit is coupled to the semiclassical [40].

Armed with these considerations, any formulation of quantum mechanics can be employed to derive the semiclassical limit of noninteracting fermionic systems. We show in section 2.4 how the classical limit first derived by Thomas and Fermi arises from the full quantum theory in the case of fermions constrained by Dirichlet boundary conditions. In chapter 3 we discuss similarly the case where particles are confined only by a smooth external coupling. For that the tools described in the next two sections will be of major importance.

2.2 Semiclassical Asymptotics for Observables

Observables of a system of noninteracting fermions can be evaluated by summing over the contributions from each occupied quantum state (single-particle state), e.g., if $\hat{O}$ is a self-adjoint operator in the Hilbert space of a single particle $\mathcal{H}$, then in the N-particle sector of the Fock space its expectation value on a noninteracting fermionic ground-state Ψ is given by

$$\langle \Psi | \hat{O}_N | \Psi \rangle = \sum_{i=1}^{\infty} \langle \psi_i | \hat{O} | \psi_i \rangle \, \theta \left(E_F(N) - E_i \right), \tag{2.9}$$

where $\hat{O}_N$ is the representation of $\hat{O}$ on $\bigotimes_{i=1}^{N} \mathcal{H}_{\rm i}$ and the Hilbert spaces $\mathcal{H}_{\rm i}$ are all isomorphic (as the fermions are indistinguishable). It will be important for the derivation of the expectation value of observables in the semiclassical limit that it is understood how to approximate sums such as that of Eq. 2.9. A hint on promising procedures is given by recalling that the classical analog of Eq. 2.9 would not involve a discrete summation, but instead an integral over a continuum set of occupied classical phase space states.

2.2.1 Euler-MacLaurin Summation

The idea of estimating sums over discrete sets by integrals (and vice-versa) is an old one [5, 53, 107]. For instance, the Euler-MacLaurin (EM) formula was discovered almost 300 years ago [36, 73, 82]. It is valid for any $f(x)$ with continuous derivatives at any x in the summation domain. For the case where f has at least m derivatives, it may be written explicitly as,

$$\sum_{k=1}^{n} f(k) = \int_{1}^{n} \mathrm{d}x f(x) + \frac{1}{2}\left[f(1) + f(n)\right] + \sum_{r=1}^{m} \frac{B_{2r}}{(2r)!}\left[f^{(2r-1)}(n) - f^{(2r-1)}(1)\right] + R_m, \quad (2.10)$$

where B_k denotes the k-th Bernoulli number [1], $f(j) = \mathrm{d}^j f(x)/\mathrm{d}x^j$ and R_m is a remainder integral [5, 15].

The EM expansion is useful in a variety of contexts where f is a slowly-varying function or has only a finite number of nonvanishing derivatives [15, 82]. However, as Eq. 2.10 shows, the EM formula is expected to be problematic whenever the summand has any kind of singular behavior in the complex plane. For instance, in cases where a function varies fast enough in some domain (e.g., if it contains a pole), its derivatives become large and the coefficients of the above expansion clearly go to infinity. We should note however that the EM formula

was proven to be useful in demonstrating the connection between semiclassical WKB and Thomas-Fermi theory [74]. This will be further discussed in chapters 3 and 4.

In any case, most of the interesting phenomena in the natural sciences arises from some type of singular behavior. Therefore, generally speaking the Euler-MacLaurin formula finds overall limited applicability. The next subsection provides an alternative method which will serve as the basis for later developments.

2.2.2 Poisson Summation and Dual Representations of Sums

Our first hint towards the semiclassical limit of quantum-mechanical observables of many-particle systems was obtained by considering their classical limit. Quantum corrections are expected to introduce wave phenomena such as oscillations (see e.g., Fig. 2.1 and [38]). As discussed, in this instance, the EM summation formula is expected to fail. Thus, in this subsection we show an alternative method, that of Poisson summation, which, as will be seen, is capable of generating the semiclassical behavior of the sums represented by Eq. 2.9.

Before introducing the Poisson summation formula we note that it is motivated by the elementary observation that functions may be represented in a variety of equivalent ways, some of which are more useful than others in different contexts. For example, special functions can be written as integral representations or as series expansions with the same domain. Integral transforms provide a qualitatively different example as they map functions on some space to another, so that while a function and its integral transform contain the same information, they are not equal, but *dual*.

Poisson summation provides a dual representation of discrete sums,

$$\sum_{j=0}^{N-1} f(j) = \sum_{k=-\infty}^{\infty} \int_{\alpha-1/2}^{N+\alpha-1/2} \mathrm{d}\lambda f(\lambda) e^{2\pi i k \lambda}, |\alpha| < 1/2, \tag{2.11}$$

where $f(\lambda)$ is assumed to fulfill the following two criteria: i) it matches $f(j)$ when $\lambda = j \in \mathbb{N}$, and ii) it satisfies Dirichlet conditions in any subinterval of unit length of $(\alpha-1/2, N+\alpha-1/2)$ [25]. Note that with $\alpha = 0$, the $k = 0$ term of the Poisson summation is equal to that of the Euler-MacLaurin formula (in fact there exists a correspondence between the EM and Poisson summation formulas which is explicitly shown in [15]).

The Poisson summation formula allows the conversion of a finite sum of known coefficients into an infinite sum of Fourier integrals over those. Thus, it may seem to have made the initial problem harder. The following semiclassical argument shows why this is not the case. In particular, we shall see that the r.h.s of Eq. 2.11 has a beautiful physical interpretation which also reveals why it is more amenable to an asymptotic treatment compared to its original representation.

Let $\rho(x, E_F)$ denote the particle density for a system with Fermi energy E_F corresponding to N particles,

$$\rho(x, E_F) = \sum_{j=0}^{\infty} |\psi_j(x)|^2 \theta[E_F(N) - E_j] = \sum_{m=-\infty}^{\infty} \int_{-1/2}^{N-1/2} \mathrm{d}\lambda |\psi_\lambda(x)|^2 e^{2\pi i m \lambda}, \tag{2.12}$$

where in accordance with the description above $\psi_\lambda(x)$ is required to match the discrete eigenstates $\psi_j(x)$, $\forall\ j \in \mathbb{Z}^+$, and be continuously differentiable almost everywhere (i.e.,

except at isolated points) in both λ and x. Then, we can rewrite it as

$$\rho(x, E_F) = \sum_{m=-\infty}^{\infty} B_m[x, E_F(N)] e^{iG_m[x, E_F(N)]}. \tag{2.13}$$

Now consider the expression of the particle density in terms of the Schrodinger equation propagator [41],

$$\rho(x, E_F) = \lim_{T\to\infty} \int_{-T}^{T} \frac{\mathrm{d}t}{t - i\eta} e^{iE_F t/\hbar}(x, t|x, 0), \ \eta \to 0^+. \tag{2.14}$$

By employing a semiclassical approximation to the quantum propagator we necessarily obtain a corresponding approximate particle density. We find the former by recalling the discussion of subsections 2.1.2 and 2.1.3. They imply the semiclassical limit of the quantum propagator can be represented by

$$(x, t|x, 0) \sim \sum_{\text{cl. paths}, q(0)=q(t)=x} A[q_{\text{cl}}(x)] e^{iS[q_{\text{cl}}(t)]/\hbar}, \ \hbar \to 0^+, \tag{2.15}$$

where $A[q_{\text{cl}}]$ is proportional the density of classical trajectories in a neighborhood of q_{cl}. Thus, it depends only on quantities evaluated at the classical orbit with boundary conditions $q_{\text{cl}}(0) = q_{\text{cl}}(t) = x$ [55, 98].

With the above result, a semiclassical approximation to the particle density is obtained

$$\rho(x, E_F) \sim \int_{-\infty}^{\infty} \frac{\mathrm{d}t}{t - i\eta} e^{iE_F t/\hbar} \left(\sum_{\text{cl. paths}, q(0)=q(t)=x} A[q_{\text{cl}}] e^{iS[q_{\text{cl}}(t)/\hbar]} \right). \tag{2.16}$$

The dominant behavior of the above integral in the limit where $\hbar \to 0$ can be obtained with the method of stationary phase approximation [14, 28, 68]. It is given by

$$\rho(x, E_F) \sim \sum_{j=-\infty}^{\infty} \sum_{\text{cl. paths}} C_j[q_{j,\text{cl}}, E_F(N)] \exp\left[\frac{i}{\hbar} \int_{C_j} p(q'_{\text{cl}}, E_F) \mathrm{d}q' + i\beta_j \right], \ \beta_j \in \mathbb{Z}\pi, \tag{2.17}$$

where the classical paths being summed now correspond to to those which are closed and along which a particle travels with energy E_F, irrespective of the elapsed time.

Here it is important to understand that because the ground-state particle density is a time-independent observable, the classical paths appearing in Eq. 2.17 include a primitive path $q$cl and an infinite number of repetitions of the latter which we have labeled by j, where $j < 0$ means that the path is travelled in the opposite direction relative to those paths with $j > 0$. The index j classifies topologically inequivalent classical orbits, that is, those which cannot be deformed onto each other by a small local perturbation.

The clear resemblance between equations 2.13 and 2.17 indicates the interpretation that each term of the Poisson summation formula may be associated in the semiclassical limit to a class of topologically equivalent paths of the classical system which corresponds to the quantum-mechanical. Because of this interpretation, Berry has described the Poisson formula as a *topological sum* [12, 12]. We will make extensive use of it in section 2.4 and chapter 3.

2.3 Uniform Asymptotic Approximations

In the previous section we have shown an approach towards the derivation of semiclassical approximations to the observables of noninteracting fermionic systems. For this to be useful, knowledge is required of the semiclassical limit of the eigenstates of the single-particle quantum Hamiltonian characterizing the noninteracting system. In this section we present those for the case of interest to this thesis, that of one-dimensional particles confined by a smooth external potential $v(x)$.

The most traditional way of studying the semiclassical limit (for this section, the only limit that is relevant is $\hbar \to 0^+$) of the quantum states $\psi(x)$ of a Hamiltonian of the form

$$\hat{H} = -\frac{\hbar^2}{2}\frac{\mathrm{d}^2}{\mathrm{d}x^2} + v(x),\ x \in \mathbb{R} \tag{2.18}$$

is via the WKB [19, 58, 106] approximation. In this method, an ansatz of the form

$$\Psi(x) = e^{\frac{i}{\hbar}A(x)},\ A(x) = A_0(x) + \hbar A_1(x) + ..., \tag{2.19}$$

is applied to the Schrodinger equation, and the coefficients $A_j(x)$ are obtained by solving simple coupled differential equations [23, 55]. If $\hbar \to 0$, it is expected that the terms $A_j(x)$ with $j > 1$ will become irrelevant in the expansion of $A(x)$. Thus, retaining only $A_0(x)$ and $A_1(x)$, we obtain the so-called WKB wave functions,

$$\psi_j^{\mathrm{WKB}}(x) \sim \begin{cases} \frac{N_j}{[E_j - v(x)]^{1/4}} \cos\left[\int_{x_L}^{x} \sqrt{2[E_j - v(x')]}\mathrm{d}x' - \frac{\pi}{4}\right] & x_L < x < x_R, \\ \frac{N_j}{2|E_j - v(x)|^{1/4}} \exp\left[-\int_{x_L}^{x} \sqrt{2|E_j - v(x')|}\mathrm{d}x'\right] & x < x_L - \eta, \\ \frac{N_j}{2|E_j - v(x)|^{1/4}} \exp\left[-\int_{x_R}^{x} \sqrt{2|E_j - v(x')|}\mathrm{d}x'\right] & x > x_R + \eta, \end{cases}$$

where $\eta \to 0^+$, E_j is obtained from the WKB quantization condition [11, 23] and x_L and x_R denote the two turning points of the classical trajectory corresponding to E_j.

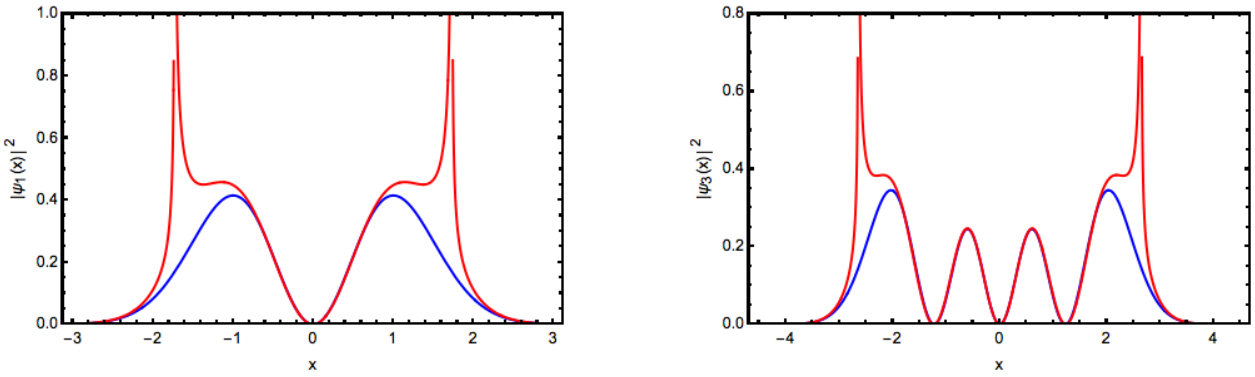

Figure 2.2: Left: harmonic Oscillator orbital densities $|\psi_1(x)|^2$ computed exactly (blue) and with WKB (red). Right: harmonic oscillator orbital densities $|\psi_3(x)|^2$ computed exactly (blue) and with WKB (red).

While WKB provides a quick avenue towards the semiclassical limit, a quick look at the WKB wave function reveals two major problems: it is not defined at the turning points x_L and x_R, and it is also discontinuous across them. Figure 2.2 illustrates these problems by showing orbital densities obtained with WKB wave functions for the states $j = 1$ and $j = 3$ corresponding to $v(x) = 1/2x^2$.

The singular behavior of the (primitive) semiclassical wave function is a manifestation of the fact that that the classical probability density for a particle to be found in the configuration space interval $(x, x + \mathrm{d}x)$ diverges exactly at those points where the speed of a classical particle vanishes. In fact, let $P_{\mathrm{cl}}(x, E)$ denote the probability to locate a classical particle in the aforementioned interval. Then,

$$P_{\mathrm{cl}}(x, E)\mathrm{d}x = \frac{\mathrm{d}t(\mathrm{d}x, E)}{T(E)}, \tag{2.20}$$

where $T(E)$ denotes the period of the classical orbit with energy E. It follows that

$$P_{\mathrm{cl}}(x, E) = \frac{1}{p(x, E)T(E)}, \;\; p(x, E) = \sqrt{2[E - v(x)]} = \frac{\mathrm{d}x}{\mathrm{d}t}. \tag{2.21}$$

Thus, the pathological behavior of WKB around turning points of the classical motion is not an anomaly. It is a result of the singular nature of classical phase space motion when projected to the configuration space.

The above discussion makes it clear that approximations to the particle density (and other local observables) which are based on WKB will inherit its representation-dependent singularities [69]. To avoid this one may look for an alternative semiclassical wave function. Because WKB works greatly in the bulk region which is far from turning points, this would ideally reduce to WKB when it is appropriate but would also somehow include the smoothing effect of quantum mechanics near the classical turning points. These characteristics might be said to define a uniform semiclassical approximation.

Semiclassical uniform approximations are generally obtained in terms of canonical functions which unfold the singularities intrinsic to primitive asymptotic treatments (e.g., WKB) [10, 11, 23, 98]. The Airy function

$$Ai(z) = \frac{1}{2\pi}\int_{-\infty}^{\infty} e^{i(t^3/3+zt)}\mathrm{d}t, \tag{2.22}$$

is the oldest and most popular of this group of special functions [2]. Its preponderance is attributed to the ubiquity of the fold catastrophe which arises as a coalescence of two non-degenerate critical points of a mapping [23, 98]. For example, the stationary WKB wave function can only be written if the corresponding classical Hamilton-Jacobi equations have known solutions. Each defines a critical point of the classical action functional. In one dimension, for a generic classically-allowed position and energy, there exists two real solutions corresponding to positive and negative momentum. However, at a turning point there is a single zero momentum critical point of the action. As a result, the projection of the constant energy Lagrangian submanifold on configuration space is singular and the stationary spatial WKB wave function loses its validity [6] as we explicitly saw above. We

will show below there exists a semiclassical Airy uniform approximation to the quantum-mechanical wave function. It is also based on the solutions to classical equations of motion, but it encodes this information in a way that avoids the aforementioned issues altogether [11, 23, 62].

In 1937 Langer proved that a semiclassical wave function existed which did not have any of the singularities associated to the classical motion. Sufficient and necessary conditions for its validity are that $v(x)$ must be such that the corresponding zeroes of the squared classical momentum $p^2(x, E)$ (turning points) are simple, and $p(x, E)$ is analytic everywhere except where it vanishes. From now on we assume these requirements are satisfied. Let E denote the energy of a classical bound state, $\omega(E)$ the classical frequency of the periodic orbit with energy E, x_- the l.h.s turning point for a particle with energy E and $S(x, x_-, E)$ the classical action measured from x_-, i.e., $S(x, x_-, E) = \int_{x_-}^{x} p(x', E)\mathrm{d}x'$. Then, the corresponding Langer wave function can be written as:

$$\phi_-(x, E) = \sqrt{\frac{2m\omega(E)}{p(x, E)}} \left[\frac{3}{2}\frac{S(x, x_-, E)}{\hbar}\right]^{1/6} Ai\left[-\left(\frac{3}{2}\frac{S(x, x_-, E)}{\hbar}\right)^{2/3}\right], \tag{2.23}$$

where $Ai(t)$ is the Airy function evaluated at t [1]. To simplify notation, we define

$$z(x, E) = \left[\frac{3}{2}\frac{S(x, x_-, E)}{\hbar}\right]^{2/3}. \tag{2.24}$$

An identical approximation can be made where x_- is replaced by x_+ and the action rewritten as $S(x_+, x, E)$ so it remains positive semidefinite in the classically-allowed region. While the Airy uniform approximation was originally built for probems with a single turning point, it may be extended (non-uniquely) for the case where there are two such points [77]. In this work we employ the following prescription: let x_m be defined such that $S(x_m, x_-, E) = S(x_+, x_m, E) = S(x_+, x_-, E)/2$. Then, for $x \leq x_m$ one may employ the left Langer wave function $\phi_-(x, E)$, while the right is used otherwise. Both will be denoted by $\phi(x, E)$ from

now on.

Note that for any smooth $v(x)$ where E defines a classical bound state state with two turning points, $\phi(x, E)$ is defined for all real x. In the classically-forbidden region, the action (and any quantities derived from it) must be analytically continued so that $\phi(x, E)$ remains real and well-behaved. For example, for $x < x_-$, it follows that $p(x, E) = e^{i\pi/2}|p(x, E)|$, $S(x, E) = e^{3\pi i/2}|S(x, x_-, E)|$, and $z(x, E) = (e^{3\pi i/2}3/2|S(x_-, x, E)|/\hbar)^{2/3}$, so

$$\phi(x, E) = \sqrt{\frac{2m\omega(E)}{|p(x, E)|}}\,|z(x, E)|^{1/4} Ai\left(|z(x, E)|\right), x < x_-. \tag{2.25}$$

In particular, $\phi(x, E)$ is a continuous function of x across the transition region (between that which is classically-allowed and forbidden). Its behavior is oscillatory in the bulk of the classically-allowed region ($z_F(x) >> 0$) [1]. For large negative values of $z_F(x)$, i.e., for x far from turning points in the classically-forbidden regions, it decays exponentially as expected for a bound finite system. Further, if the asymptotic forms of the Airy function are employed where the WKB wave function is well-defined, $\phi(x, E)$ is seen to be locally equivalent to that.

These remarks suggest the Langer wave function provides a promising starting point for the construction of uniform approximations to the semiclassical particle and kinetic energy densities. This will be verified to be true explicitly in chapter 3.

2.4 Warm-up Exercise: Dirichlet Fermions

This chapter is ended with a non-trivial example of the ideas exposed in the previous sections.

Define as Dirichlet fermions those which have zero probability to be located outside of a compact interval, e.g., $[0, 1]$, i.e., their wave functions satisfy vanishing Dirichlet boundary conditions at $x = 0$ and $x = 1$. We consider noninteracting particles with the same spin, so

they are only correlated by the Pauli principle. The single-particle hamiltonian governing all properties of the system is given by

$$\hat{H^{\gamma}} = -\frac{\gamma^2}{2}\frac{\mathrm{d}^2}{\mathrm{d}x^2} + v(x),\ x \in [0,1]. \tag{2.26}$$

where $\gamma > 0$ is the semiclassical scaling parameter, $v(x)$ is a smooth external potential and we have set $m = \hbar = 1$. The domain of $\hat{H}$ consists only of those functions which are square integrable in $[0,1]$ and vanish at $x = 0$ and $x = 1$. We only treat systems with ground-state energy $E_0 > v(x),\ \forall\ x \in [0,1]$. In the next chapter we lift the latter two requirements and remove the Dirichlet boundary conditions.

First we derive the ground-state density matrix, then we take the limit where $x' \to x$ so the particle density is obtained. A derivation of these results using completely different methods can be found in references [22, 33].

2.4.1 One-Particle Density Matrix

The single-particle density matrix for a system of N noninteracting Dirichlet fermions is given by

$$n_D(x,x') = \sum_{j=0}^{N-1} \overline{\phi}_j(x)\phi_j(x'),\ x,x' \in [0,1], \phi_j(0) = \phi_j(1) = 0\ \forall\ j \in \mathbb{N}, \tag{2.27}$$

where $\phi_j(x)$ denotes the eigenstate of $\hat{H}$ with energy E_j, such that $E_j < E_i$ for all $j < i$ and $\overline{z}$ identifies the complex conjugate of z.

To find the limit of $n_D^{\gamma}(x,x')$ as $\gamma \to 0^+$, we can employ WKB orbitals adapted to Dirichlet boundary conditions. They correspond to uniform approximations for the studied system since we assume that the equations $E_i = v(x)$ have no solution on [0,1]. Then, it follows that

primitive semiclassical wave functions are continuously differentiable for any energy $E > E_0$. By following the same idea given in our previous discussion of WKB one finds that,

$$\phi_j^{\gamma,\mathrm{WKB}}(x) = \sqrt{\frac{2\omega_j}{\pi p_j}} \sin[S_j(x)/\gamma], \tag{2.28}$$

where we employ the notation of the previous section. The WKB energies which should be employed in the computation of ω_j and p_j are obtained by requiring that $\phi_j^{\gamma,\mathrm{WKB}}$ satisfies the appropriate boundary conditions for this problem:

$$S_j^{\gamma}(1) = \int_0^1 \mathrm{d}x' \sqrt{2\left[E_j^{\gamma,\mathrm{WKB}} - v(x)\right]} = \gamma j \pi. \tag{2.29}$$

The implication of the above quantization condition is that, as expected, the spectrum of the Hamiltonian (and with it every other quantity in eq. 2.28) depends on γ. For the sake of simplicity, we adopt in the remainder of this derivation a simpler notation in which only explicit γ dependence is shown and any reference to WKB is removed, though it should be kept in mind that γ-scaled WKB energies are being employed to calculate any classical property which is needed to construct the semiclassical Dirichlet density matrix.

From the above we have the WKB Dirichlet density matrix,

$$n_D^{\gamma}(x,x') = \sum_{j=0}^{N^{\gamma}-1} \frac{2\omega_j}{\pi} \frac{1}{\sqrt{p_j(x)p_j(x')}} \sin[S_j(x)/\gamma] \sin[S_j(x')/\gamma], \tag{2.30}$$

which can be further simplified to

$$n_D^{\gamma}(x,x') = \sum_{j=0}^{N^{\gamma}-1} \frac{\omega_j}{\pi} \frac{1}{\sqrt{p_j(x)p_j(x')}} \left[\cos[\gamma^{-1}(S_j(x) - S_j(x'))] - \cos[\gamma^{-1}(S_j(x) + S_j(x'))]\right], \tag{2.31}$$

and rewritten as an infinite sum with the aid of the Poisson summation formula:

$$n_D^{\gamma}(x,x') = \frac{1}{\pi}\sum_{m=-\infty}^{\infty}\int_{N_0}^{N_F^{\gamma}} \frac{\mathrm{d}\lambda\ \omega_\lambda}{\sqrt{p_\lambda(x)p_\lambda(x')}}\left[\cos[\gamma^{-1}(S_\lambda(x)-S_\lambda(x'))]-\cos[\gamma^{-1}(S_\lambda(x)+S_\lambda(x'))]\right]e^{2\pi i m\lambda}, \tag{2.32}$$

where $N_0 = -1/2$ and $N_F^{\gamma} = N^{\gamma} - 1/2$. As $\gamma \to 0$ the integrand above oscillates fast under small variations of λ. This can be employed to obtain an approximation to each of the shown integrals. In particular, if integration by parts is performed it is found that

$$n_D(x,x') = \frac{\omega_F}{\pi\sqrt{p_F(x)p_F(x')}}\sum_{m=-\infty}^{\infty}(I_1 - I_2) + O(\gamma), \tag{2.33}$$

where

$$I_1 = \frac{1}{2}\int_{-1/2}^{N^{\gamma}-1/2}\mathrm{d}\lambda\left[e^{i(S_\lambda(x)/\gamma - S_\lambda(x')/\gamma + 2\pi m\lambda)} + e^{-i(S_\lambda(x)/\gamma - S_\lambda(x')/\gamma - 2\pi m\lambda)}\right], \tag{2.34}$$

and

$$I_2 = \frac{1}{2}\int_{-1/2}^{N^{\gamma}-1/2}\mathrm{d}\lambda\left[e^{i(S_\lambda(x)/\gamma + S_\lambda(x')/\gamma + 2\pi m\lambda)} + e^{-i(S_\lambda(x)/\gamma + S_\lambda(x')/\gamma - 2\pi m\lambda)}\right]. \tag{2.35}$$

Note that we have neglected contributions from the lower-bound of the integration domain (it can be shown they are irrelevant in the semiclassical limit). The integrals in I_1 and I_2 are still not simple enough to allow for an exact evaluation. However, they may be again approximated with the method of integration by parts. We work the following example in detail as the prescription will be adopted for each of the integrals encapsulated by I_1 and I_2.

Let

$$I_f = \int_{-1/2}^{N^\gamma - 1/2} \mathrm{d}\lambda \; e^{if(\lambda)} = \int_{f(-1/2)}^{f_F^\gamma} \mathrm{d}f \frac{e^{if}}{\mathrm{d}f/\mathrm{d}\lambda}, \tag{2.36}$$

where

$$f(\lambda) = 2\pi m\lambda + S_\lambda(x)/\gamma + S_\lambda(x')/\gamma, \tag{2.37}$$

and $f_F^\gamma = f\left(N^\gamma - 1/2\right)$. By employing the relations

$$\left(\frac{\mathrm{d}f}{\mathrm{d}\lambda}\right)^{-1} = \frac{1}{2\pi m + \alpha_\lambda(x) + \alpha_\lambda(x')}, \; \alpha_\lambda(x) = \gamma^{-1}\frac{\partial S_\lambda(x)}{\partial \lambda}, \tag{2.38}$$

we find to leading order in γ,

$$I_f \sim \frac{e^{i[S_F(x)/\gamma + S_F(x')/\gamma] - m\pi}}{2\pi m + \alpha_F(x) + \alpha_F(x')} + O(\gamma). \tag{2.39}$$

After performing the same steps for the other integrals associated to I_1 and I_2 we find the result is

$$n_D(x,x') \sim \frac{\omega_F}{\pi\sqrt{k_F(x)k_F(x')}} \sum_{m=-\infty}^{\infty} \left[\sin[1/\gamma(S_F(x) - S_F(x'))]S_1 - \sin[1/\gamma(S_F(x) + S_F(x'))]S_2\right] \tag{2.40}$$

where we have only shown the leading terms in the limit where $\gamma \to 0^+$, and

$$S_1 = \sum_{m=-\infty}^{\infty} \frac{e^{-i\pi m}}{\frac{\alpha_F(x) - \alpha_F(x')}{2} - m\pi}, \; S_2 = \sum_{m=-\infty}^{\infty} \frac{e^{-i\pi m}}{\frac{\alpha_F(x) + \alpha_F(x')}{2} - \pi m}. \tag{2.41}$$

Fortunately the above sums can be evaluated exactly, so the infinite number of terms which

initially appeared in the Poisson representation of the density matrix have been reduced to an almost unbelievably simple semiclassical approximation [33]:

$$n_D^{\gamma}(x,x') \sim \frac{\omega_F}{\pi\sqrt{p_F(x)p_F(x')}}\left(\frac{\sin[1/\gamma(S_F(x)-S_F(x'))]}{\sin\left(\frac{\alpha_F(x)-\alpha_F(x')}{2}\right)} - \frac{\sin[1/\gamma(S_F(x)+S_F(x'))]}{\sin\left(\frac{\alpha_F(x)+\alpha_F(x')}{2}\right)}\right). \quad (2.42)$$

The semiclassical particle density is obtained from the one-particle density matrix by taking the limit where $x \to x'$ [22, 68]. It can be written as a dominant term corresponding to the Thomas-Fermi density and an oscillatory correction of lower-order in γ,

$$\rho_D^{\gamma}(x) \sim \frac{p_F(x)}{\pi\gamma} - \frac{\omega_F \cos[2S_F(x)/\gamma]}{p_F(x)\sin[\alpha_F(x)]}. \quad (2.43)$$

Here one is reminded again of the singular nature of the Thomas-Fermi density (the first term on the r.h.s) as it arises from the part of the diagonal element of $n_D^{\gamma}(x,x')$ which corresponds to a removable singularity.

Extensive discussion of the behavior of the Dirichlet density matrix and one-particle density including their relevance to electronic structure can be found in [22, 33].

Chapter 3

Semiclassical Approximations for Many-Fermion Systems

3.1 Introduction

The present chapter focuses on the semiclassical limit of sums of quantum mechanical probability densities over the lowest N bound levels. In particular, we employ the methods discussed extensively in chapter 2 to construct uniform semiclassical approximations to the particle and kinetic energy densities of noninteracting fermionic systems in one dimension.

A literature review is given in subsection 3.1.1. In section 3.2 we introduce relevant definitions and establish notation. Sections 3.3 and 3.4 contain the main developments of this chapter: i) derivations of the uniform approximation to the semiclassical particle and kinetic energy

A portion of the text in this chapter is a reprint of the material as it appears in Corrections to Thomas-Fermi Densities at Turning Points and Beyond Raphael F. Ribeiro, Donghyung Lee, Attila Cangi, Peter Elliott, Kieron Burke, Phys. Rev. Lett. 114, 050401 (2015).

densities, ii) a discussion of their analytic properties, and iii) their physical interpretation. We conclude with a discussion of open problems. Appendices I and II provide further comments on the smallness of higher-order terms neglected in the treatment employed in the main text.

3.1.1 Literature Survey

In this section we provide a summary of previous research related to the problem solved later in this chapter. It is important to recognize the priorly obtained limiting behaviors for the particle and kinetic energy densities, as later we show the approximations derived in section 3.4 provide a unified description of all of them.

Primitive semiclassical approximations of limited range of validity have been obtained before for both the particle and kinetic energy densities [22, 57, 63, 93]. For instance, Kohn and Sham gave region-dependent discontinuous approximations to the one-dimensional fermionic ground-state density [57] using semiclassical Green's function theory. Lee and Light built a similar approximation by heuristic generalization of some properties of the problem of a particle in a linear potential, but had to resort to discontinuous ad-hoc corrections from a different model to improve its accuracy [63]. More recently, Cangi et al. obtained a uniform approximation to the particle and kinetic energy densities, but only in the case of vanishing Dirichlet boundary conditions and Fermi energy above any critical point of the potential energy function [22] (see also section 2.4). Similarly, Roccia and Brack constructed semiclassical approximations for the density and kinetic energy densities in a classically-allowed region by employing the Van-Vleck-Gutzwiller [44, 104] semiclassical Green's function [93, 94]. As a result, their approximations are strongly singular at turning points and cannot be continued to the classically-forbidden region.

Aside from the approaches just discussed, many variations are discussed in the older literature

of a variety of subfields of theoretical physics and chemistry, e.g., [4, 7, 43, 81, 100]. Most of the failures of older models can be either ascribed to a reliance on primitive semiclassical methods (e.g., WKB) as a starting point or inadequate formalism upon which perturbation theory is performed.

3.1.2 Definitions

For an isolated non-relativistic system of noninteracting $2N$ spin-1/2 fermions bound to a smooth external potential $v(x)$ with nondegenerate energy levels E_k, the ground-state wave function Ψ can be written as the normalized antisymmetric tensor product of N single-particle states (orbitals) $\psi_i(x),\ i = 1, 2, ..., N$ satisfying $(\hat{H}\psi_i)(x) = E_i\psi_i(x)$, where $E_i < E_j,\ \forall\, i < j$. The corresponding particle density $\rho(x; 2N) \equiv n(x)$ is defined as the expectation value of the operator $\sum_{i=1}^{N} \delta(x - \hat{x_i})$,

$$n(x) = \mathrm{Tr}\left[\hat{\rho}\sum_{i=0}^{N-1}\delta\left(x-\hat{x_i}\right)\right] = 2\sum_{i=0}^{N-1}|\psi_i(x)|^2. \tag{3.1}$$

The kinetic energy of the same fermionic system can be obtained as the expectation value of the kinetic energy operator $\hat{T}$.Thus, we we define the kinetic energy density $t(x)$,

$$t(x) = 2\sum_{i=0}^{N-1}\psi_i^*(x)\left(\hat{T}\psi_i\right)(x). \tag{3.2}$$

The operator identity $\hat{T} = \hat{H} - \hat{V}$ may be employed so $t(x)$ can be rewritten in a form that will find use later:

$$t(x) = 2\sum_{i=0}^{N-1}\frac{p^2(x, E_i)}{2m}|\psi_i(x)|^2, \tag{3.3}$$

where m is the fermionic mass, and $p^2(x, E_i)/2m = E_i - v(x)$.

Note that a nondegenerate fermionic ground state can be completely specified by its potential energy function $v(x)$ and number of particles N. Hence, we define the Fermi energy E_F so it lies between the energy of the lowest occupied and highest unoccupied orbitals, i.e., $E_{N-1} < E_F < E_N$. In this way, we may characterize a one-dimensional fermionic ground state by $v(x)$ and E_F. Assuming, without loss of generality, that each orbital is occupied by a single fermion of unit mass, the particle and kinetic energy densities for N noninteracting bound fermions may be rewritten as:

$$n(x) = \sum_{i=0}^{\infty} |\psi_i(x)|^2 \theta\left(E_F - E_i\right), \tag{3.4}$$

$$t(x) = \frac{1}{2} \sum_{i=0}^{\infty} |\psi_i(x)|^2 p^2(x, E_i) \theta\left(E_F - E_i\right), \tag{3.5}$$

where the spectrum of $\hat{H}$ is assumed discrete for notational purposes.

3.2 Uniform Semiclassical Approximations

3.2.1 Particle Density

Our aim in this section is to obtain closed-form uniform approximations to the one-dimensional non-interacting fermionic density which respect the leading-order asymptotics of $n(x)$ everywhere in configuration space. As opposed to the derivation presented in section 2.4, the semiclassical scaling parameter γ is not explicitly shown, though it is implied that we work in the limit where semiclassical asymptotics is reliable. We choose to retain $\hbar$ in all equations. This is done to aid clarity (as γ-scaling is omitted). Later we apply semiclassical scaling in the Appendices to show that terms neglected in intermediate steps of the following derivations

are irrelevant in the semiclassical limit.

Without loss of generality we assume orbitals are singly-occupied and the fermions have $m = 1$. The external potential $v(x)$ is required to be analytic and to have non-vanishing first derivative at the turning points of all classical orbits with $E < E_F$. Under these conditions, the orbitals of non-interacting fermionic system can be uniformly and accurately approximated by the Langer wave functions described in the previous chapter. It follows from Eq. 3.4 that the same is true for $n(x)$. Thus, our treatment has as its starting point Eq. 3.4 with Langer wave functions (eq. 2.23) employed as occupied orbitals. In what follows E_F will always be chosen so that the classical action (see below) $S(E_F, x_+, x_-)$ satisfies the semiclassical quantization condition

$$S(E_F, x_+, x_-) = N\pi\hbar. \tag{3.6}$$

This choice enforces normalization of the associated Thomas-Fermi density (the leading term in any asymptotic expansion of the particle density) to N particles [37, 74, 101]. Also equivalent is to assume the Fermi level corresponds to the energy of a state with half-integer quantum number $j = N - 1/2$ in the WKB quantization condition

$$\frac{1}{2\pi\hbar}\oint \mathrm{d}x' p[x', E(j)] = (j + 1/2)\,. \tag{3.7}$$

For this reason every quantity evaluated at $j = N - 1/2$ will be denoted by a subscript F. Note the above implies the Fermi energy defines a compact Lagrangian submanifold of phase space, so that no states in the continuum spectrum of $\hat{H}$ are occupied.

In the first step of our derivation we employ the finite Poisson summation formula (see previous chapter and [25]). It allows the rewriting of the particle density in a way that

(despite appearances) is amenable to a semiclassical treatment:

$$\sum_{j=0}^{N-1} |\psi_j|^2 = \sum_{k=-\infty}^{\infty} \int_{1/2}^{N-1/2} d\lambda \, |\psi(\lambda)|^2 e^{2\pi i k \lambda}, \tag{3.8}$$

where the conditions satisfied by $\psi(\lambda)$ are described in section 2.2.2.

Using the finite Poisson summation formula and the Langer semiclassical uniform approximation to the wave function for each occupied energy level we obtain for the density $n(x)$

$$n(x) = \sum_{k=-\infty}^{\infty} \int_{-1/2}^{N-1/2} \mathrm{d}\lambda \frac{2\omega(\lambda) z^{1/2}(x,\lambda)}{p(x,\lambda)} Ai^2[-z(x,\lambda)] e^{2\pi i k \lambda}. \tag{3.9}$$

In the integrals above, physical quantities defined previously as functions of E are written as functions of λ via the mapping $E = E(\lambda)$ (e.g., $\omega(E) = \omega(E(\lambda)) \equiv \omega(\lambda)$) which we assume can be well approximated by $E_{\mathrm{WKB}}(\lambda)$. Because our assumptions imply non-degeneracy of energy levels and $\mathrm{d}E/\mathrm{d}\lambda \neq 0$ for all $E \leq E_F$, the map $E(\lambda)$ is bijective in the integration interval.

Our strategy consists of a perturbative evaluation of the integrals in Eq. 3.9, followed by resummation of the dominant contributions to the asymptotic expansion of each. The terms in Eq. 3.9 where $k = 0$ and $k \neq 0$ are treated in different subsections, since their asymptotic treatments and physical interpretations are of a different nature, though, as will be seen, deeply connected.

Dominant Behavior

The leading asymptotic contribution to the density in the semiclassical limit is well-known to emerge from the zeroth component of the Poisson summation formula [11, 18]. In other words, Thomas-Fermi theory may be obtained by approximating the summation in the

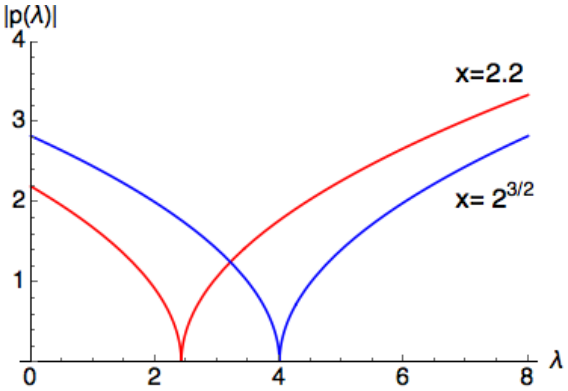

(a) Generic behavior of $|p(\lambda, x)|$ for fixed x.

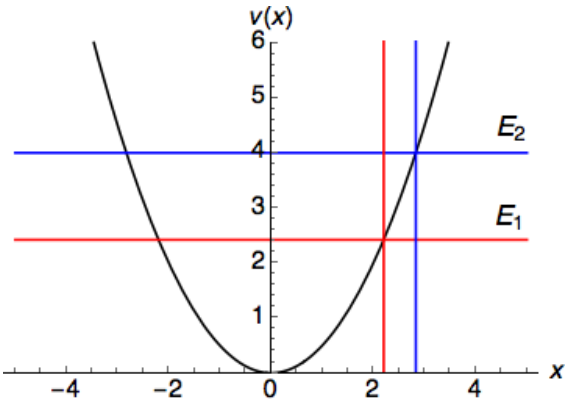

(b) Typical $v(x)$; the energies E_1 and E_2 correspond to those with turning points at the two values of x indicated in Figure 1.

definition of $n(x)$ by an integral over classical (or WKB) probability densities [11, 22, 74]. Thus, we expect

$$n_0(x) = 2\int_{-1/2}^{N-1/2} \mathrm{d}\lambda \frac{\omega(\lambda)}{p(x,\lambda)} z^{1/2}(x,\lambda) Ai^2[-z(x,\lambda)], \tag{3.10}$$

to contain the classical limit of the one-particle density $n(x)$. In what follows x will be regarded as a parameter, so it will be assumed constant throughout all subsequent developments unless explicitly stated otherwise. For ease of notation we omit the spatial dependence of physical quantities at intermediate steps of the derivation. Then, upon using the identity $\hbar\omega(\lambda)\mathrm{d}\lambda = p(\lambda)\mathrm{d}p(\lambda)$, $n_0(x)$ can be rewritten in a simpler form as a Riemann-Stieltjes integral [108]:

$$n_0(x) = 2\hbar^{-1}\int_{-1/2}^{N-1/2} \mathrm{d}p(\lambda) p(\lambda) f^{-1}(p) Ai^2\left[f^{-2}(p)p^2(\lambda)\right], \tag{3.11}$$

where $f(p) = f(p(\lambda)) = p(\lambda)/\sqrt{z(\lambda)}$. Both $p(\lambda)$ and $z(\lambda)$ are of bounded variation in any compact interval of the (x, λ) plane (see Figures 1 and 2). Additionally, the integrand is continuous in the integration domain. Therefore, the integral is well-defined.

If $f(p)$ were constant as is the case for the linear potential $v(x) = x$, a closed-form solution

would exist for $n_0(x)$. For well-behaved $v(x)$ we expect $f(p(\lambda))$ to be a slowly-varying function of λ. In fact, as the semiclassical limit defined in Section 2.1 is approached, the variation of f with respect to λ tends to be small (see Appendix I). This suggests the following zeroth order approximation, obtained under the assumption that $f(p)$ is constant,

$$n_0^{(0)} = \frac{p(\lambda)}{\hbar}\sqrt{z(\lambda)}\left(Ai^2[-z(\lambda)] + \frac{1}{z(\lambda)}Ai'^2[-z(\lambda)]\right)\Bigg|_{\lambda=-1/2}^{\lambda=N-1/2}. \tag{3.12}$$

To extract corrections to $n_0^{(0)}$ we take partial derivatives of the above with respect to p (noting that in this case $\partial/\partial p = \partial N/\partial p\ \partial/\partial N$), change N to λ, and then apply the integration operator $\int_{-1/2}^{N-1/2} \mathrm{d}p(\lambda)$ to both sides. After rearranging terms we find:

$$\begin{aligned} n_0 = \ & \frac{p(\lambda)}{\hbar}\sqrt{z(\lambda)}\left(Ai^2[-z(\lambda)] + z^{-1}(\lambda)Ai'^2[-z(\lambda)]\right)\Bigg|_{\lambda=-1/2}^{\lambda=N-1/2} + \frac{1}{\hbar}\int_{-1/2}^{N-1/2}\mathrm{d}p(\lambda)\frac{\partial f}{\partial p}z(\lambda)Ai^2\left[-z(\lambda)\right] \\ & - \frac{1}{\hbar}\int_{-1/2}^{N-1/2}\mathrm{d}p(\lambda)\frac{\partial f}{\partial p}Ai'^2\left[-z(\lambda)\right], \end{aligned} \tag{3.13}$$

where $f'(p) = \partial f/\partial p$. The identity $\partial f/\partial p = \partial z/\partial p\ \partial f/\partial z$ allows us to rewrite the correction to $n_0^{(0)}(x)$ in a simple form:

$$n_0 = n_0^{(0)} + L_0 + \frac{1}{\hbar}\int_{-1/2}^{N-1/2}\mathrm{d}\left\{Ai[-z(\lambda)]Ai'[-z(\lambda)]\right\}\frac{\partial f}{\partial z}, \tag{3.14}$$

where L_0 corresponds to the first term on the r.h.s of Eq. 3.13 evaluated at $\lambda = -1/2$. Further integration by parts gives:

$$n_0 = n_0^{(0)} + \frac{1}{\hbar}\left[\left.\frac{\partial f}{\partial z}\right|_{z=z_F} Ai[-z_F]Ai'[-z_F] - \int_{-1/2}^{N-1/2}\mathrm{d}z(\lambda)\frac{\partial^2 f}{\partial z^2}Ai[-z(\lambda)]Ai'[-z(\lambda)]\right] + L(x). \tag{3.15}$$

where L contains all previously integrated terms evaluated at $\lambda = -1/2$, i.e.,

$$\hbar L = \left[-p(\lambda)\sqrt{z(\lambda)}\left(Ai^2[-z(\lambda)] + \frac{1}{z(\lambda)}Ai'^2[-z(\lambda)]\right) - \left.\frac{\partial f}{\partial z}\right|_{z=z(\lambda)} Ai[-z(\lambda)]Ai'[-z(\lambda)]\right]\Bigg|_{\lambda=-1/2}. \tag{3.16}$$

A hint that $L(x)$ will turn out to be negligible under our assumptions is that $\lambda = -1/2$

corresponds in the WKB approximation to a classical system with zero action, i.e.,

$$\oint \mathrm{d}x p\left[x, E(-1/2)\right] = 0. \tag{3.17}$$

In this case,the classical motion is supported on a minimum of $v(x)$. In Appendix I we show explicitly that both $L(x)$ and the integral in Eq. 3.15 can be safely ignored under the scaling given in Section 2.2. Hence, we find n_0 may be approximated under conditions of small $\hbar$ and large N by:

$$n_0 \sim \frac{p_F}{\hbar}\sqrt{z_F}\left(Ai^2[-z_F] + z_F^{-1}Ai'^2[-z_F]\right) + \left(\frac{\omega_F}{p_F\alpha_F} - \frac{p_F}{2\hbar z_F^{3/2}}\right) Ai[-z_F]Ai'[-z_F], \tag{3.18}$$

where $\alpha_F(x) = z_F^{1/2}(x)\partial z(x,\lambda)/\partial\lambda|_{\lambda=N-1/2}$.

Note that as x approaches a turning point corresponding to the Fermi energy, $\alpha_F(x) \to 2\hbar\omega_F z_F^{3/2}(x)/p_F^2(x)$. Thus, Eq. 3.18 reduces to Eq. 3.12 (minus the terms depending on $\lambda = -1/2$) in a neighborhood of each turning point. This is consistent with the assumption that there exists a region near the turning points where the potential may be linearized and where its properties become identical to those of the linear potential, a central requirement of this work. Further, use of the Airy function asymptotic expansions for large positive z_F recovers the Thomas-Fermi limit for the density at leading order (see Appendix I).

Leading Corrections to Dominant Term

Let $n_1(x)$ denote the sum of the components of the Poisson summation formula with $k \neq 0$. Then, using the integral representation of $Ai^2(-z)$ [71], $n_1(x)$ can be expressed as:

$$n_1 = 2\sum_{k=-\infty}^{\infty'}\int_{-1/2}^{N-1/2}\mathrm{d}\lambda\frac{\omega(\lambda)\sqrt{z(\lambda)}}{p(\lambda)}e^{2\pi ik\lambda}\int_{\mathcal{C}}\mathrm{d}t\frac{e^{\left(t^3/12+z(\lambda)t\right)}}{4i\pi^{3/2}\sqrt{t}}, \tag{3.19}$$

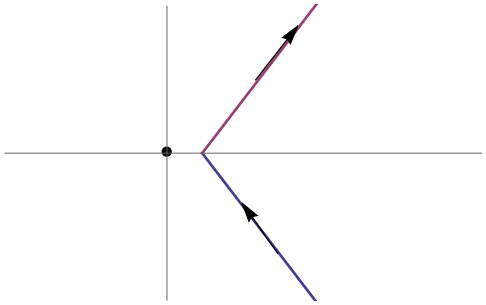

(c) The contour represents a closed curve starting at $\infty e^{-i\pi/3}$ and ending at $\infty e^{i\pi/3}$. The black dot represents a branch point at $t = 0$, and the branch cut is positioned at Re $t < 0$. For details, see Ref. [71].

where the primed summation implies that $k \neq 0$ and the contour $\mathcal{C}$ is given in Figure 3. To obtain approximate forms for the integrals in Eq. 3.19 a choice of perturbative method must be made. For that, we recourse to the following arguments. It is well-known that the semiclassical limit of the fermionic particle density is expressed in terms of quantities that depend only on the Fermi energy [22, 68, 70, 74]. Similarly, as consequence of the Darboux-Christoffel formula the fermionic ground-state harmonic oscillator particle and kinetic energy densities can be written exactly in terms of the lowest unoccupied orbital $\psi_N(x)$ [51], e.g.,

$$n^{\text{SHO}}(x; N) = \frac{1}{2}\left(\frac{\mathrm{d}\psi_N(x)}{\mathrm{d}x}\right)^2 + \frac{1}{2}p_F^2(x)\psi_N^2(x), \tag{3.20}$$

where units were chosen so $\hbar = m = \omega = 1$, single-occupation of the orbitals $\{\psi_0, ..., \psi_{N-1}\}$ was assumed, and for the harmonic oscillator $p_F(x) = \sqrt{2(N - 1/2x^2)}$. These motivate our assumption that the dominant contribution to each of the integrals in $n_1(x)$ originates from a small neighborhood of $\lambda = N - 1/2$ in the integration domain.

Define

$$F(\lambda) = 2\pi k\lambda - iz(\lambda)t, y(\lambda) = \alpha(\lambda)z^{-1/2}(\lambda), \tag{3.21}$$

so $\partial F/\partial\lambda = F'(\lambda) = 2\pi k - iy(\lambda)t$. Then, upon switching the integration order in Eq. 3.19

we obtain:

$$n_1 = 2 \sum_{k=-\infty}^{\infty'} \int_{\mathcal{C}} \mathrm{d}t \frac{e^{t^3/12}}{4i\pi^{3/2}\sqrt{t}} \int_{-1/2}^{N-1/2} \mathrm{d}F(\lambda) \frac{\omega(\lambda)\sqrt{z(\lambda)}}{p(\lambda)F'(\lambda)} e^{iF(\lambda)}. \tag{3.22}$$

From integration by parts we further find

$$n_1 = \frac{2\omega_F\sqrt{z_F}}{p_F} \sum_{k=-\infty}^{\infty'} (-1)^k \int_{\mathcal{C}} \mathrm{d}t \frac{\exp\left[(t^3/12 + z_F t)\right]}{4i\pi^{3/2}\sqrt{t}} \frac{1}{2\pi ik + z_F^{-1/2}\alpha_F t} + R_1. \tag{3.23}$$

The first term in the r.h.s of the above may give a useful approximation to $n_1(x)$ as long as the remainder R_1 is relatively small. In Appendix I, we show explicitly this is in fact the case at the semiclassical limit.

The factor $(2\pi ik + \alpha_F t/\sqrt{z_F})^{-1}$ may be expanded as a convergent power series in $t/(2\pi iky_F^{-1})$ within the disk $|t| < t_r = |2\pi ky_F^{-1}|$. While y_F can be made arbitrarily small (but different from zero) by the scaling defined in Section 2.2, no matter how large t_r is, the integration domain will contains regions where $|t| \geq t_r$. If term-by-term integration is performed, then the resulting series will be divergent. Similar phenomenon arises in the case of many asymptotic expansions, such as the exponential and the Stieltjes integral [14, 28]. The behavior of this class of asymptotic expansions is well-understood, see, e.g., [14, 28]. For instance, the accuracy of estimates based on the leading term increases as the radius of convergence of the associated geometric series is enlarged. In addition, approximations obtained by the inclusion of higher-order corrections become progressively more accurate, but only until one reaches the parameter-dependent optimal truncation point where the error made by the asymptotic expansion is minimal, and beyond which the pathological behavior of the series starts to show (the magnitude of higher-order approximations increases unboundedly).

For each value of k in Eq. 3.19, we are only interested in the lowest-order terms. Further, as previously mentioned, the radius of convergence of the geometric series expansion of $(2\pi ik + \alpha_F t/\sqrt{z_F})^{-1}$ is arbitrarily large in the semiclassical limit. Therefore, the pathological

effects of the singularity in the integrand of Eq. 3.23 emerge only at high-order corrections for which we have no use.

Thus, we expand $(2\pi ik + \alpha_F t/\sqrt{z_F})^{-1}$ as a geometric series in $t/(2\pi iky_F^{-1})$ and follow it by changing the order of summation and integration to encounter:

$$n_1 \sim 2\frac{\omega_F\sqrt{z_F}}{p_F}\sum_{j=0}^{\infty}\left(\alpha_F z_F^{-1/2}\right)^j \sum_{m=-\infty}^{\infty'}\frac{(-1)^m}{(2m\pi)^{j+1}}\int_{\mathcal{C}}\mathrm{d}t\frac{\exp\left(t^3/12+z_F t\right)}{-4\pi^{3/2}\sqrt{t}}(it)^j. \tag{3.24}$$

The expression above may be simplified by use of the identities:

$$\sum_{m=-\infty}^{\infty'}\frac{(-1)^m}{(2\pi m)^{j+1}} = \frac{(-1)^j 2(2^j-1)\zeta(j+1)}{\pi^{j+1}2^{2j+1}},\ \text{for } j \text{ odd, 0 otherwise,} \tag{3.25}$$

$$\frac{\partial^j}{\partial z_F^j}\int_{\mathcal{C}}\mathrm{d}t\frac{\exp\left(t^3/12+z_F t\right)}{4i\pi^{3/2}\sqrt{t}} = \frac{\partial^j}{\partial z_F^j}Ai^2[-z_F], \tag{3.26}$$

where $\zeta(p)$ is the Riemann zeta function [1]. It follows that:

$$n_1 \sim \frac{\omega_F\sqrt{z_F}}{p_F}\sum_{j=1}^{\infty}(-1)^j\ \left(\alpha_F z_F^{-1/2}\right)^{2j-1}\frac{(2^{2j-1}-1)\zeta(2j)}{\pi^{2j}4^{j-1}}\frac{\partial^{2j-1}}{\partial z_F^{2j-1}}Ai^2[-z_F]. \tag{3.27}$$

This expression could be further simplified by using the binomial expansion for multiple derivatives of a product and a recently discovered formula for the jth derivative of the Airy function (so-called Airy polynomial [20]). The end result is:

$$n_1 \sim \frac{\omega_F}{p_F}\sum_{q=0}^{2}\sum_{j=0}^{\infty}(-z_F)^{-3j-q}\,\xi_{3j+q}(\alpha_F)Ai^{(q+1)/\mathbb{Z}_3}[-z_F]Ai'^{(1-q)/\mathbb{Z}_3}[-z_F], \tag{3.28}$$

where for $u \in \mathbb{Z}, u/\mathbb{Z}_3 = u \bmod 3$, and each of the $\{\xi_j(\alpha_F)\}$ is a different power series in α_F,

e.g.:

$$\xi_0(\alpha) = \sum_{k=1}^{\infty} \frac{(-1)^{k-1} 2\left(2^{2k-1}-1\right) B_{2k}}{(2k)!} \alpha^{2k-1}, \tag{3.29}$$

$$\xi_1(\alpha) = \frac{7\alpha_F^3}{1440} + \frac{31\alpha_F^5}{17280} + \frac{127\alpha_F^7}{302400} + \frac{21127\alpha_F^9}{27371520} + \frac{32532971\alpha_F^{11}}{2615348736000} + ... \tag{3.30}$$

$$\xi_2(\alpha) = \frac{31\alpha_F^5}{24192} + \frac{127\alpha_F^7}{345600} + \frac{73\alpha_F^9}{1013760} + \frac{1414477\alpha_F^{11}}{11887948800} + ... \tag{3.31}$$

where B_{2k} identifies the $2k$th Bernoulli number. The power series $\xi_j(\alpha)$ seem to be related to periodic functions. For example,

$$\xi_0(\alpha) = \csc(\alpha) - \frac{1}{\alpha}. \tag{3.32}$$

This is an important feature of the leading term in the expansion given for $n_1(x)$. Recall that $\alpha_F(x)$ (restricted to $x_-(E_F) < x < x_m(E_F)$, or $x_m(E_F) < x < x_+(E_F)$) is the angle-variable canonically conjugate to the Fermi action corresponding to the periodic orbit at E_F. Therefore, unless its image is restricted, $\alpha_F(x)$ takes an infinite number of values which differ by $\pm 2\pi k, k \in \mathbb{Z}$. It is an interesting fact that in the approximation obtained for $n(x)$ by summing the leading terms of $n_0(x)$ and $n_1(x)$ such constraint is completely *unnecessary*. When the dominant term of Eq. 3.28 (that with $(q, j) = (0, 0)$) is added to Eq. 3.18, we obtain an approximation for $n(x)$ where $\alpha_F(x)$ only occurs as the argument of a periodic function, as expected. Thus the approximation obtained by combining $n_0(x)$ and the first correction coming from $n_1(x)$ is single-valued and well-defined everywhere. Since the first few terms of some of the $\xi_j(\alpha_F)$ also appear in series expansions of trigonometric functions

of α_F (around $\alpha_F = 0$), it is expected that the connection between the corrections of $n_0(x)$ and $n_1(x)$ remains at higher-orders.

If only the dominant term in Eq. 3.28 is retained (see Appendix I), then

$$n_1(x) \sim \frac{\omega_F}{p_F(x)} \xi_0(\alpha_F(x)) Ai[-z_F(x)] Ai'[-z_F(x)]. \tag{3.33}$$

The addition of the above to Eq. 3.18 generates the following semiclassical uniform approximation to the fermionic particle density:

$$n^{\mathrm{sc}}(x) = \frac{p_F(x)}{\hbar} \left[\left(\sqrt{z} \mathrm{Ai}^2(-z) + \frac{\mathrm{Ai}'^2(-z)}{\sqrt{z}} \right) + \left(\frac{\hbar\omega_F \csc[\alpha_F(x)]}{p_F^2(x)} - \frac{1}{2z^{3/2}} \right) \mathrm{Ai}(-z)\mathrm{Ai}'(-z) \right]_{z=z_F(x)}. \tag{3.34}$$

Discussion

Equation 3.34 expresses the quantum density of a fermionic system in one-dimension in terms of quantities evaluated along the complexified Lagrangian manifold defined by $H(x,p) = E_F$ where $H(x,p) = p^2/2m + v(x)$. It must be noted that while individual classical objects such as the action or momentum become purely imaginary in regions where tunneling happens, $n^{\mathrm{sc}}(x)$ remains a real positive semidefinite function for all $x \in \mathbb{R}$ as required for a probability measure. In addition, $n^{\mathrm{sc}}(x)$ is continuous everywhere. It also has continuous first derivative except at the matching point (defined in Section 2.3) $x_m(E_F)$. However, in the limit of large N, small $\hbar$,and fixed $N\hbar$,

$$\lim_{\epsilon \to 0} \left| \frac{\left. \frac{\mathrm{d}n^{\mathrm{sc}}(x)}{\mathrm{d}x} \right|_{x=x_m+\epsilon} - \left. \frac{\mathrm{d}n^{\mathrm{sc}}(x)}{\mathrm{d}x} \right|_{x=x_m-\epsilon}}{n(x_m)} \right| \sim \frac{\hbar\omega_F}{9N\hbar\sqrt{2[E_F - v(x_m)]}}. \tag{3.35}$$

Because ω_F and E_F only depend on N and $\hbar$ via the Fermi action $I_F = N\hbar$ the above indicates that in the semiclassical limit (see Appendix I) the discontinuity in the first derivative of the particle density at x_m is irrelevant.

Higher-order corrections to the semiclassical density can in principle be included by accounting for the contributions neglected to reach Eq. 3.34, e.g., the deviation of the Langer uniform approximation from the exact single-particle states of $\hat{H}$, the remainders of the various asymptotic approximations to integrals, etc. Nonetheless as will be shown in the next chapter, the result obtained above is already of high accuracy for a variety of potentials even when the number of occupied states is $O(1)$ (see also[91]).

Towards a physical interpretation of the various terms in $n^{\rm sc}(x)$, we recall the particle density can be expressed in terms of the propagator $\hat{K}(t) = e^{-i\hat{H}t/\hbar}$ in the configuration space representation, i.e.,

$$n(x, E_F) = \lim_{T\to\infty} \int_{-T}^{T} \frac{{\rm d}t}{t - i\gamma} e^{iE_F t/\hbar} K(x, x, t), \tag{3.36}$$

where time-reversal invariance guarantees the Green's function is well-defined for negative propagation times [55]. As we have shown in the section 2.1.2 the propagator $K(x, x, t)$ admits an interpretation in terms of an integral over the space of closed paths based on x [39]. In the semiclassical limit, $K(x, x, t)$ is expressed as a sum over amplitudes associated to topologically inequivalent closed classical orbits [45, 69]. These are classified by the Morse index μ. In the case of interest to the system discussed in this chapter μ is simply given by the number of times the velocity vector of a closed orbit with $x(0) = x(T) = x$ and energy E changed its sign [6]. As we have shown in section 2.2.2, the same interpretation can be ascribed to the different components of the Poisson summation formula (see also [12, 13]). By using the asymptotic forms of $Ai(-z)$ and $Ai'(-z)$ in the allowed regions for classical motion at E_F, it is therefore unsurprising that the leading terms terms of $n^{\rm sc}(x)$ are decomposed into the two expected classes: a dominant non-oscillatory density (Thomas-Fermi) arising from the first two terms of Eq. 3.34, corresponding to the direct $t \to 0$ orbit with $\mu = 0$, and an oscillatory correction obtained from the third term of Eq. 3.34 which stems from the closed classical orbits with Morse index different from zero (see Appendices I and II).

The uniform semiclassical approximation to the particle density simplifies in different regions of configuration space. *Classically-allowed:* For $z_F(x) >> 1$, the asymptotic form of the Airy function applies, leading to

$$n^{\rm sc}(x) \to \frac{p_F(x)}{\hbar\pi} - \frac{\omega_F \cos\left[2S_F(x)/\hbar\right]}{2\pi p_F(x)\sin\alpha_F(x)}, \tag{3.37}$$

(simplifying Eq. (3.36) of Ref. [57]; see also [63]). The dominant smooth term arises from the direct short-time classical orbit[11, 68]. The oscillatory contributions are generated by single- (in $n_0(x)$) and multiple- (in $n_1(x)$) reflections from each turning point [11, 63, 68, 93]. *Evanescent:* For x far outside the classically allowed region for the density, $-z_F(x) >> 1$, and

$$n^{\rm sc}(x) \to \left[\frac{p_F(x)}{3S_F(x)} - \frac{\omega_F}{p_F(x)\sin\alpha_F(x)}\right]\frac{e^{-2|S_F(x)|/\hbar}}{4\pi}, \tag{3.38}$$

generalizing the approximation of Ref. [57]. *Turning point:* At a Fermi energy turning point x_0, where $v'(x_0) \neq 0$, we recover the known leading term for the particle density

$$n^{\rm sc}(x_0) = c_0\hbar^{-2/3}|dv/dx|^{1/3}, \tag{3.39}$$

where $c_0 = (2/9)^{1/3}/\Gamma^2(1/3)$. As promised all of the limits which may be obtained from the previous literature are recovered by $n^{\rm sc}$.

3.2.2 Kinetic Energy Density

The kinetic energy density (KED) can be found by reasoning which is very similar to that for the particle density. We start with the finite Poisson summation formula representation for the KED defined in Eq. 3.3 with $m = 1$, singly-occupied orbitals and ψ_j replaced by

Langer wave functions $\phi(\lambda)$ (Eq. 2.23):

$$t = \frac{1}{2}\sum_{k=-\infty}^{\infty}\int_{-1/2}^{N-1/2} \mathrm{d}\lambda\; p^2(\lambda)|\phi(\lambda)|^2 e^{2\pi i k\lambda}. \tag{3.40}$$

The dominant component can be rewritten as another Riemann-Stieltjes integral,

$$t_0 = \frac{1}{\hbar}\int_{-1/2}^{N-1/2} \mathrm{d}p(\lambda) p^3(\lambda) f^{-1}(p) Ai^2\left[-p^2(\lambda)f^{-2}(p)\right]. \tag{3.41}$$

Assuming $f(p)$ is constant we again recover a result which is exact for a linear potential,

$$t_0^{(0)} = \frac{p^3(\lambda)}{6\hbar}\left(z^{1/2}(\lambda)Ai^2\left[-z(\lambda)\right] + z^{-1/2}(\lambda)Ai'^2[-z(\lambda)] + z^{-3/2}(\lambda)Ai[-z(\lambda)]Ai'[-z(\lambda)]\right)\Big|_{-1/2}^{N-1/2}. \tag{3.42}$$

Upon re-setting $N-1/2 \to \lambda$ in the above, following it by taking a partial derivative with respect to p (for fixed x, but varying λ as usual), integrating both sides from $-1/2$ to $N-1/2$, and then rearranging terms it is found that:

$$\begin{aligned} t_0 = \; & t_0^{(0)} + \frac{1}{2\hbar}\int_{-1/2}^{N-1/2} \mathrm{d}p(\lambda)\left\{\frac{p^4(\lambda)f'(p)}{f^2(p)}Ai^2\left[-\frac{p^2(\lambda)}{f^2(p)}\right] - \frac{p^2(\lambda)f'(p)}{2\hbar}Ai'^2\left[-\frac{p^2(\lambda)}{f^2(p)}\right]\right\} \\ & - \frac{1}{2\hbar}\int_{-1/2}^{N-1/2} \mathrm{d}p(\lambda) f^2(p) f'(p) Ai\left[\frac{-p^2(\lambda)}{f^2(p)}\right] Ai'\left[\frac{-p^2(\lambda)}{f^2(p)}\right]. \end{aligned} \tag{3.43}$$

Each of the remaining integrals can be evaluated perturbatively. In particular, we change variables from p to z so as to obtain for the first two:

$$\begin{aligned} & \frac{1}{2\hbar}\int_{-1/2}^{N-1/2} \mathrm{d}p(\lambda)\frac{p^4(\lambda)f'(p)}{f^2(p)}Ai^2\left[-\frac{p^2(\lambda)}{f^2(p)}\right] - \frac{1}{2\hbar}\int_{-1/2}^{N-1/2} \mathrm{d}p(\lambda)p^2(\lambda)f'(p)Ai'^2\left[-\frac{p^2(\lambda)}{f^2(p)}\right] \\ & = \frac{1}{2\hbar}\int_{-1/2}^{N-1/2} \mathrm{d}z(\lambda)\frac{\partial p(\lambda)}{\partial z(\lambda)}\frac{\partial f}{\partial p}p^2(\lambda)\left\{z(\lambda)Ai^2[-z(\lambda)] - Ai'^2[-z(\lambda)]\right\}. \end{aligned} \tag{3.44}$$

As noted before, under the scaling discussed in Appendices I and II, $\frac{\partial f}{\partial z}$ is small, so the

dominant term of the above can be obtained by integration by parts:

$$\frac{1}{2\hbar}\int_{-1/2}^{N-1/2} \mathrm{d}\left\{Ai[-z(\lambda)]Ai'[-z(\lambda)]\right\}\frac{\partial f}{\partial z}p^2(\lambda) = \frac{1}{2\hbar}\frac{\partial f}{\partial z}p^2(\lambda)Ai[-z(\lambda)]Ai'[-z(\lambda)]\Big|_{\lambda=-1/2}^{\lambda=N-1/2}$$
$$-\frac{1}{2\hbar}\int_{-1/2}^{N-1/2}\mathrm{d}z\left[\frac{\partial}{\partial z}\left(p^2(\lambda)\frac{\partial f}{\partial z}\right)\right]Ai[-z]Ai'[-z]. \tag{3.45}$$

By the arguments discussed in Appendix I the latter term in the above equation, the last of the integrals in Eq. 3.43 and all terms depending on $\lambda = -1/2$ can be neglected. Hence, the following provides the dominant component of the the defined kinetic energy density in the semiclassical limit:

$$t_0 = \frac{p_F^3\sqrt{z_F}}{6\hbar}\left[Ai^2\left[-z_F\right] + \frac{1}{z_F}Ai'^2[-z_F] + \left(\frac{3\hbar\omega_F}{p_F^2\alpha_F} - \frac{1}{2z_F^2}\right)Ai[-z_F]Ai'[-z_F]\right]. \tag{3.46}$$

The above may be rewritten in a way that makes manifest its relation to the dominant term in the semiclassical uniform approximation to the particle density given in eq. 3.18,

$$t_0(x) = \frac{p_F^2(x)}{6}n_0(x) + \frac{\omega_F p_F(x)}{3\alpha_F(x)}Ai[-z_F(x)]Ai'[-z_F(x)]. \tag{3.47}$$

The higher-order terms emerging from the $k \neq 0$ components of Eq. 3.40 are obtained by performing essentially the same calculation done for the analogous terms of $n(x)$,

$$t_1(x) \sim \frac{1}{2}\left[\omega_F p_F(x)\csc(\alpha_F(x)) - \frac{\omega_F p_F(x)}{\alpha_F(x)}\right]Ai[-z_F(x)]Ai'[-z_F(x)]. \tag{3.48}$$

In fact, the relationship between $n_1(x)$ and $t_1(x)$ is simple,

$$t_1(x) = \frac{p_F^2(x)}{2}n_1(x). \tag{3.49}$$

Our final expression for the kinetic energy density can thus be written as:

$$t^{\mathrm{sc}}(x) = \frac{p_F^2(x)}{6}n^{\mathrm{sc}}(x) + \frac{p_F(x)\omega_F}{3\mathrm{sin}\alpha_F(x)}Ai[-z_F(x)]Ai'[-z_F(x)]. \tag{3.50}$$

As a result of its simple relation to $n^{\rm sc}$ an analysis of neglected terms in the approximations made in this section would be identical to that in the previous. Further discussion of this point is given in Appendix II. In Ref. [91], the behavior of the semiclassical kinetic energy density was illustrated with a Morse potential including 21 bound states. Chapter 4 includes a variety of other numerical studies of the accuracy of $t^{\rm sc}(x)$.

Discussion

Equations 3.46, 3.49, and 3.50 indicate a strong similarity between the uniform approximations obtained for the particle and kinetic energy densities. This is unsurprising from the classical point of view, for a classical distribution of particles of unit mass $\rho_{\rm cl}(x,p)$ has kinetic energy density given by

$$t_{\rm cl}(x) = \frac{1}{2\pi\hbar}\int {\rm d}p \rho_{\rm cl}(x,p)\frac{p^2}{2}. \tag{3.51}$$

Thus, if the classical phase space distribution $\rho_{\rm cl}(x,p) = 2\theta[E_F - H(x,p)]$ is employed, then the Thomas-Fermi kinetic energy density given by $p_F^3/6\pi\hbar$ is obtained. Because the one-dimensional particle density is given in the classical limit by $n_{\rm TF}(x) = p_F(x)/\pi\hbar$, the Thomas-Fermi kinetic energy density can be rewritten as

$$t_{\rm TF}(x) = \frac{p_F^2(x)}{6} n_{\rm TF}(x). \tag{3.52}$$

This in turn explains the factor of 1/6 in Eq. 3.50 as a manifestation of the classical limit of the quantum mechanical kinetic energy density.

3.3 Conclusion

We presented detailed derivations of uniform semiclassical approximations to the noninteracting fermionic ground-state density and kinetic energy density in one-dimension. Open questions naturally emerge from our treatment. They may be classified into internal or external. The former corresponds to inquiries that can be discussed within the framework developed here, whereas the latter regard applications to different systems and further generalizations.

A simple internal question is whether there is a general relationship between the terms in the expansions for $n_0(x)$ and $n_1(x)$ which would allow the generation of higher-order terms in n_1 from those of n_0. For example, Eq. 3.18 contains the factor α_F^{-1} which is the leading term in the Laurent series of $\csc(\alpha_F)$ around the pole at $\alpha_F = 0$. The remaining terms of this series are obtained from n_1. Because α_F is an angle variable and $\csc(\alpha_F)$ is the simplest trigonometric function which has a simple pole at zero, n_1 could have been conjectured from n_0 without any of the extensive calculations done in Section 3.4. This is important because n_0 contains the Thomas-Fermi term which can be easily calculated for any noninteracting model, but n_1 is much less trivial as it includes non-perturbative effects due to an infinite number of topologically distinct closed orbits in a complexified phase space. Note that we do not comment here on the accuracy of our approximations for any given potential $v(x)$. In the semiclassical limit, as described by γ-scaling in the Appendices, the derivation here given guarantees that corrections to $n^{\mathrm{sc}}(x)$ vanish pointwise (though with different rates in distinct regions of $\mathbb{R}$), i.e, can be made arbitrarily small for sufficiently small γ. But for a fixed $v(x)$ and number of particles, we have not explored the difficult question of predicting, in general, the quantitative accuracy of the main results of this chapter.

The behavior of various expectation values for observables depending only on local operators is also worth further study. For instance, the energy of a noninteracting fermionic system

can be estimated with Eqs. 3.34 and 3.50 by adding the configuration space integral of $v(x)n^{\rm sc}(x)$ to that of $t^{\rm sc}(x)$. As shown in Ref. [91] (and in the next chapter), a pointwise comparison of $n^{\rm sc}(x)$ and $t^{\rm sc}(x)$ with the corresponding TF approximations indicates the uniform approximations include all of the quantum effects missed by Thomas-Fermi theory. On the other hand, the expectation values of configuration space observables $O(\hat{x})$ are obtained by taking the integral of $n(x)O(x)$ over all space. In some cases, e.g., the harmonic oscillator, this averaging perfectly cancels out errors in the Thomas-Fermi approximation, so that TF theory provides exact results. The effect would obviously be reduced for any system that cannot be reasonably approximated by a harmonic oscillator, but it implies further study of this issue is warranted. Such investigation is undertaken in chapter 4.

It would also be interesting to find alternative derivations of the uniform approximations given here. Semiclassical formulas can often be derived in more than one way, emphasizing distinct aspects of a result. For instance, Refs. [22, 33, 34] provide three distinct derivations of the semiclassical approximation to $n(x)$ with $E_F > v(x)\ \forall\ x \in [0,1], n(0) = n(1) = 0$. Another example is Berry and Tabor's derivation of the EBK density of states via the Poisson summation formula [12], followed shortly later by an alternative which employed the trace of a semiclassical action-angle variable propagator[13]. Each different methodology brings a new light to previously obtained results. In the case of this paper, it would be particularly beneficial to have an alternative systematic construction, since our derivation employed various identities exclusive to Airy functions, making it far from obvious how to extend the employed treatment to general systems in any finite number of dimensions.

The simplest extensions of the formalism developed here which would still be limited to cases where classical dynamics is trivial are: a) the study of radial Coulomb problems, b) the treatment of systems with multiple potential wells, e.g., a periodic potential or a simple double well, and c) the development of uniform approximations to the density matrix.

It is unclear if the obtained semiclassical uniform approximations can be systematically

amended to study radial Coulomb problems. For instance, the fast variation of the Coulomb potential near its center would forbid the use of the results given here. However, only the spherically symmetric s-states have substantial amplitude near the origin. Therefore, it could be that except for such (which in any case will likely require a uniform approximation not based on Airy functions [62]), our treatment remains valid.

Multiple potential wells in the weak coupling regime (high-energy barriers and/or large separations) would pose no challenge to the approximations here utilized, as to leading order in perturbation theory in the coupling constant each well can be treated independently and so the uniform approximations here presented would apply immediately as long as the Fermi energy is sufficiently below all local maxima of the potential energy function. However, it is also uncertain whether there exists simple extensions of the formalism here presented which would i) account for tunneling effects between regions separated by a barrier, and ii) provide a non-singular description of the behavior of the particle density as the Fermi energy crosses critical points of the external potential $v(x)$.

The one-particle density matrix can be employed to evaluate the exchange energy. Therefore, there exists large interest in the development of semiclassical approximations to the density matrix which contain the Thomas-Fermi limit and its dominant corrections. For instance, Elliott et al. [33] have recently demonstrated the low cost and high accuracy of exchange energies obtained from a semiclassical approximation to the density matrix. However, their result only applies to systems which satisfy Dirichlet boundary conditions and for which a particle with the Fermi energy would encounter no turning points in any of its possible classical histories. Hence, another possibility for future research is the application of the methods here used to obtain a uniform approximation to the density matrix. However, the introduction of another degree of freedom poses additional technical difficulties, as a new set of classical singularities is introduced to the problem and much less analytical results exist for integrals of products of Airy functions with different arguments.

3.4 Appendix I - Corrections to the Semiclassical Particle Density

In the derivations of $n_0(x)$ and $n_1(x)$, we neglected two types of terms: remainder integrals, such as the last term of Eq. 3.15, and integrated quantities evaluated at the minimum of the potential well $V_0 = E(-1/2)$, e.g., Eq. 3.16. In this appendix we show that under the scaling $\hbar \to \hbar\gamma, N_\gamma \to N/\gamma$, the aforementioned quantities become negligible relative to those included in Eq. 3.34 when γ is small.

Before doing so, let us recall two basic facts about our choice of scaling: i) because the limit where $\gamma \to 0$ implies $\hbar_\gamma = \gamma\hbar \to 0$, the local de Broglie wavelength associated to the Fermi energy, $|\lambda_{F\gamma}(x)| = \gamma\hbar/|p_{F\gamma}(x)|$ is almost vanishing outside a small neighborhood of $p_F^{-1}(0)$. This condition also characterizes the regions where the WKB approximation can be employed unrestrictedly [11, 23]; ii) as $\gamma \to 0$, the Fermi energy is preserved, but the spacing between energy eigenvalues of the original system is reduced to enforce the condition that N/γ states are occupied. This can be seen by examining the behavior of the scaled quantization condition for the Fermi action,

$$\frac{1}{2\pi\gamma\hbar}\oint p_{F,\gamma}(x)\mathrm{d}x = \frac{N}{\gamma}, \tag{3.53}$$

whence it is seen that $p_{F\gamma}(x) = p_F(x)$, and so $E_{F\gamma} = E_F$. The analysis that follows will shed more light on some of these points.

First, note that under γ-scaling, $z_F(x) \to z_{F\gamma}(x) = \gamma^{-2/3} z_F(x)$, so

$$n_{0\gamma} = \frac{p_F}{\hbar\gamma}\left[\gamma^{-1/3}\sqrt{z_F}Ai^2(-z_{F\gamma}) + \frac{\gamma^{1/3}}{\sqrt{z_F}}Ai'^2(-z_{F\gamma}) + \gamma\left(\frac{\hbar\omega_F}{p_F^2\alpha_F} - \frac{1}{2\sqrt{z_F}^3}\right)Ai(-z_{F\gamma})Ai'(-z_{F\gamma})\right]. \tag{3.54}$$

For any x different from a turning point, γ can be chosen small enough that the Airy function and its first derivative are arbitrarily close to the leading term of their asymptotic expansions. Hence, in the classically-allowed region we find,

$$n_{0\gamma} \sim \frac{p_F}{\gamma\hbar\pi} - \frac{\omega_F \cos(2S_F/\gamma\hbar)}{2\pi p_F \alpha_F} + O(\gamma) \ , z_F(x) > 0, \gamma \to 0. \tag{3.55}$$

The first term is the TF contribution, while the second is the leading, spatially-oscillating correction. Note that the oscillations become infinitely rapid in the limit. On the other hand, in the classically-forbidden region,

$$n_{0\gamma} \sim e^{-2|S_F|/\hbar\gamma} \left[\frac{\omega_F}{4\pi|p_F||\alpha_F|} - \frac{|p_F|}{6\pi|S_F|} + O(\gamma) \right], \ z_F(x) < 0, \gamma \to 0 \tag{3.56}$$

Here, no TF contribution ever arises, and every term vanishes exponentially with $1/\gamma$. Near a turning point of the Fermi energy the semiclassical particle density is given by:

$$n_{0\gamma} \sim \gamma^{-2/3} \frac{1}{\Gamma^2(1/3)} \left(\frac{2}{9\hbar^2} \left| \frac{\mathrm{d}v}{\mathrm{d}x}(x_0) \right| \right)^{1/3} + O(x - x_0), \ x - x_0 \to 0. \tag{3.57}$$

At this point we pause to note that the above considerations explicitly indicate that just as it occurs with other local observables, there exists no simple global expansion of the particle density in powers of $\hbar$. However, the local expansions shown above are all encapsulated by the basic result expressed in Eq. 3.54 which will thus be used to determine negligible terms as $\gamma \to 0$ without the necessity of examining the behavior of individual terms in each region with qualitatively different behavior for the particle density.

We can now look at the remainder integral in Eq. 3.15:

$$R_0 = \hbar^{-1} \int_{z_{-1/2}}^{z_F} \mathrm{d}z \frac{\partial^2 f}{\partial z^2} Ai[-z] Ai'[-z] = -\frac{1}{2\hbar} \left[\frac{\partial^2 f}{\partial z^2} \bigg|_{z_{-1/2}}^{z_F} Ai^2[-z_F] - \int_{z_{-1/2}}^{z_F} \mathrm{d}z \frac{\partial^3 f}{\partial z^3} Ai^2[-z] \right]. \tag{3.58}$$

Recalling that $z \in O\left(\hbar^{-2/3}\right)$, we find $R_{0\gamma}$ is $O\left(\gamma^{2/3} Ai^2[-z_{F,\gamma}]\right)$. Thus, as $\gamma \to 0$ it vanishes relative to the terms included in Eq. 3.54.

In deriving n_0 we also neglected

$$L(x) = \frac{1}{\hbar}\left[-p_\lambda \sqrt{z(\lambda)}\left(Ai^2[-z(\lambda)] + \frac{1}{z(\lambda)} Ai'^2[-z(\lambda)]\right) - \left.\frac{\partial f}{\partial z}\right|_{z(\lambda)} Ai[-z(\lambda)]Ai'[-z(\lambda)]\right]\Bigg|_{\lambda=-\frac{1}{2}+\delta} \tag{3.59}$$

where we added to $-1/2$ a small constant $\delta \to 0$, for the Langer approximation requires turning points to be simple zeros of the classical momentum. This is not the case when $\lambda = -1/2$. In fact, the classical region for the corresponding state is a point. Therefore, any contribution to $n_0(x)$ from this term is exponentially small and can be safely ignored.

Our final approximation for $n_1(x)$ (Eq. 3.33) transforms under γ scaling as:

$$n_{1\gamma}(x) = \frac{\omega_F}{p_F}\xi_0(\alpha_F) Ai[-\gamma^{-2/3} z_F(x)] Ai'[-\gamma^{-2/3} z_F(x)]. \tag{3.60}$$

As expected (based on the discussion in section 3.3) $n_{1\gamma}$ is $O\left(\gamma^0\right)$, i.e., of the same order in γ as the last two terms of Eq. 3.55. In the classically-allowed region for a particle at the Fermi energy,

$$n_{1\gamma} \sim -\frac{\omega_F \xi_0(\alpha_F)}{2\pi p_F}\cos(2S_F/\gamma\hbar) + O(\gamma)\ , z_F(x) > 0, \gamma \to 0. \tag{3.61}$$

Hence, the leading correction to the Thomas-Fermi term in Eq. 3.55 is of the same order as the dominant term of $n_1(x)$. Similarly, in the forbidden region for the Fermi energy,

$$n_{1\gamma} \sim \frac{\omega_F e^{-2|S_F|/\gamma\hbar}}{4\pi|p_F|}\left(\mathrm{csch}(|\alpha_F|) - |\alpha_F|^{-1}\right) + O(\gamma),\ z_F(x) < 0, \gamma \to 0, \tag{3.62}$$

while near a Fermi energy turning point,

$$n_{1\gamma} \sim \left[\frac{1}{\Gamma(1/3)\Gamma(2/3)}\right]\left(\frac{\omega_F^2}{6}+\frac{2v''(x_0)}{15}\right)\left[\frac{\mathrm{d}v}{\mathrm{d}x}(x_0)\right]^{-1}+O(x-x_0),\ x-x_0\to 0. \quad (3.63)$$

We also neglected two types of terms in the derivation of $n_1(x)$. The first is

$$R_1(x) = -2\sum_{k=-\infty}^{\infty'}\int_{\mathcal{C}}\mathrm{d}t\frac{e^{t^3/12}}{4i\pi^{3/2}\sqrt{t}}\int_{-1/2}^{N-1/2}\mathrm{d}F(\lambda)\frac{e^{iF(\lambda)}}{iF(\lambda)}\frac{\partial}{\partial\lambda}\frac{\omega(\lambda)\sqrt{z(\lambda)}}{p(\lambda)F'(\lambda)}, \quad (3.64)$$

while the second consists of

$$\begin{aligned} R_2(x) \sim\ & \frac{\omega_F}{p_F}\sum_{p=0}^{2}\sum_{j=1}^{\infty}(-z_F)^{-3j-p}\,\xi_{3j+p}(\alpha_F)Ai^{(1+p)/\mathbb{Z}_3}[-z_F]Ai'^{(1-p)/\mathbb{Z}_3}[-z_F]+ \\ & \frac{\omega_F}{p_F}\sum_{p=1}^{2}(-z_F)^{-p}\,\xi_p(\alpha_F)Ai^{(1+p)/\mathbb{Z}_3}[-z_F]Ai'^{(1-p)/\mathbb{Z}_3}[-z_F]. \end{aligned} \quad (3.65)$$

That $R_2(x)$ is of a higher order than Eq. 3.33 is easy to see because $z_{F\gamma}$ is $\mathrm{O}(\gamma^{-2/3})$ and $\alpha_{F\gamma}=\alpha_F$. Thus, all terms in Eq. 3.65 are relatively small compared to those in $n_1(x)$ as $\gamma\to 0$.

In the case of $R_1(x)$ the next-order term in integration by parts will contain factors of $1/F_\lambda'^2$ and $1/F_\lambda'^3$. This will yield various power series in x if the argument on section 3.3 is followed. Each contains terms in γ that vanish relative to $n_1(x)$.

3.5 Appendix II - Higher-order Terms and Limiting Behaviors of the Semiclassical Kinetic Energy Density

From the equations defining our approximations to t_0 (Eq. 3.46) and t_1 (Eq. 3.49), it is clear that except for the introduction of p_F^2 and rational factors, the expressions for the uniform approximation to the kinetic energy density share the same structure of those corresponding to n_0 and n_1, respectively. Therefore, the considerations given in the previous Appendix can be applied almost verbatim to explain the smallness of the terms neglected in the derivation of $t^{\rm sc}$. In this appendix, we apply, for the sake of completeness, γ-scaling to Eq. 3.50 in the regions where the kinetic energy density behaves qualitatively different. This will provide further insight into the distinguishing features of the semiclassical approximations to the particle and kinetic energy densities.

In the classically-allowed part of the configuration space of a particle with the Fermi energy, the kinetic energy density behaves asymptotically as:

$$t_\gamma \sim \frac{p_F^3}{6\gamma\hbar\pi} - \frac{\omega_F p_F \cos(2S_F/\gamma\hbar)}{4\pi\sin(\alpha_F)} \ , \gamma \to 0, \ z_F(x) > 0, \tag{3.66}$$

whereas in the evanescent and transition regions,

$$t_\gamma \sim \left(\frac{2|p_F|^3}{3|S_F|} - \frac{3\omega_F|p_F|}{\sinh|\alpha_F|}\right)\frac{e^{-2|S_F|/\gamma\hbar}}{24\pi}, \gamma \to 0, \ z_F(x) < 0, \tag{3.67}$$

$$t_\gamma \sim -\frac{|dv/dx|}{9\Gamma(2/3)\Gamma(1/3)} + O(x - x_0), \ x - x_0 \to 0. \tag{3.68}$$

In comparison to Eq. 23 of ref. [91], Eq. 3.67 contains an extra factor of 2 multiplying $|p_F|^3$.

The former has a typo.

The above equations illustrate for one last time: i) the relative dominance of the Thomas-Fermi term $p_F^3/6\pi\hbar$ in comparison to all others as $\gamma \to 0$, ii) the exponential smallness of contributions to the kinetic energy coming from regions where the Fermi energy classical motion is forbidden, and iii) the absence of a global power series expansion in any single variable which is valid for all of configuration space.

Chapter 4

Numerical and Analytical Studies of Corrections to Thomas-Fermi

4.1 Introduction

It is the aim of this chapter to investigate the properties of the approximations derived in the previous in a variety of situations of relevance to atomic systems. We employ the uniform semiclassical approximations to obtain universal corrections to 1D Thomas-Fermi kinetic and potential energies in regions of configuration space where the behavior of a system is qualitatively different. We also establish a general result on the depletion of the particle density in a classically-allowed region due to tunneling. Comparisons between semiclassical and exact numerical data illustrate our results.

4.2 Notation

In this chapter we will employ the main results of Chapter 3 (eqs. 3.34 and 3.50) to obtain information on energetic contributions emanating from different configuration space regions. To make mathematical expressions simpler we introduce definitions which are only employed in this chapter. For instance, the following provides a simple notation for products involving Airy functions and/or their derivatives,

$$a(z) = Ai(-z), \quad A_0 = -aa', \quad A_1 = a^2, \quad A_2 = a'^2, \quad a_0 = a(0) = \frac{3^{-2/3}}{\Gamma(2/3)}. \tag{4.1}$$

Next we combine different products of Airy functions which appear repeatedly in this work:

$$K_0(z) = \pi \left[z^{1/2} A_1(z) + z^{-1/2} A_2(z) \right], \quad K_1(z) = \pi A_0(z), \quad K_2(z) = K_0(z) - \frac{K_1(z)}{2z^{3/2}}. \tag{4.2}$$

Asymptotic expansions and integrals of the above expressions which will be useful later are summarized in Appendix I.

In the notation just given the semiclassical particle density can be written in a simple form:

$$n^{\rm sc}(x) = f[p_F(x), \tilde{p}_F(x), S_F(x)], \text{ with } \tilde{p}_F(x) = \frac{\omega_F}{p_F(x) \sin\alpha_F(x)}, \tag{4.3}$$

and

$$f(p, \tilde{p}, S) = \frac{p}{\pi} K_2[z(S)] + \frac{\tilde{p}}{\pi} K_1[z(S)]. \tag{4.4}$$

We also recall that $z(S) = [3S/2]^{2/3}$, and $S(x) = \int_{x_0}^{x} p(x')\mathrm{d}x'$. Similarly, for the semiclassical

kinetic energy density it follows that:

$$t^{\rm sc}(x) = h[p_F(x), \tilde{p}_F(x), S_F(x)], \quad h(p, \tilde{p}, S) = \frac{p^2}{6}\left[\frac{p}{\pi}K_2(S) + \frac{2\tilde{p}}{\pi}K_1(S)\right]. \tag{4.5}$$

4.3 Methods

We consider hamiltonians of the conventional type

$$\hat{h} = -\frac{1}{2}\nabla^2 + v(x), x \in \mathbb{R}. \tag{4.6}$$

with smooth potential energy functions $v(x)$ which either vanish or diverge positively at large $|x|$. In the former case, we require the existence at least one bound state for the employed methods to be valid. As in previous instances, here we will study the ground-state of N noninteracting fermions at 0K. Particle and kinetic energy densities are defined as in chapter 3. In situations where the semiclassical scaling is relevant it is explicitly shown. Otherwise, not. We employ units where $\hbar = m = 1$.

4.3.1 Numerical

One of the great features of the uniform semiclassical approximations for the particle and kinetic energy densities derived in the previous chapter is that they allow us to evaluate these quantities for a given $x \in \mathbb{R}$ with minimal effort irrespective of the number of fermions which live in the system. This is quite to the contrary of the general procedure of numerically solving the Schrodinger equation for systems with a large number of particles, which involves finding eigenvectors of large matrices for which the cost scales asymptotically as M^3 (where M is the dimension of the Hilbert space). Below we describe the numerical methods employed in the computations we performed to compare semiclassical and Thomas-Fermi theory with

exact results.

Accurate numerical solutions for the Schrodinger equation were extracted with the Matrix Numerov method [84] whenever the studied potential gave rise to a Schrodinger equation which we could not solve analytically. A grid spacing of 10^{-3} was chosen and the size L of the system depended on the external potential and the Fermi energy. This choice of parameters was guided by the requirement that kinetic and total energies were converged (relative to a reduction in grid spacing and enlargement of L) up to the 4th decimal digit. In every case we checked that both the exact particle and kinetic energy densities were at least of $O(10^{-5})$ when $x = \pm L$.

4.3.2 Analytical

Several potentials are employed to illustrate our results. Some of these have analytical solutions for any choice of γ (as defined in the previous section), e.g., the harmonic $x^2/2$ [59] and Morse oscillators $D_e[1 - \exp(-ar)]^2$ [79]. Therefore, these are the most amenable for testing the behavior of semiclassical quantities as $\gamma \to 0$ (and $N \to \infty$). The Poschl-Teller potential $-v_0/\cosh^2 x$ with $v_0 \in \mathbb{R}^+$ also has analytic solutions, but only when $v_0 = \lambda(\lambda+1)/2, \lambda \in \mathbb{N}$ [85]. An external potential we studied for which the associated Schrodinger equation has no analytical solution is the quartic $v(x) = x^4$. All listed potentials are infinitely differentiable and, except for the Morse, symmetric around $x = 0$.

We always choose $N = 1$ as our original system, and take $\gamma \to 0$. In all cases, a larger initial value of N makes convergence more rapid toward the semiclassical limit (except for the $v(x)$ which go to zero at infinity, in which case when N is large enough we expect the semiclassical approximation to be less accurate - see below). In Fig. 4.1 we show the external potentials studied in this chapter.

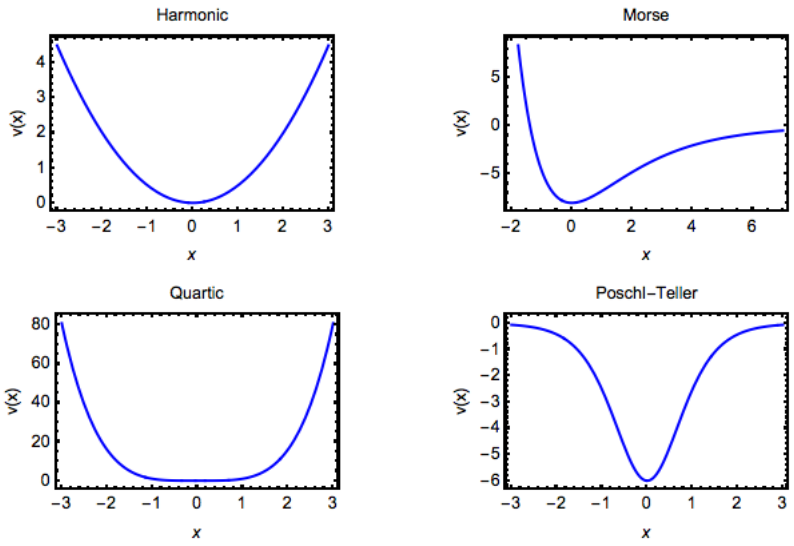

Figure 4.1: External potentials employed for the quantitative analysis of the uniform semiclassical approximations

Thomas-Fermi energies must be calculated numerically whenever the WKB quantization condition cannot be solved analytically for the semiclassical spectrum. However, in case the latter condition is satisfied, Thomas-Fermi kinetic and potential energies can be obtained without much effort, i.e., without the need to perform complicated integrations over configuration space. This is the case for all of the external potentials we study here. Appendix II provides the applied method.

4.4 Dominant Corrections to the Classical Limit

4.4.1 General Considerations

We start the analysis of leading corrections to TF theory by demonstrating in what way the predictions of quantum mechanics approach those of its classical limit as $\gamma\hbar \to 0^+$ and $N/\gamma \to \infty$. Figure 4.2 illustrates the behavior of particle densities as $\gamma \to 0^+$. In particular, we show exact densities for the harmonic well with $N = 1$ and $\gamma = 1, 1/4$ and $1/16$. In

each case where $\gamma \neq 1$ we multiply the density by γ so all of them are on the same scale. We also show the Thomas-Fermi density. We see the exact particle density approaches the TF only in a *weak* or distributional sense as γ goes to zero(see e.g., [22, 40]). This simply means that any expectation value obtained with Thomas-Fermi theory will agree with that obtained with the quantum theory in the limit where $\gamma \to 0^+$. Note that, pointwise, the TF density does not everywhere have relative error approaching zero. For example, in the evanescent region, the TF density is identically zero, leading to 100% error relative to the exact density.

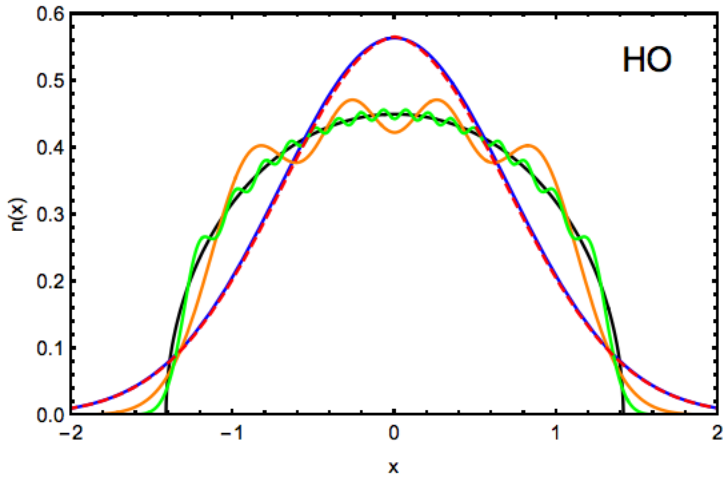

Figure 4.2: Harmonic oscillator particle densities with $N = 1$, for $\gamma = 1$ (blue), 1/4 (orange), 1/16 (green); $n^{\mathrm{TF}}(x)$ (black) and $n^{\mathrm{sc}}(x)$ (dashed, red)

Figure 4.2 also gives the semiclassical particle density for $N = \gamma = 1$. We only show its behavior for $\gamma = 1$, as, for all other values of γ the semiclassical is everywhere indistinguishable from the exact curve. In order to emphasize this fact, we plot in Fig. 4.3 the ratio of semiclassical and exact particle densities for different values of γ. It clearly approaches 1 everywhere, thus showing its relative error vanishes for sufficiently small γ, for all values of x. This shows that indeed the semiclassical particle density is a *uniform* asymptotic approximation and suffers none of the difficulties of previous works [57, 63, 93], despite the qualitatively different behavior of spatially-varying properties in the traveling, transition and evanescent regions.

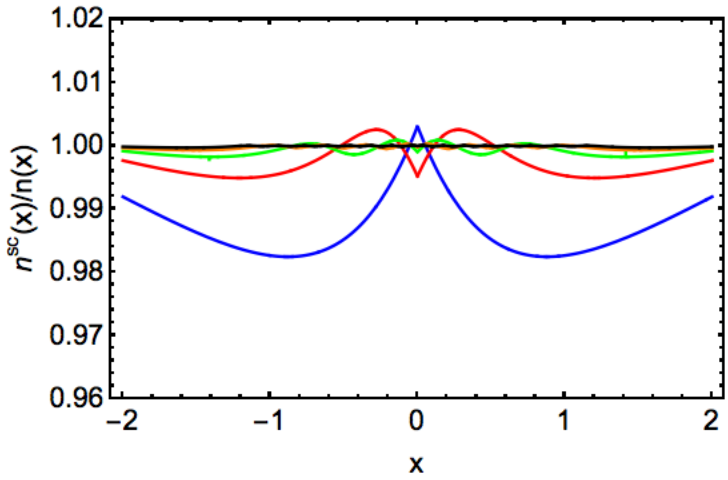

Figure 4.3: $n^{\text{sc}}(x)/n(x)$ for the harmonic oscillator with $\gamma = 1, 1/2, 1/4, 1/8, 1/16$ (blue, red, green, orange, black, respectively)

4.4.2 Pointwise Analysis

Figures 4.2 and 4.3 demonstrate the greater pointwise accuracy of semiclassical approximations relative to that of Thomas-Fermi theory. In this section we perform a quantitative analysis of this point.

We begin our discussion with the harmonic well. Consider again a single particle in the unit frequency harmonic oscillator. We use the density-error measure introduced in [91], which is:

$$\eta = \frac{1}{N}\int_{-\infty}^{\infty} \mathrm{d}x |n^{\text{sc}} - n(x)|. \tag{4.7}$$

Table 4.1 shows the pointwise error as a function of γ for both the particle and the kinetic energy densities (which we denote by η_T). Even for $\gamma = 1$, the error is far smaller than TF, and vanishes much more rapidly with decreasing γ, a result that we expected based on the qualitative discussion of the prior subsection.

Another beautiful illustration of the pointwise accuracy of the semiclassical results is seen by considering the particle and kinetic energy densities at the classical turning points of a

Table 4.1: Semiclassical (η, η_T) and TF (η^{TF}, η_T^{TF}) pointwise errors for the particle and kinetic energy densities

γ	η	η^{TF}	η_T	η_T^{TF}
1	0.0118	0.6183	0.0321	0.1685
1/2	0.0026	0.5982	0.0080	0.0898
1/3	0.0015	0.5905	0.0037	0.0615
1/4	0.0007	0.5864	0.0020	0.0469
1/5	0.0005	0.5839	0.0013	0.0379

phase space Fermi energy orbit. The explicit formulas are [57, 90, 91]

$$n_{TP}^{\gamma} \to \frac{c_0}{l_F}\gamma^{-2/3} - \frac{b_F}{2l_F\sqrt{3}\pi}, \quad t_{TP}^{\gamma} \to -\frac{l_F^{-3}}{12\sqrt{3}\pi}\gamma^{2/3}, \tag{4.8}$$

where

$$c_0 = (2/9)^{1/3}/\Gamma^2(1/3), \tag{4.9}$$

$$l_F = (2F)^{-1/3}, \; F = |v_F'|(x_{TP}), \text{ and } b_F = \left|\frac{l_F^4}{3}\left[\omega_F^2 + \frac{4v_F''}{5}\right](x_{TP})\right|. \tag{4.10}$$

In Fig. 4.4, we plot $\gamma^{2/3} l_F n_{TP}^{\gamma}/c_0$ and $(t^{\rm sc}/t)(x_{TP})$ for the harmonic and Morse potentials (with $N = 1$). These show that as $\gamma \to 0$ the turning point particle and kinetic energy densities rapidly approach the limits given by eqs. 4.8 and 4.10 irrespective of the external potential. Thus, the universality of the small γ limit is demonstrated. Corresponding TF quantities are identically zero. Table I shows the high accuracy of the semiclassical uniform

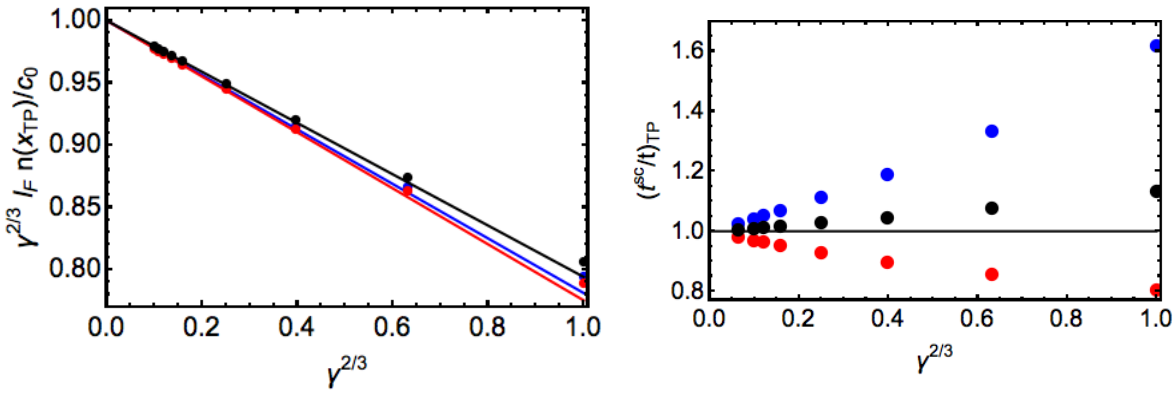

Figure 4.4: Left: $\gamma^{2/3} l_F n^{\gamma}(x_{TP})/c_0$ vs $\gamma^{2/3}$ for harmonic oscillator (black) and left (blue) and right (red) turning points of the Morse potential (all with $N = 1$). Continuous lines represent the semiclassical behavior as $\gamma \to 0$ given by eq 4.8. Right: $t^{sc}/t|_{TP}$ vs $\gamma^{2/3}$ for harmonic oscillator (black) and left (blue) and right (red) turning points of the Morse potential (all with $N = 1$). The continuous line represents the semiclassical behavior as $\gamma \to 0$ given by eq. 4.10

approximation for the case of the quartic potential.

Table 4.2: Error in quartic potential semiclassical turning point densities as a function of γ ($N = 1$).

γ	$n^{sc}/n(x) - 1$
1	-3.8×10^{-3}
1/2	-9.5×10^{-3}
1/4	-3.5×10^{-3}
1/8	-1.4×10^{-3}
1/16	-5.4×10^{-4}
1/32	-2.1×10^{-4}

4.4.3 Regional Particle Number and Energies

The previous subsection demonstrated the far greater accuracy of the semiclassical uniform approximations relative to Thomas-Fermi theory when absolute pointwise errors are employed as a comparison norm. In this section we employ the uniform semiclassical approximations to obtain dominant corrections to Thomas-Fermi observables emanating from the classically-forbidden and allowed regions (as determined by the Fermi energy). For example, we will analytically determine the depletion in particle number in the classically-allowed

region, i.e., the tunneling effect on the particle density in the semiclassical limit.

We will justify a variety of upcoming arguments with semiclassical scaling, so we recall that according to the discussion of section 2.1, the semiclassical limit is obtained when $\gamma \to 0^+$. This implies the particle number $N_\gamma = N/\gamma \to \infty$ while $\hbar_\gamma = \gamma\hbar \to 0$. Because the Fermi energy is invariant under these transformations (see Eq. 3.6), any other classical property which depends strictly only on the phase space orbit defined by the Fermi energy ϵ_F also remains constant (e.g., the classical frequency at ϵ_F, etc.)

Let $f(x)$ denote either $n(x)$, $v(x)n(x)$ or $t(x)$. Then, we define the contributions from different configuration space regions to the expectation value of the particle number N, and total potential and kinetic energies V and T by,

$$f^L_{\text{allow}} = \int_{x_L}^{x_m} \mathrm{d}x f(x), \quad f^R_{\text{allow}} = \int_{x_m}^{x_R} \mathrm{d}x f(x), \tag{4.11}$$

$$f^L_{\text{forbid}} = \int_{-\infty}^{x_L} \mathrm{d}x f(x), \quad f^R_{\text{forbid}} = \int_{x_R}^{\infty} \mathrm{d}x f(x), \tag{4.12}$$

where L/R denotes left and right Fermi energy turning points and x_m is the Fermi mid-phase point defined in section 2.3. Thus, it follows the expectation value of N, T or V can be obtained with

$$\int_{-\infty}^{\infty} \mathrm{d}x f(x) = \sum_{S=L,R} \left(f^S_{\text{allow}} + f^S_{\text{forbid}} \right). \tag{4.13}$$

The above definitions allows us to discriminate average behavior of a system in different regions and will prove useful in determining leading corrections to Thomas-Fermi.

Our strategy to analytically find the corrections to TF for observables in different spatial regions relies on the following observations: corrections to TF particle density in the bulk of the classically-allowed region (where $z_F >> 0$) are oscillations of frequency $O(1/\gamma)$ and amplitude $O(\gamma^0)$ (see eq 3.37) while deep into the region which is classically-unaccessible for a particle at the Fermi energy corrections to TF are exponentially small (see eq. 3.38). These suggest that if there are corrections to TF of $\mathrm{O}(\gamma^\alpha)$, with $\alpha < 1$ (recall that TF energies scale as $1/\gamma$, so the next-order term is expected to be $\mathrm{O}(\gamma^0)$), they can only be due to a small neighborhood of the turning point (at which $z_F \to 0$), where the behavior of the particle and kinetic energy densities are qualitatively different relative to the prior mentioned regions (see e.g., eq. 3.39). In particular, near turning points, classical quantities evaluated at the Fermi level such as $z_F(x)$ and $p_F(x)$ are simply related so that the semiclassical approximations become even simpler. This can be seen by noting that in the neighborhood of a turning point x_{TP} for a particle with the Fermi energy ϵ_F, we may write

$$v(x) = v(x_{TP}) + (x - x_{TP})v'_F(x_{TP}) + (x - x_{TP})^2 \frac{v''_F}{2} + ... \tag{4.14}$$

Defining,

$$y = (x - x_{TP})/l_F, \tag{4.15}$$

it then follows that,

$$p_F \to \sqrt{y}\left[1 - g_F y + O(y^2)\right],\ g_F = \frac{1}{2} l_F^4 v_F'', \tag{4.16}$$

$$S_F = \frac{2}{3} y^{3/2}\left[1 - \frac{3 g_F y}{5} + O(y^2)\right],\quad z_F = y\left[1 - \frac{2 g_F y}{5} + O(y^2)\right], \tag{4.17}$$

$$\tau_F / l_F = 2(l_F y)^{1/2}\left[1 + \frac{g_F y}{3} + O(y^2)\right]. \tag{4.18}$$

This yields a semiclassical approximation to the particle density valid only in a small neighborhood around turning points,

$$n^{\mathrm{sc,TP}} \sim \frac{1}{l_F \pi}\left[\sqrt{z_F} K_0\left(z_F\right) + b_F K_1(z_F)\right]. \tag{4.19}$$

There are some interesting aspects to this formula. First, it agrees with that of a 1D Airy gas [56]. Second, we see that the coefficient b_F contains the second-derivative of the potential at the turning point. Thus it vanishes if the Fermi energy is at a point of inflection of the potential, and either adds to or subtracts from the linear contribution to b_F depending on which side of that point x is located at. A similar approximation may be derived for the kinetic energy density near one of the Fermi energy turning points.

From Eq. 4.19 (and its analogous for the kinetic energy density) the dominant corrections to TF energies will be derived in the classically-allowed and forbidden regions below. Numerical confirmation will be presented by comparing analytical results to the exact for the cases of the Morse and harmonic potentials.

Tunneling Effect on Particle Number

We start with some considerations on the number of particles in a given region. In the classical limit it is obvious that all particles are located only in regions which are classically-allowed, so TF predicts $N_{\text{forbid}} = 0$ in any circumstance. To obtain the correction to the classical behavior according to the uniform semiclassical approximation, define

$$\Delta N_{\text{allow}} = \sum_{S=L/R} \int_{x_S}^{x_m} dx \Delta n(x), \tag{4.20}$$

where x_L and x_R denote the left and right-hand-side turning points as usual. Inserting the semiclassical particle density given in eq. 4.19 and using the relationship

$$pdx = \sqrt{z}dz, \tag{4.21}$$

which is valid everywhere in the classically-allowed region, we find ultimately:

$$\Delta N_{\text{allow}}^{sc,TP\gamma} \rightarrow \Delta N_0 + \sum_{S=L/R} b_F^S a_0^2 \gamma^{2/3} + ..., \tag{4.22}$$

where

$$\Delta N_0 = -\frac{1}{3\sqrt{3}\pi}. \tag{4.23}$$

Applying the same reasoning to the region that is not accessible classically we find

$$\Delta N_{\text{forbid}}^{sc,TP\gamma} \to -\Delta N_{\text{allow}}^{sc,TP\gamma}, \tag{4.24}$$

i.e., term-by-term in the γ-expansion, the change in the particle number in the evanescent region precisely cancels that of the allowed region. This is an explicit demonstration that the semiclassical density, which is *not* exactly normalized in general, *is* normalized to this order in the γ expansion.

Additionally, since the TF density is entirely within the allowed region, we find that to leading order, approximately 0.03 electrons leak out beyond each turning point into the evanescent region. This is a universal result for all 1D potentials. It is illustrated in Fig. 4.5.

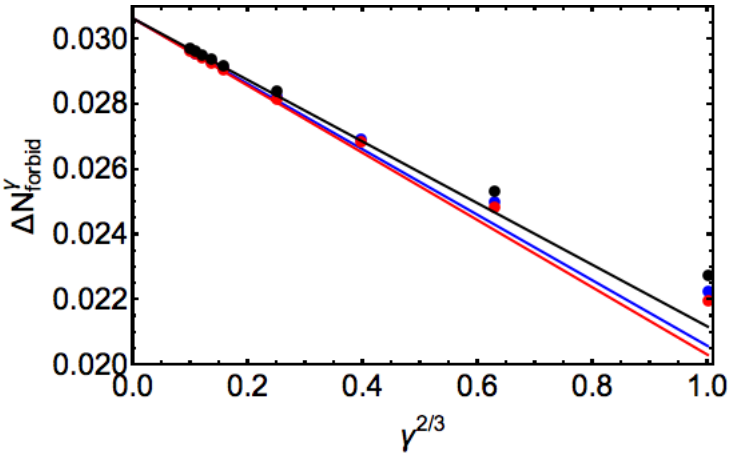

Figure 4.5: Average particle number in left or right classically-forbidden regions for the harmonic oscillator (black) and left (blue) and right (red) turning points of the Morse potential (all with $N = 1$); the straight lines correspond to the predictions implied by Eq. 4.24 decomposed into contributions from the classically-forbidden regions beside each turning point

Leading Corrections to the Thomas-Fermi Potential and Kinetic Energies

The next simplest observable we can address is the total potential energy. A similar analysis yields:

$$\Delta V_{\text{allowed}}^{sc,TP\gamma} \to -\epsilon_F \Delta N_0 + \sum_{S=L/R} a_0^2 \epsilon_F \left[b_F^S - \frac{1}{\left(10 l_F^S\right)^2 \epsilon_F} \right] \gamma^{2/3} + ... \tag{4.25}$$

The first term is universal, again showing dependence only on the semiclassical Fermi energy, determined by Eq. 3.6. In fact, we may write this as $-\epsilon_F \Delta N_{\text{allowed}}$, i.e., it is as if the fraction of a particle that spills out of the allowed region has potential energy equal to the Fermi energy.

But, just as before, we find the corrections in the classically-allowed region exactly cancels that of the forbidden, leaving zero contribution to the total potential energy. This is true for both the the contribution which is independent of γ and for the $\mathrm{O}(\gamma^{2/3})$ coefficient. Figure 4.6 illustrates how the behavior implied by Eq. 4.25 is approached in the case of the Morse and harmonic potentials.

Finally, we repeat the calculation for the kinetic energy, finding

$$\Delta T_{\text{allowed}}^{TP\gamma} \to \sum_{S=L/R} \frac{a_0^2}{5\left(l_F^S\right) 2} \gamma^{2/3} + ... \tag{4.26}$$

In figure 4.7 we illustrate the emergence this universal limit as $\gamma \to 0$ (in the evanescent region) for the Morse and harmonic oscillators. Here again, the leading correction to TF in the classically-allowed region is cancelled by that of the classically-forbidden.

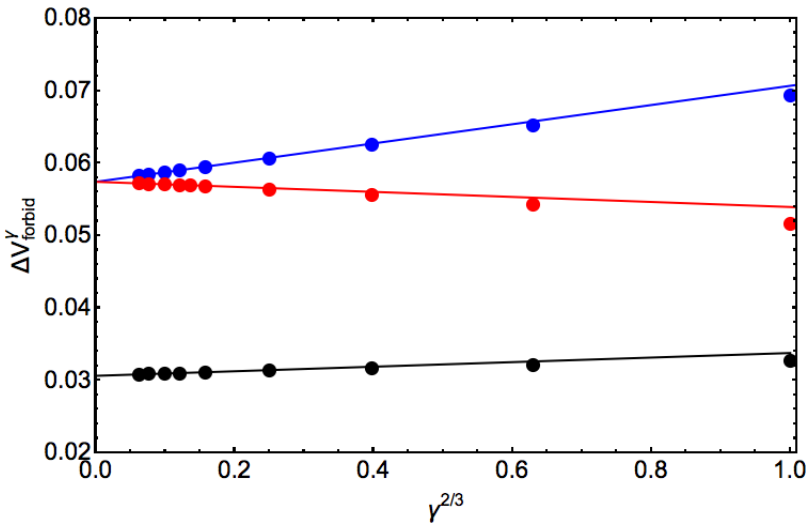

Figure 4.6: Average potential energy in the left or right classically-forbidden regions for the harmonic oscillator (black) and Morse potentials (for which left evanescent region results are given in blue and right are in red) with $N = 1$; straight lines correspond to the predictions implied by the appropriate decomposition of minus Eq. 4.25 into contributions due to each each turning point

4.5 Global Analysis of Energies

In this section we explore the accuracy of semiclassical total potential and kinetic energies for the harmonic, Morse and quartic oscillators.

Figure 4.8 illustrates the results for the harmonic well. As priorly mentioned, Thomas-Fermi kinetic and potential energies match the exact for this system, so the performance of the semiclassical approximation is necessarily worse relative to TF. Figure 4.8 includes straight lines which indicate a small error of $O(\gamma)$ in the expectation values predicted by the uniform semiclassical approximations. This is pertinent because Thomas-Fermi energies scale as $1/\gamma$. Thus, leading corrections are expected to be $O(\gamma^0)$, but they vanish (see discussion of previous section). Because the semiclassical approximation only guarantees that the leading correction to TF is given exactly, its error is necessarily $O(\gamma^\alpha)$ with $\alpha > 0$. This is consistent with the observations of the previous subsection: the leading energetic corrections to TF from the classically-allowed and forbidden regions are either $O\left(\gamma^{2/3}\right)$ or

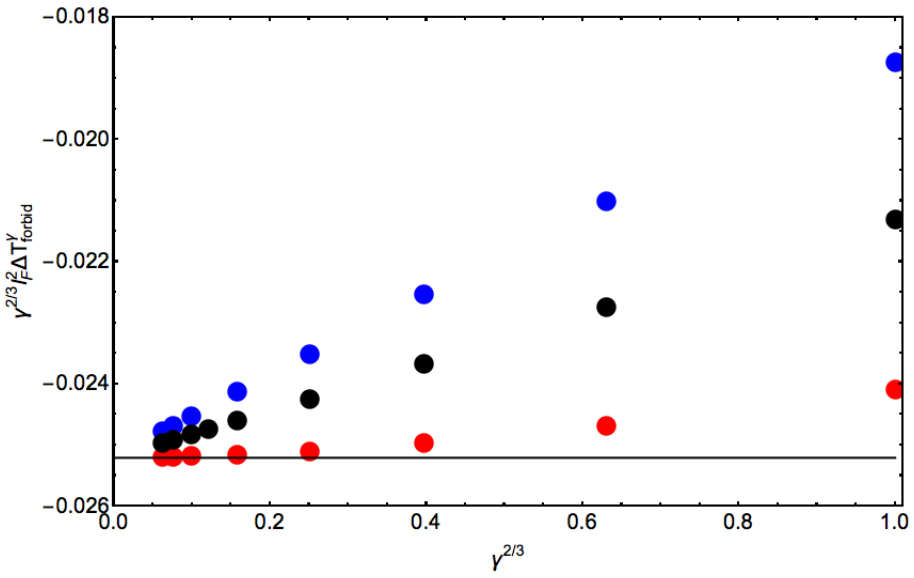

Figure 4.7: Average $l_F^2 \gamma^{2/3} \times$ kinetic energy from the left or right classically-forbidden regions for the harmonic oscillator (black) and Morse potentials (for which left evanescent region results are given in blue and right are in red) with $N = 1$; the straight line corresponds to the predictions implied by the appropriate decomposition of minus Eq. 4.26 into contributions due to each turning point

$O(\gamma^0)$ in the classically-allowed and forbidden regions, but they have opposite signs in each domain, and therefore, cancel yielding no net correction to the expectation value predicted by Thomas-Fermi theory.

For the Morse oscillator TF potential energies are again exact, but kinetic energies are not. In any case, it can be seen from Fig. 4.9 that the latter are accurately predicted by TF. The semiclassical total kinetic energies do not show improvement relative to TF results. In fact, the O(γ) error of TF kinetic energies is 0.01 according to the least squares fit shown in Fig. 4.9, while that of the semiclassical approximation is 0.05. As argued in detail for the harmonic oscillator, these results in no way discredit the semiclassical approximation.

The quartic potential provides a case where all TF observables are inexact. In this case, the semiclassical total potential energies are consistently more accurate than those predicted by TF. However, the opposite trend is seen for the total kinetic energy.

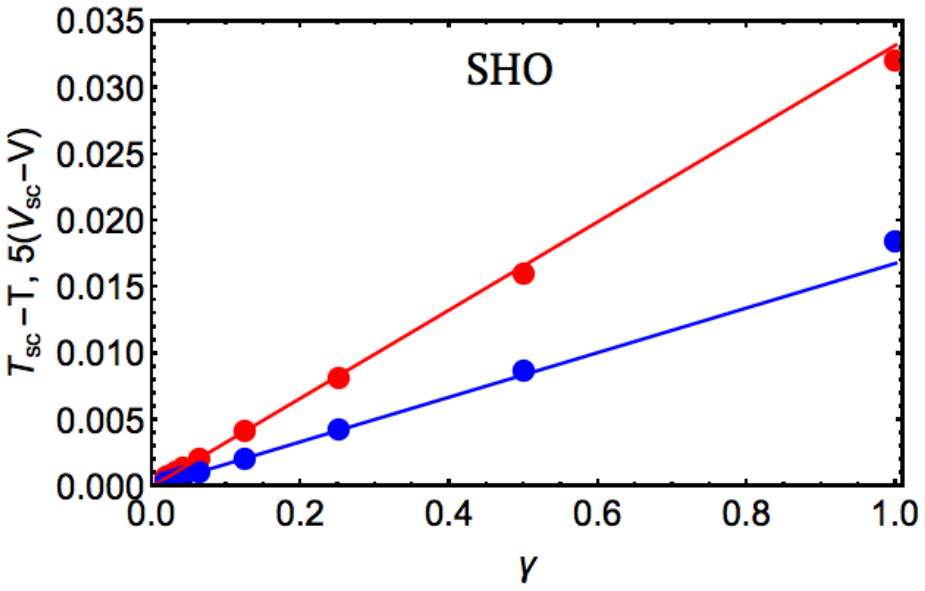

Figure 4.8: Errors in $N = 1$ harmonic oscillator total semiclassical kinetic and potential energies as a function of γ; straight lines correspond to a least squares fit to the results for all $\gamma < 1/32$.

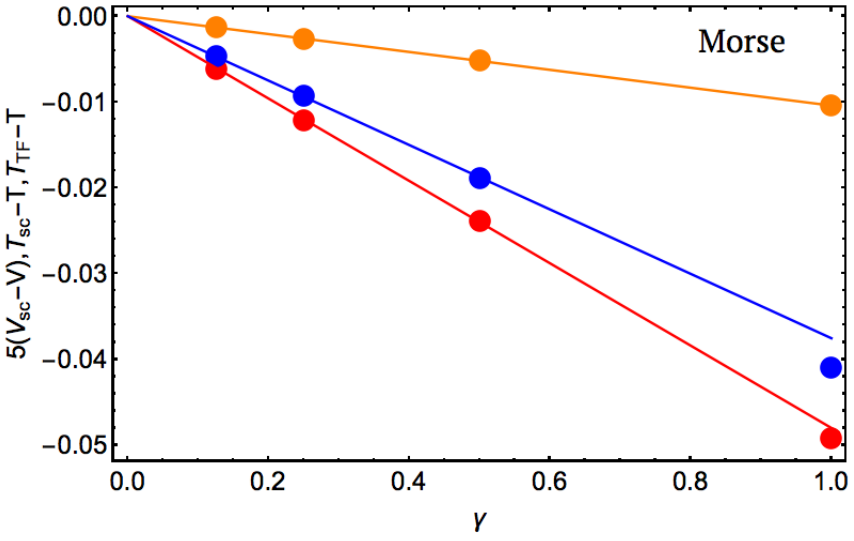

Figure 4.9: Semiclassical and TF total kinetic (red and orange, respectively) and semiclassical total potential energy (blue) errors for the Morse potential as a function of γ; straight lines correspond to a least squares fit to the points with $\gamma < 1$.

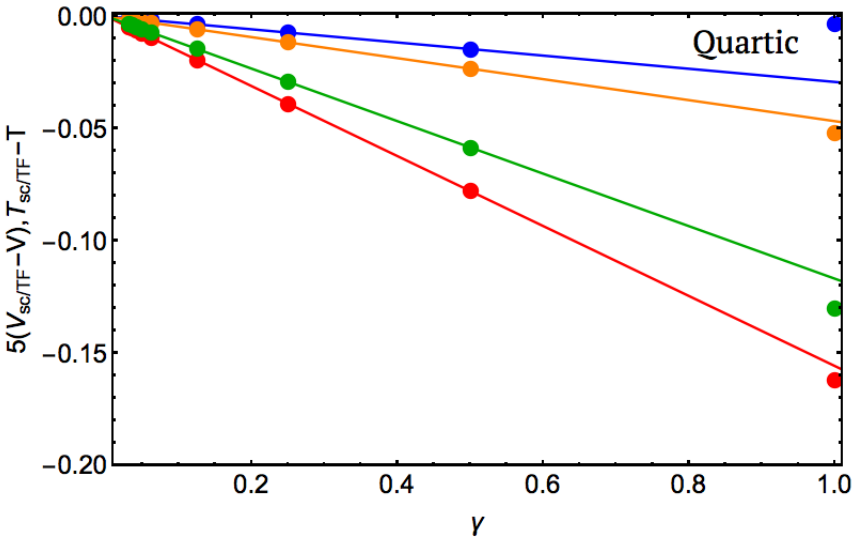

Figure 4.10: Semiclassical and TF total kinetic (red and orange, respectively) and potential energies (blue and green, respectively) errors for the quartic potential as a function of γ; straight lines correspond to a least squares fit to the points with $\gamma < 1$.

4.6 Breakdown of Semiclassical Approximation?

Two basic assumptions of the semiclassical approximations are that i) $\omega_F \neq 0$, and ii) $v_F'(x_{L/R}) \neq 0$. If the latter is not verified, then the Langer semiclassical wave function fails entirely to be a uniform approximation to the quantum-mechanical, thus invalidating the starting point of the derivations in chapter 3. The former means that the Fermi energy is located within the discrete part of the spectrum of a given potential (in other words the corresponding classical motion is bound), which we assumed from the beginning. In this section we look at the symptoms of a breakdown in n^{sc} and t^{sc} when the potential well described by $v(x)$ is sufficiently shallow that both ω_F and $v_F'(x_{L/R})$ are near zero.

We employ the Poschl-Teller potential described before with $v_0 = 1$ in which case there exists only one bound state with energy equal to $-1/2$. The semiclassical Fermi energy is -0.086. We compare this extreme case to that of $v_0 = 3$ and $v_0 = 6$ which give rise to two and three bound states, respectively (Fig. 4.11). In every case, we choose $N = \gamma = 1$. Table 1 gives numerical results while Figs. 4.12 and 4.13 compare semiclassical, Thomas-Fermi and exact

particle and kinetic energy densities.

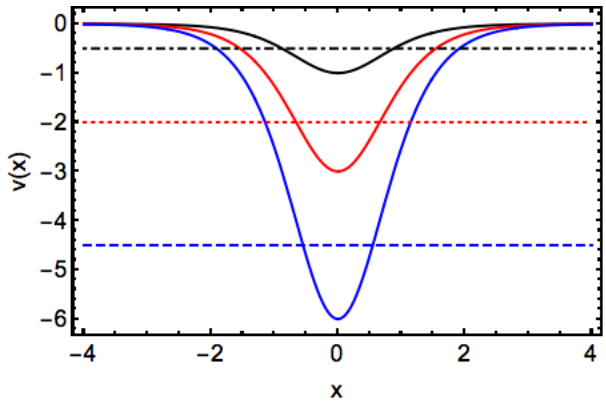

Figure 4.11: Poschl-Teller potentials (continuous lines) and lowest-energy states (dashed horizontal lines); $v(x)$ with $v_0 = 1$ corresponds to the black curve; $v_0 = 3$ to the red and $v_0 = 6$ to the blue.

Table 4.3: Poschl-Teller percent errors in energies for $N = 1$, pointwise particle density error and pointwise kinetic energy error/exact kinetic energy.

v_0	$\%\Delta T^{\text{sc}}$	$\%\Delta T^{TF}$	$\%\Delta V^{\text{sc}}$	$\%\Delta V^{TF}$	$\%\Delta E^{\text{sc}}$	$\%\Delta E^{TF}$	η	η^{TF}	η_T/T	η_T^{TF}/T
1	13.3	12.1	−4.1	−3.0	−9.9	−8.1	0.07	0.20	0.75	1.1
3	7.7	11.4	−1.0	−0.5	−2.8	−2.9	0.02	0.23	0.33	1.0
6	2.4	8.8	−0.8	−0.2	−1.2	−1.4	0.01	0.24	0.21	0.9

Table 4.3 verifies our expectations. As the depth of the probed well increases, the semiclassical approximations have their accuracy improved. This follows according to any measure chosen to check semiclassical pointwise and/or global errors for the potential and kinetic energies. Figures 4.12 and 4.13 illustrate the gradual reduction in accuracy of the uniform semiclassical approximations as the ability of a potential to bind particles becomes weaker. Significantly, while we see a systematic reduction in the efficacy of the predictions of the semiclassical approximation it does not provide any egregious or qualitative incorrect behavior for either the particle or kinetic energy density.

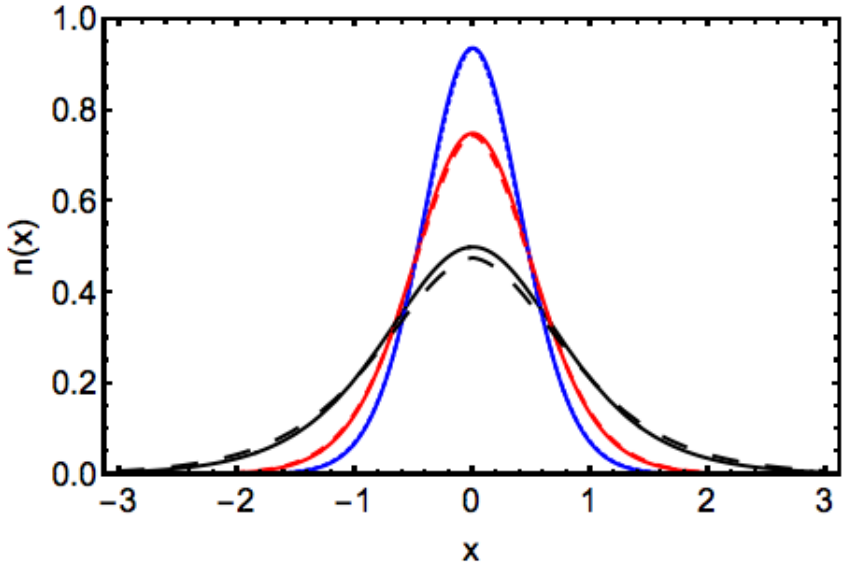

Figure 4.12: Poschl-Teller semiclassical (dashed) and exact (continuous) particle densities for $N = 1$, $v_0 = 1$ (black), 3 (red) and 6 (blue).

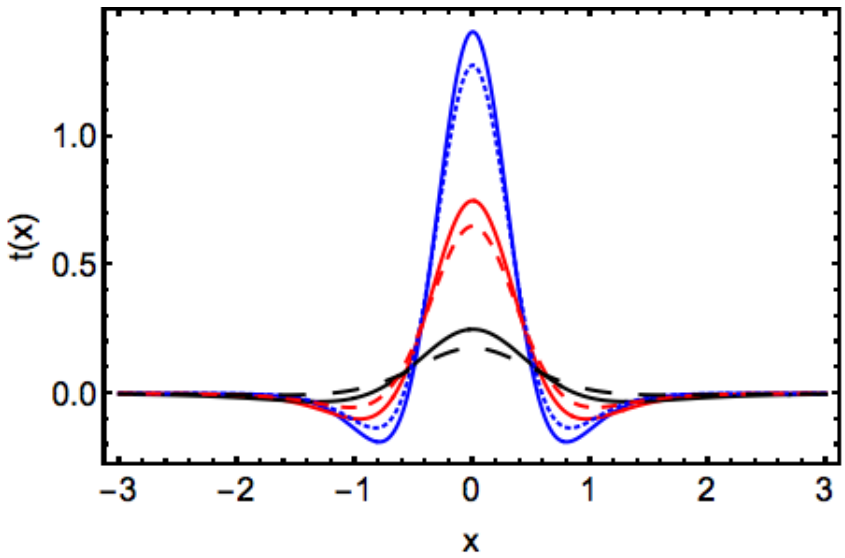

Figure 4.13: Poschl-Teller semiclassical (dashed) and exact (continuous) kinetic energy densities for $N = 1$, $v_0 = 1$ (black), 3 (red) and 6 (blue).

4.7 Conclusions

In this chapter we have explored some properties of the uniform semiclassical approximations to the particle and kinetic energy densities of noninteracting fermionic systems confined by a smooth external potential derived in chapter 3. Both local and global behavior were examined. In particular, we have demonstrated the high pointwise accuracy of the semiclassical approximations. These indisputably capture the dominant corrections to the classical limit in the region where the quantum-mechanical particle density oscillates and also in those where it decays exponentially. However, we found that dominant corrections to the energetics given by the classical limit in these dissimilar regions cancel exactly. This leads to the large accuracy of averages obtained with Thomas-Fermi theory, despite its poor pointwise behavior. Further study is needed to determine whether there exists a given class of external potentials for which total potential and kinetic energies predicted by the uniform semiclassical approximations are consistently more accurate relative to TF. Currently, we do not know what factors determine whether semiclassical total energies are better or worse than those given by TF.

We have also checked the behavior of the uniform semiclassical approximations in a situation where vital assumptions required for their derivation are almost violated. The results only indicated mild symptoms of a breakdown.

4.8 Appendix I - Relevant Properties of Airy functions

4.8.1 Asymptotic Expansions

Below we list the asymptotic expansions of $z^{1/2}A_1(z), z^{-1/2}A_2(z), A_0(z)$ (see section 4.2) in the three regions where they behave qualitatively different [103].

In the traveling region,

$$z^{1/2}A_1(z) \sim \frac{1+\sin(2S)}{2\pi} - \frac{5\cos(2S)}{72\pi S} + O(1/S^2),\ z >> 0, \tag{4.27}$$

$$z^{-1/2}A_2(z) \sim \frac{1-\sin(2S)}{2\pi} - \frac{7\cos(2S)}{72\pi S} + O(1/S^2),\ z >> 0, \tag{4.28}$$

$$A_0(z) \sim -\frac{\cos(2S)}{2\pi} + \frac{6+\sin(2S)}{72\pi S} + O(1/S^2),\ z >> 0. \tag{4.29}$$

In the classically-forbidden region (branches are chosen such that multiplication by $p = i\sqrt{p}$ gives the correct signs in the density or kinetic energy density semiclassical approximations),

$$z^{1/2}A_1(z) \sim ie^{-2|S|}\left(\frac{1}{4\pi} - \frac{5}{144\pi|S|} + O(1/S^2)\right),\ z << 0 \tag{4.30}$$

$$z^{-1/2}A_2(z) \sim -ie^{-2|S|}\left(\frac{1}{4\pi} + \frac{7}{144\pi|S|} + O(1/S^2)\right),\ z << 0 \tag{4.31}$$

$$A_0(z) \sim -e^{-2|S|}\left(\frac{1}{4\pi} + \frac{1}{144\pi|S|} + O(1/S^2)\right),\ z << 0. \tag{4.32}$$

In a small neighborhood of a turning point,

$$z^{1/2}A_1(z) \sim a_0^2 + \frac{z^{3/2}}{\sqrt{3}\pi} + \frac{z^{5/2}}{12\pi^2 a_0^2} + O(z^{7/2}),\ z \to 0 \tag{4.33}$$

$$z^{-1/2}A_2(z) \sim \frac{a_0^4 z^{-1/2}}{9} - \frac{z^{3/2}}{2\sqrt{3}\pi} - \frac{z^{5/2}}{18\pi^2 a_0^2} + O(z^{7/2}),\ z \to 0 \tag{4.34}$$

$$A_0(z) \sim -\frac{1}{2\sqrt{3}\pi} - \frac{z}{12\pi^2 a_0^2} + \frac{a_0^2 z^2}{2} + O(z^3), z \to 0$$

4.8.2 Integrals

To derive corrections to Thomas-Fermi in the allowed and forbidden regions (section 4.4) we had to evaluate a variety of integrals containing products of Airy functions. Here we show those which are needed to verify our results. Let,

$$I_p^m = \int_0^\infty \mathrm{d}z z^{m+1/2} K_p(z), \tag{4.35}$$

then it follows that

$$I_0^0 = -\frac{1}{6\sqrt{3}},\ I_0^1 = \frac{\pi a_0^2}{5}, \tag{4.36}$$

$$I_1^{-1/2} = \frac{1}{6\sqrt{3}},\ I_1^{1/2} = -\frac{1}{12\pi a_0^2}. \tag{4.37}$$

4.9 Appendix II - Basic Results of Thomas-Fermi Theory

In this appendix we collect some basic results of 1D Thomas-Fermi theory which are needed to obtain some data shown in the main text (sections 4.5 and 4.6). The particle and kinetic energy densities are given in terms of the potential $v(x)$ and Fermi energy ϵ_F by

$$n^{\mathrm{TF},\gamma}(x) = \frac{p_F(x)}{\pi\gamma}\theta[E_F - v(x)],\quad t^{\mathrm{TF},\gamma}(x) = \frac{\pi^2\left[n^{\gamma}_{\mathrm{TF}}(x)\right]^3}{6}\gamma^2. \tag{4.38}$$

From these it follows that as expected both the TF kinetic and potential energies scale as $1/\gamma$.

The total kinetic and potential energies can be obtained by evaluating the integrals,

$$T^{\mathrm{TF}} = \int_{-\infty}^{\infty} \mathrm{d}x\ t^{\mathrm{TF}}(x),\quad V^{\mathrm{TF}} = \int_{-\infty}^{\infty} \mathrm{d}x\ v(x)n^{\mathrm{TF}}(x), \tag{4.39}$$

where we have taken $\gamma = 1$ (in view of the relations above, the generalization to arbitrary γ is obvious). However, in many cases it is possible to evaluate TF kinetic and potential energies without having to perform the spatial integrations given above. Particularly, if the semiclassical Fermi energy can be obtained analytically (as is the case for all of the potential energy functions discussed in this chapter), then it is also the case for the total TF kinetic

and potential energies.

Let $E^{\mathrm{WKB}}(n;\beta)$ be the energy given as a function of quantum number n for a system with potential energy function $v(x;\beta) = \beta v(x)$. Then, it follows from the Hellmann-Feynman theorem [64] that,

$$\frac{\partial E^{\mathrm{WKB}}(n;\beta)}{\partial \beta} = V^{\mathrm{WKB}}(n;\beta), \quad T^{WKB}(n;\beta) = E^{\mathrm{WKB}}(n;\beta) - V^{\mathrm{WKB}}(n;\beta). \tag{4.40}$$

After setting $\beta = 1$ to the above results, the procedure first given by March and Plaskett in [74] to relate WKB and Thomas-Fermi theory can be employed to give TF energies:

$$V^{\mathrm{TF}} = \int_{-1/2}^{N-1/2} \mathrm{d}j \; V^{\mathrm{WKB}}(j), \quad T^{\mathrm{TF}} = \int_{-1/2}^{N-1/2} \mathrm{d}j \; T^{\mathrm{WKB}}(j). \tag{4.41}$$

This reformulation of the problem still requires one to evaluate integrals to obtain the TF kinetic and potential energies. However, these are generally much simpler relative to eq. 4.39. For instance, for the Morse potential:

$$E^{\mathrm{WKB}}(n;\beta) = a\sqrt{2\beta D_e}\left(j+\frac{1}{2}\right) - \frac{1}{2}a^2\left(j+\frac{1}{2}\right)^2. \tag{4.42}$$

It follows quickly that,

$$V^{\mathrm{WKB}}(j) = a\sqrt{D_e/2}\left(j+\frac{1}{2}\right). \tag{4.43}$$

Because integrals over polynomial functions are simple, TF energies for the Morse system (and any other studied in this chapter) can be obtained with no numerical effort.

Chapter 5

A Model of One-Dimensional Quantum Transport

5.1 Introduction

In this chapter we develop a novel mathematical treatment for a model of one-dimensional quantum transport. In particular, we establish a formal relationship between the properties of an idealized molecular junction and those of the corresponding isolated (conducting) molecule.

Our model consists of two main ingredients: i) noninteracting one-dimensional fermions prepared at featureless leads in the limit where the stationary bias goes to zero (we work within the framework of the Landauer model [26, 27, 60]) and ii) a short-range (vanishing outside of a finite interval of $\mathbb{R}$) potential $v(x)$ representing the effects of the molecular coupling. Only basic principles are shown, so no discussion of feasibility or cost for realistic computations is given.

In section 2 we review the required background (scattering theory and Green's functions), while section 3 contains the theory first exposed in this work. In section 4 we illustrate the main result of this chapter with a semiclassical approximation. The novelties introduced by this work are put into context in section 5, which also includes general discussion. The appendix contains intermediate results necessary for some derivations included in the main text.

5.2 Background

This work is restricted to one-dimensional systems, but the principles illustrated can be generalized to three dimension, e.g., with periodic boundary conditions in the other two directions [26, 27]. We use atomic units throughout.

Molecular conductance can be interpreted with the tools of scattering theory [26, 27], and one-dimensional scattering has been extensively studied, e.g., in [8, 32]. In this section we review some of these results and fix the notation that will be later employed.

Consider scattering off an external potential here denoted by $v(x)$. We assume it is symmetric with respect to a parity transformation, i.e., $v(-x) = v(x)$. This is employed to simplify some of the further considerations, but it is not necessary in principle. It is also assumed that $v(x)$ is of finite range, i.e., it vanishes for $x > a$. This constraint can be weakened. In particular, if the decay of $v(x)$ as $x \to \infty$ is exponential, then the errors induced by the discussed formalism will be exponentially small.

Transmission (t) and reflection (r) amplitudes completely characterize one-dimensional scattering. These are obtained as functions of the incoming momentum k from the conditions satisfied by a scattering wave function outside the range of influence of the external potential $v(x)$. For example, if $\chi(x)$ denotes a scattering state incoming from the left, then the

transmission and reflection amplitudes can be defined by the asymptotic conditions,

$$\chi(x) = \begin{cases} e^{ik(x+a)} + re^{-ik(x+a)}, & x \leq a, \\ te^{ik(x-a)}, & x \geq a. \end{cases} \tag{5.1}$$

From r and t transmission and reflection probabilities are obtained via the usual quantum-mechanical prescription [29], i.e., $T = |t|^2, R = |r|^2$.

Parity and time-reversal symmetry simplifies the study of one-dimensional quantum scattering. In particular, in this case the scattering matrix admits the simple form,

$$S = \begin{pmatrix} \sqrt{R} & i\sqrt{T} \\ i\sqrt{T} & \sqrt{R} \end{pmatrix} e^{i\theta}. \tag{5.2}$$

This implies knowledge of the transmission amplitude $t = \sqrt{T}e^{i\theta}$ is sufficient to determine the reflection amplitude r by using $r = \sqrt{R}e^{i(\theta-\pi/2)}$.

Because later results depend on various properties of Green's functions we also list here some of their useful relations. Let L_k be a linear differential operator with a domain consisting of generalized functions satisfying outgoing boundary conditions at infinity of the class,

$$\Phi(x) \to ce^{ik|x|}, |x| \to \infty, c \in \mathbb{C}. \tag{5.3}$$

If $\phi_L(x)$ and $\phi_R(x) = \phi_L(-x)$ are the solutions of $L_k\phi(x) = 0$ satisfying the above given boundary conditions at $x = -\infty$ and $x = +\infty$, respectively, then the Green's function $g(x, x'; k)$ can be written as

$$g(x, x'; k) = \begin{cases} \phi_L(x)\phi_R(x')/W(k) & x' > x, \\ \phi_L(x')\phi_R(x)/W(k) & x > x', \end{cases} \tag{5.4}$$

where $W(k)$ is the Wronskian determinant for the Schrodinger equation, i.e.,

$$W(k) = \begin{vmatrix} \phi_L(x) & \phi_R(x) \\ \frac{d}{dx}\phi_L(x) & \frac{d}{dx}\phi_R(x) \end{vmatrix}. \tag{5.5}$$

By using the basis formed by Eq. 5.1 and a corresponding scattering state incoming from the right, we can find a Green's function suitable for the study of one-dimensional scattering in accordance with the above,

$$g^{(+)}(x,y;k) = \begin{cases} te^{ik|x-y|}/ik, & x < -a, y > a, \\ \frac{e^{ik|x-y|}}{ik} + \frac{r}{t}\frac{e^{ik(|x|+|y|)}}{ik}, & x > y > a > 0, \end{cases} \tag{5.6}$$

where the + superscript reminds outgoing boundary conditions with $\mathrm{Im}(\epsilon(k) > 0)$ are employed. In particular, $g^{(+)}(x,y;k)$ is simply related to the Green's function defined in Eq. 5.4 via

$$g^{(+)}(x,y;k) = \lim_{\eta \to 0^+} g(x,y;k+i\eta). \tag{5.7}$$

From the previous results it follows that t and r can be obtained in terms of Green's functions evaluated beyond the range where $v(x)$ is effective:

$$\begin{cases} t(k) = ik\ e^{-2ika} g^{(+)}(a,-a;k), \\ r(k) = e^{-2ika}\left[ik\ g^{(+)}(a,a;k) - 1\right], \end{cases} \tag{5.8}$$

where to obtain the second expression, the limit $x \to y \to a_+$ was taken.

As an example consider $v(x) = -\delta(x)/\alpha$. Then,

$$g^{(+)}(a,a;k) = \frac{1}{ik}\left(1 - \frac{1}{ik\alpha + 1}e^{2ika}\right), \tag{5.9}$$

$$g^{(+)}(a,-a;k) = \frac{e^{2ika}\alpha}{1+ik\alpha}, \tag{5.10}$$

whence $r(k) = -1/(1+ik\alpha)$ and $t(k) = ik\alpha/(1+ik\alpha)$.

Note the transmission amplitude can also be directly obtained from the Green's function with

$$t(k) = -\frac{i}{k}\frac{\partial^2 g^{(+)}(a,-a;k)}{\partial x \partial y}e^{-2ika}. \tag{5.11}$$

A similar result for the reflection amplitude follows from consideration of the parametrization for the S-matrix given in Eq. 1. Thus, the Green's function can be used to directly obtain the S-matrix.

5.3 Generalized Dyson Equation and Self-Energy

The main result of this work is derived in this section: a Dyson-like equation relating an isolated molecule Dirichlet Green's function $g_0(x,y;k)$ to that of a system in which the molecule is coupled to featureless leads with outgoing boundary conditions at infinity. In particular, for the Dirichlet system we assume $H_0 = -1/2\mathrm{d}^2/\mathrm{d}x^2 + v(x), \psi(\pm a) = 0$, whereas for the coupled system the Hamiltonian is the same, though we denote it by H, for the boundary conditions require the wave functions of bound states to be square integrable whereas scattering states oscillate at long distances.

The following family of Hamiltonians will prove useful throughout the derivation:

$$H_{\beta\alpha} = -\frac{1}{2}\frac{\mathrm{d}^2}{\mathrm{d}x^2} + v(x) + \beta^{-1}\delta(x+a) + \alpha^{-1}\delta(x-a), \tag{5.12}$$

where $\beta, \alpha \geq 0$, $v(x)$ is of finite range r, and $|a| > r$. Note that by varying (β, α) we can interpolate between the systems defined by H and H_0 above. For example, it is obvious that $H_{\infty\infty} = H$, and it can be shown that $H_{00} = H_0$. For a given pair (β, α) the associated Green's function to $H_{\beta\alpha}$ will be denoted $g_{\beta\alpha}$. To simplify notation we will in this section omit the dependence of the Green's function on the energy, and also introduce the following definitions: $g_0 \equiv g_{00}, g_\infty \equiv g_{\infty\infty}, g_L \equiv g_{0\infty}$, and $g_{L\alpha} \equiv g_{0\alpha}$. In fact these subscripts will be employed whenever possible to identify properties of the system for which the Hamiltonian is $H_{\beta\alpha}$. Then, for example, $H_{00} \equiv H_0$, $H_{0\infty} = H_L$, etc.

The derivation can be summarized by three steps: in the first we relate g_0 and g_L; the second connects g_∞ and g_L, while the third gives a relationship between g_0 and g_∞ which is a generalized Dyson equation (the main result of this chapter).

The Green's function for $H_{L\alpha}$ can be related to that of H_0 by the integral equation:

$$g_{L\alpha}(x, y) = g_0(x, y) + \int \mathrm{d}z g_0(x, z) v_\alpha(z) g_{L\alpha}(z, y), \tag{5.13}$$

where $v_\alpha = \delta(x - a)/\alpha$. By standard techniques it is written as:

$$g_{L\alpha}(x, y) = g_0(x, y) + \frac{f_0(x) f_0(y)}{\alpha - h_0}, \tag{5.14}$$

where $f_{L\alpha}(x) = g_{L\alpha}(x, a)$, $h_{L\alpha} = f_{L\alpha}(a)$.

With the objective of expressing $g_0(x, y)$ in terms of $g_{L\alpha}(x, y)$ we invert 5.14 to find:

$$g_0(x, y) = g_{L\alpha}(x, y) - \frac{1}{\alpha - h_\alpha} f_0(x) f_0(y) \tag{5.15}$$

Note $h_{L\alpha} = g_{L\alpha}(a, a) = h_0\alpha/(\alpha - h_0)$ and $f_{L\alpha}(x) = f_0(x)\alpha(\alpha + h_{L\alpha})$ (this follows from eq. 5.14). Note that as $\alpha \to 0, h_{L\alpha} \to -\alpha$. However, by defining $K_{L\alpha}(x) = f_{L\alpha}(x)/h_{L\alpha} = g_{L\alpha}(x, a)/g_{L\alpha}(a, a)$ this issue is resolved, since $K_{L\alpha}(x) = K_{0,0}(x) = g_0(x, a)/g_0(a, a)$, so it is

independent of α. From now on we will write $K_{L\alpha}(x) = K(x)$ unless we wish to emphasize the value of α we are using to evaluate $K(x)$. Hence, we rewrite the above as:

$$g_0(x,y) = g_{L\alpha}(x,y) - \frac{h_0^2}{\alpha - h_0}\frac{f_0(x)}{h_0}\frac{f_0(y)}{h_0}, \tag{5.16}$$

$$g_0(x,y) = g_{L\alpha}(x,y) - \frac{h_0^2}{\alpha - h_0}K(x)K(y). \tag{5.17}$$

As $\alpha \to 0$ we find to leading order (and here we have to specify that $\epsilon = k^2/2$ is not an eigenvalue of the box hamiltonian otherwise the limiting process we take becomes undefined; it is sufficient to set $\mathrm{Im}(k) > 0$):

$$g_0(x,y) = g_{L\alpha}(x,y) + h_0 K(x)K(y),\ \alpha \to 0. \tag{5.18}$$

For $\alpha = 0$, we evaluate $K(x)$ with L'Hôpital's rule:

$$K(x) = K_L(x) = \lim_{\eta \to 0^+} \frac{g_L(x, a-\eta)}{g_L(a-\eta, a-\eta)}, \tag{5.19}$$

$$K(x) = \frac{\partial g_L(x,y)/\partial y|_{y=a}}{\mathrm{d}g_L(x,x)/\mathrm{d}x|_{x=a}}. \tag{5.20}$$

It is important to note that in the denominator the limit is taken on the diagonal element of the Green's function (a single-variable function). It follows that:

$$g_0(x,y) = g_L(x,y) + f_0 K(x)K(y), \tag{5.21}$$

$$g_0(x,y) = g_L(x,y) + f_0(y)\frac{\frac{\partial g_{L(x,a)}}{\partial y}}{\frac{\mathrm{d}g_L(a,a)}{\mathrm{d}x}}. \tag{5.22}$$

Finally,

$$g_0(x,y) = g_L(x,y) + c^{-1}g_0(y,a)\frac{\partial g_L(x,a)}{\partial y} \tag{5.23}$$

where $c = \mathrm{d}g_L(a,a)/\mathrm{d}x$.

The identities derived in Appendix I allow us to rewrite the above as:

$$g_0(x,y) = g_L(x,y) - \frac{i}{2k}\frac{\partial g_L(x,a)}{\partial y}\frac{\partial g_0(a,y)}{\partial x}. \tag{5.24}$$

By using the Green's function integral equation we can additionally relate g_∞ to g_L, and as a result g_∞ to $g_0(x,y)$. This latter relationship is what we are after, since $g_\infty(x,y)$ is the Green's function for a system trapped by two hard-walls (thus corresponding to a model of an isolated molecule), while g_0 is the Green's function corresponding to a model of a molecule coupled to featureless external leads. Introducing the relationship found for $g_L(x,y)$ in terms of $g_0(x,y)$, we find,

$$g_0(x,y) = g_\infty(x,y) + \frac{\frac{\partial g_\infty(x,-a)}{\partial y}}{\frac{\mathrm{d}g_\infty(-a,-a)}{\mathrm{d}y}}\ g_L(-a,y) + \frac{\frac{\partial g_L(x,a)}{\partial y}}{\frac{\mathrm{d}g_L(a,a)}{\mathrm{d}x}}\ g_0(a,y). \tag{5.25}$$

To get rid of any factor involving $g_L(x,y)$ or its partial derivatives in eq. 5.25, we employ the results derived in Appendix I as well as the following identities:

$$g_L(-a,y) = g_0(-a,y) - \frac{1}{2}g_0(a,y)\frac{\partial g_L(-a,a)}{\partial y}, \tag{5.26}$$

$$\frac{\partial g_L(x,a)}{\partial y} = \frac{\partial g_\infty(x,a)}{\partial y} - \frac{1}{2}\frac{\partial g_\infty(x,-a)}{\partial y}\frac{\partial g_L(-a,a)}{\partial y}, \tag{5.27}$$

where the first equation was obtained from 5.23 (after replacing c by 2 as derived in Appendix I), and the second from 5.25 (with the same priorly mentioned replacement). After applying the above and additional results obtained in Appendix 1 we obtain

$$g_0(x,y) = g_\infty(x,y) - \frac{i}{2k}\frac{\partial g_\infty(x,-a)}{\partial y}\frac{\partial g_0(-a,y)}{\partial x} - \frac{i}{2k}\frac{\partial g_\infty(x,a)}{\partial y}\frac{\partial g_0(a,y)}{\partial x}, -a \leq x,y \leq a.$$

This provides a partial differential equation equation relating the Green's function of a system modeled by the external potential $v(x)$ satisfying open boundary conditions, in terms of the Green's function for the same system satisfying closed boundary conditions.

The self-energy may be read from the Dyson-like equation given above by recalling that it can be defined by the integral equation,

$$g(x,y;k) = g_0(x,y;k) + \int \mathrm{d}z\mathrm{d}z' g_0(x,z;k)\Sigma(z,z';k)g(z',y;k). \tag{5.28}$$

Hence, it follows that for the model studied in this chapter, the self-energy operator is given in real-space by:

$$\Sigma(x,x';k) = -\frac{i}{2k}\delta'(x-a)\delta'(x'-a) - \frac{i}{2k}\delta'(x+a)\delta'(x'+a). \tag{5.29}$$

5.4 Quantum Transport Properties

While the derived Dyson-like equation relates the isolated and connected Green's functions for a model system in 1D, it is unlikely to be exactly solvable for any system of practical interest. However, as shown in section 5.2, S-matrix elements and therefore, transport observables, can be directly obtained from the mixed second derivative of the connected Green's function $g(x, y)$ ($g_0(x, y)$ in the notation of the previous section) evaluated at the box endpoints $x = a, y = -a$. This quantity can be obtained without solving the Dyson-like equation given above. To see that, let γ denote the 2x2 Hessian matrix of any Green's function evaluated at the endpoints, i.e.,

$$\gamma_{\pm\pm} = \frac{i}{2k} \frac{\partial^2 g(x,y)}{\partial x \partial y}\bigg|_{x=\pm a, y=\pm a}. \tag{5.30}$$

Then, the generalized Dyson equation given above can be manipulated to give:

$$\gamma_{-+} = \frac{\gamma^0_{-+}}{\det\gamma^0 + \mathrm{Tr}\ \gamma^0 + 1}. \tag{5.31}$$

Because $t(k) = 2\gamma_{-+}e^{-2ika}$, we explicitly see that the transmission can be obtained from the isolated Green's function Hessian matrix. In the next section we explore a simple approximations to Eq. 5.31.

5.5 Example: Semiclassical Approximation

In this section we illustrate the use of Eq. 5.31 by using a semiclassical approximation. For simplicity we assume the energy of the incoming particle $\epsilon = k^2/2 > v(x),\ \forall\ x \in \mathbb{R}$. Then, WKB applied to a system with Dirichlet boundary conditions gives the following Green's

function,

$$g^{(0)}(x,y;k) = \frac{\cos[\theta_L(x) - \theta_R(y)] - \cos[\theta_L(x) + \theta_R(y)]}{\sqrt{k(x)k(y)}\sin\Theta}, \tag{5.32}$$

where $-a \leq x < y \leq a$, $\theta_L(x) = \int_{-a}^{x} \mathrm{d}x\ k(x)$, $\theta_R(x) = \int_{a}^{x} \mathrm{d}x\ k(x)$, and $\Theta = \theta_L(a)$. From this we can calculate the mixed second derivative Green's function matrix $\gamma_{\eta,\zeta}$ defined above,

$$\gamma^0 = i \begin{pmatrix} \cot(\Theta) & \csc(\Theta) \\ \csc(\Theta) & \cot(\Theta) \end{pmatrix}. \tag{5.33}$$

It follows from Eq. 5.31 that

$$\gamma_{-+}(k) = \frac{e^{i\Theta}}{2}, \tag{5.34}$$

whence we obtain the approximate transmission amplitude,

$$t(k) = e^{i\Theta}e^{-2ika} = e^{i\int_{-a}^{a}[k(x)-k]\mathrm{d}x}, \tag{5.35}$$

so the semiclassical approximation to the one-dimensional scattering phase-shift emerges. Note that semiclassical transmission above barrier has unit probability as the phenomenon of reflection above barrier is exponentially small and cannot be described with primitive semiclassical theory.

5.6 Summary

We have analytically constructed the self-energy operator in real-space for the case of a conducting system connected to two featureless leads in the limit of zero bias. This can be shown to be the long-distance limit for a tight-binding chain in which the leads are described

by a nearest-neighbor hopping hamiltonian and the coupling to a central molecular system only happens at their interface [92]. As such, our model is not realistic. However, it provides an explicit example in which computations done for isolated subsystems may be employed to understand the properties of a coupled infinite system.

5.7 Appendix I - Some Useful Identities

In this appendix we derive some results used in section III. For instance, the factors $g_0(y,a)$ and $\mathrm{d}g_L(x,x)/\mathrm{d}x|_{x=a}$ can be rewritten by taking advantage that a is beyond the finite range of the potential $v(x)$. For this purpose we introduce a new Hamiltonian $H_0^{\text{free}} = -1/2\mathrm{d}^2/\mathrm{d}x^2$, defined on the real line, with

$$g_0^{\text{free}}(x,y) = e^{ik|x-y|}/ik. \tag{5.36}$$

Some of the notation introduced before was employed since H_0^{free} corresponds to $H_{\alpha\beta}$ with $v(x) = 0, \alpha = \beta = \infty$. The integral equation for the Green's function of H reads:

$$g_0(x,y) = g_0^{\text{free}}(x,y) + \int_{\mathbb{R}} \mathrm{d}z g_0^{\text{free}}(x,z)v(z)g_0(z,y). \tag{5.37}$$

Naturally, g_0 here corresponds to $H_{00}(\alpha = \beta = 0$, the hamiltonian for the coupled system which has $v(x) \neq 0)$. Taking partial derivatives w.r.t x on both sides of the previous equation and multiplying by $-i/k$ gives

$$\begin{aligned}\frac{-i}{k}\frac{\partial g_0(x,y)}{\partial x} =& \left[\theta(x-y) - \theta(y-x)\right]\frac{e^{ik|x-y|}}{ik} + \\ &\int_{\mathbb{R}} \mathrm{d}z \left[\theta(x-z) - \theta(z-x)\right]\frac{e^{ik|x-z|}}{ik}v(z)g_0(z,y).\end{aligned} \tag{5.38}$$

Now set $x = a$ and note that because a is chosen so that it lies beyond the range of influence of $v(x)$, $y < x = a$ and $v(z) = 0, \forall z \geq a$. Hence,

$$\frac{-i}{k}\frac{\partial g_0(a,y)}{\partial x} = \frac{e^{ik|a-y|}}{ik} + \int_{-\infty}^{a} \mathrm{d}z \frac{e^{ik|a-z|}}{ik} v(z) g_0(z,y). \tag{5.39}$$

We can extend the integration domain, for $v(z) = 0,\ \forall\ z > a$. Thus,

$$\frac{-i}{k}\frac{\partial g_0(a,y)}{\partial x} = \frac{e^{ik|a-y|}}{ik} + \int_{\mathbb{R}} \mathrm{d}z \frac{e^{ik|a-z|}}{ik} v(z) g_0(z,y), \tag{5.40}$$

which implies

$$\frac{-i}{k}\frac{\partial g_0(a,y)}{\partial x} = g_0^{\text{free}}(a,y) + \int_{\mathbb{R}} \mathrm{d}z g_0^{\text{free}}(a,z) v(z) g_0(z,y) \tag{5.41}$$

as well as

$$g_0(a,y) = -\frac{i}{k}\frac{\partial g_0(a,y)}{\partial x},\ y < a, v(z) = 0\ \forall\ z \geq a \tag{5.42}$$

which is the identity we wanted. Now we show that

$$\mathrm{d}g_L(x,x)/\mathrm{d}x|_{x=a} = 2. \tag{5.43}$$

For this we need g_L^{free} which has $h_L^{\text{free}} = -1/2\mathrm{d}^2/\mathrm{d}x^2$ (with domain $\psi(a) = 0\}$):

$$\begin{aligned} g_L^{\text{free}}(x,y) &= \frac{e^{ik|x-y|} - e^{ik|2a-x-y|}}{ik} \\ -\frac{1}{ik}&\frac{\left(e^{ik|x|} - e^{2ika}e^{-ikx}\right)\left(e^{ik|y|} - e^{2ika}e^{-iky}\right)}{ik\alpha^{-1} + (1 - e^{2ika})}, x, y < a. \end{aligned} \tag{5.44}$$

We also note that $\mathrm{d}g_L^{\mathrm{free}}(x,x)/\mathrm{d}x|_{x=a} = 2$. We use again the integral equation for the Green's function of $g_L(x,y)$:

$$g_L(x,y) = g_L^{\mathrm{free}}(x,y) + \int_{\mathbb{R}} \mathrm{d}z g_L^{\mathrm{free}}(x,z)v(z)g_L(z,y). \tag{5.45}$$

Taking the derivative of the diagonal element $g_L(x,x)$ with respect to x and setting $x = a$, we find the only contributing term comes from $\mathrm{d}g_L^{\mathrm{free}}(x,x)/\mathrm{d}x|_{x=a}$.This happens because $a > r$ and $v(z)$ vanishes for $|z| > r$.We find the desired relationship

$$\mathrm{d}g_L(x,x)/\mathrm{d}x|_{x=a} = 2. \tag{5.46}$$

Similar identities follow at $x = -a$. For example,

$$g_0(-a,y) = \frac{i}{k}\frac{\partial g_0(-a,y)}{\partial x}. \tag{5.47}$$

Now let g_∞^{free} correspond to the Green's function of the free particle in a box with edges $x = \pm a$,

$$g_\infty^{\mathrm{free}}(x,y) = \frac{2\mathrm{sin}k(x_< + a)\mathrm{sin}k(x_> - a)}{k\mathrm{sin}2ka}, \tag{5.48}$$

where $x_> = \max(x,y),$ and $x_< = \min(x,y)$. It follows that

$$\left.\frac{\mathrm{d}g_\infty^{\mathrm{free}}(x,x)}{\mathrm{d}x}\right|_{x=\pm a} = \pm 2. \tag{5.49}$$

For the integral equation relating g_∞ and g_∞^{free}, we find

$$g_\infty(x,y) = g_\infty^{\mathrm{free}}(x,y) + \int_{\mathbb{R}} \mathrm{d}z g_\infty^{\mathrm{free}}(x,z)v(z)g_\infty(z,y). \tag{5.50}$$

Evaluating $\mathrm{d}g_\infty(x,x)/\mathrm{d}x|_{x=\pm a}$ gives as the only contributing term $\mathrm{d}g_\infty^{\mathrm{free}}(x,x)/\mathrm{d}x|_{x=\pm a}$ which

is equal to ± 2. This happens again because $a > r$ where r is the range of $v(x)$.

Chapter 6

Epilogue

6.1 Semiclassical Fermions

A variety of novel results was given in this thesis for the nonrelativistic ground-state of noninteracting fermions living on a line. In particular, in chapter 3 we solved a long-standing problem investigated by researchers in fields as diverse as chemical, condensed matter and nuclear physics: the unravelling of general semiclassical approximations to the particle and kinetic energy densities of fermions coupled to an external potential in one dimension.

A large part of the fascination with the problems here solved is related to the quest for unifying principles in theoretical chemistry and physics. For instance, the simple approximations given by eqs. 3.34 and 3.50 are independent of particle number and may be applied to any set of spinless fermions coupled to any generic potential $v(x)$ (the generalization to spinful fermions without spin-dependent couplings is obvious). Therefore, we were able in chapter 4 to uncover universal aspects of local and global properties of one-dimensional fermionic systems. While we have limited ourselves in this thesis to the study of external potentials consisting of a single well/center, a simple perturbative argument essentially guarantees the

validity of the uniform semiclassical approximation in the weak coupling regime of a multicentered trapping potential. The case of strong coupling remains to be studied, but the methods described in this thesis may be useful in this context, too.

From a methodological point of view the main novelty of this research consists of the particular blend of techniques of semiclassical analysis employed to obtain the main results. Notably, we have shown that the Poisson summation formula is a powerful tool for the study of the local behavior of finite fermionic systems in the semiclassical limit. In chapter 2 we showed that semiclassical arguments combined with application of Poisson summation quickly led to the non-trivial density matrix for fermions confined to a box. Next, in chapter 3 we saw that the same device was equally effective in decoding the universal behavior of particle and kinetic energy densities of fermions confined only by a smooth external potential, though intermediate steps were more convoluted as a result of the richer behavior of quantum-mechanical particles in an unbounded domain.

Nevertheless, because the universe as we know consists of three spatial dimensions, one cannot help but wonder about

- the establishment of similar results for general 3D systems, and
- what are the lessons learned from this project which could be applied to the field of electronic structure theory.

It is hard to foresee generalizations of the results presented in the first part of this thesis to generic 3D external potentials. This follows from the general non-integrability of classical dynamics in the case of more than one dimension, and the richness of classical phase space structures which then exist.

The question posed by item 2 is subtler. For example, chapter 4 shows in general that an accurate local description of quantum effects on the particle and kinetic energy densities does

not necessarily guarantee improved energetics. This follows from a strong cancellation of quantum effects emanating from parts of configuration space where the particle density behaves in qualitatively different manners. The extent to which this phenomenon is generalized to 2 or 3 dimensions remains to be investigated.

To conclude we list several directions which may be pursued with the methods and results introduced by our research:

- adaptation of semiclassical uniform approximations to many-fermion systems coupled to 2D or 3D isotropic external potentials, [102]
- development of semiclassical uniform approximation to the one-particle density matrix (or equivalently, the derivation of semiclassical approximations to the one-dimensional exchange energy density given some effective fermion-fermion coupling),
- application of the semiclassical approximation to one-dimensional systems with multiple wells,
- analytical determination of next-order corrections to the semiclassical particle and kinetic energy densities, and numerical study of the effect on energetics,
- derivation of semiclassical thermal particle and kinetic energy densities.

Thus, even in the modest context of one-dimensional system many challenges still lay ahead towards a complete description of noninteracting fermionic systems in the semiclassical limit.

6.2 Quantum Transport

We have shown explicitly for a simple model of transport within a molecular junction the general behavior of a coupled system (represented by knowledge of its Green's function) can

be determined from the properties of the corresponding isolated (central) conductor confined to a compact domain by vanishing Dirichlet boundary conditions.

A few questions remain to be investigated, for instance:

- whether the chosen model can be generalized to accommodate a realistic coupling between the leads and the central conductor, e.g., one that is not limited to occur only between interface degrees of freedom,
- if accurate transmission coefficients may be obtained with computations involving a finite/truncated Hilbert space (of the isolated system satisfying Dirichlet conditions).

It would also be interesting to analyze what changes would be incurred on the self-energy operator if the leads are not assumed to be featureless.

Bibliography

[1] M. Abramowitz and I. Stegun. *Handbook of Mathematical Functions: With Formulas, Graphs, and Mathematical Tables*. Applied mathematics series. Dover Publications, 1965.

[2] G. Airy. On the intensity of light in the neighborhood of a caustic. *Transactions of the Cambridge Philosophical Society*, pages 379–402, 1838.

[3] F. Alber and P. Carloni. Ab initio molecular dynamics studies on hiv-1 reverse transcriptase triphosphate binding site: Implications for nucleoside–analog drug resistance. *Protein Science*, 9(12):2535–2546, 2000.

[4] L. C. R. Alfred. Quantum-corrected statistical method for many-particle systems: The density matrix. *Phys. Rev.*, 121:1275–1282, Mar 1961.

[5] T. M. Apostol. An elementary view of euler's summation formula. *The American Mathematical Monthly*, 106(5):409–418, 1999.

[6] V. Arnold. *Mathematical Methods of Classical Mechanics*. Graduate texts in mathematics. Springer, 1989.

[7] N. Balazs and G. Z. Jr. Quantum oscillations in the semiclassical fermion -space density. *Annals of Physics*, 77(1-2):139 – 156, 1973.

[8] V. E. Barlette, M. M. Leite, and S. K. Adhikari. Integral equations of scattering in one dimension. *American Journal of Physics*, 69(9):1010–1013, 2001.

[9] M. V. Berry. Uniform approximation for potential scattering involving a rainbow. *Proceedings of the Physical Society*, 89(3):479, 1966.

[10] M. V. Berry. Uniform approximation: a new concept in wave theory. *Sci. Prog., Oxf.*, 57:43–64, 1969.

[11] M. V. Berry and K. E. Mount. Semiclassical approximations in wave mechanics. *Reports on Progress in Physics*, 35(1):315, 1972.

[12] M. V. Berry and M. Tabor. Closed orbits and the regular bound spectrum. *Proceedings of the Royal Society of London. Series A, Mathematical and Physical Sciences*, 349(1656):pp. 101–123, 1976.

[13] M. V. Berry and M. Tabor. Calculating the bound spectrum by path summation in action-angle variables. *Journal of Physics A: Mathematical and General*, 10(3):371, 1977.

[14] N. Bleistein and R. Handelsman. *Asymptotic Expansions of Integrals*. Holt, Rinehart and Winston, 1975.

[15] R. P. Boas and C. Stutz. Estimating sums with integrals. *American Journal of Physics*, 39(7):745–753, 1971.

[16] M. Boero, K. Terakura, and M. Tateno. Catalytic role of metal ion in the selection of competing reaction paths: A first principles molecular dynamics study of the enzymatic reaction in ribozyme. *Journal of the American Chemical Society*, 124(30):8949–8957, 2002.

[17] M. Born and R. Oppenheimer. Zur Quantentheorie der Molekeln. *Annalen der Physik*, 389(20):457–484, 1927.

[18] M. Brack and R. Bhaduri. *Semiclassical Physics*. Frontiers in physics. Westview, 2003.

[19] L. Brillouin. La mecanique ondulatoire de schrödinger: une methode generale de resolution par approximations successives. *Compt. Rend.*, 183:24, 1926.

[20] Y. A. Brychkov. On higher derivatives of the bessel and related functions. *Integral Transforms and Special Functions*, 24(8):607–612, 2013.

[21] K. Burke. Perspective on density functional theory. *J. Chem. Phys.*, 136, 2012.

[22] A. Cangi, D. Lee, P. Elliott, and K. Burke. Leading corrections to local approximations. *Phys. Rev. B*, 81(23):235128, Jun 2010.

[23] M. S. Child. *Semiclassical Mechanics with Molecular Applications*. Clarendon Press, Oxford, 1991.

[24] C. J. Cramer. *Essentials of computational chemistry: theories and models*. John Wiley & Sons, 2004.

[25] B. J. B. Crowley. Some generalisations of the poisson summation formula. *Journal of Physics A: Mathematical and General*, 12(11):1951, 1979.

[26] S. Datta. *Electronic Transport in Mesoscopic Systems*. Cambridge Studies in Semiconductor Physi. Cambridge University Press, 1997.

[27] M. Di Ventra. *Electrical Transport in Nanoscale Systems*. Cambridge University Press, 2008.

[28] R. B. Dingle. *Asymptotic expansions: their derivation and interpretation*. Academic Press, London, 1973.

[29] P. Dirac. *The principles of quantum mechanics*. International series of monographs on physics. The Clarendon Press, 1935.

[30] P. A. M. Dirac. Quantum mechanics of many-electron systems. *Proceedings of the Royal Society of London. Series A, Containing Papers of a Mathematical and Physical Character*, 123(792):714–733, 1929.

[31] R. M. Dreizler and E. K. U. Gross. *Density Functional Theory: An Approach to the Quantum Many-Body Problem*. Springer–Verlag, Berlin, 1990.

[32] J. H. Eberly. Quantum scattering theory in one dimension. *American Journal of Physics*, 33(10):771–773, 1965.

[33] P. Elliott, A. Cangi, S. Pittalis, E. K. U. Gross, and K. Burke. Almost exact exchange at almost no computational cost in electronic structure. *Phys. Rev. A*, 92:022513, Aug 2015.

[34] P. Elliott, D. Lee, A. Cangi, and K. Burke. Semiclassical origins of density functionals. *Phys. Rev. Lett.*, 100(25):256406, Jun 2008.

[35] E. Engel and R. M. Dreizler. *Density Functional Theory: An Advanced Course*. Springer, Berlin, 2011.

[36] L. Euler. Methodus universalis serierum convergentium summas quam proxime inveniendi. *A general method for finding approximations to the sums of convergent series (E46)), Originally published in Commentarii academiae scientiarum Petropolitanae*, 8(1741):3–9, 1741.

[37] E. Fermi. Eine statistische Methode zur Bestimmung einiger Eigenschaften des Atoms und ihre Anwendung auf die Theorie des periodischen Systems der Elemente (a statistical method for the determination of some atomic properties and the application of this method to the theory of the periodic system of elements). *Zeitschrift für Physik A Hadrons and Nuclei*, 48:73–79, 1928.

[38] R. Feynman and A. Hibbs. *Quantum mechanics and path integrals*. McGraw-Hill, New York, NY, 1965.

[39] R. P. Feynman. Space-time approach to non-relativistic quantum mechanics. *Rev. Modern Phys.*, 20:367, 1948.

[40] S. Fournais, M. Lewin, and J. P. Solovej. The semi-classical limit of large fermionic systems. *ArXiv e-prints*, Oct. 2015.

[41] S. Golden. Statistical theory of electronic energies. *Reviews of Modern Physics*, 32(2):322, 1960.

[42] G. Grensing and W. S. (Singapur). *Structural Aspects of Quantum Field Theory and Noncommutative Geometry: ...* World Scientific, 2013.

[43] R. Grover. Asymptotic expansions of the dirac density matrix. *Journal of Mathematical Physics*, 7(12):2178–2186, 1966.

[44] M. C. Gutzwiller. Energy spectrum according to classical mechanics. *Journal of Mathematical Physics*, 11(6):1791–1806, 1970.

[45] M. C. Gutzwiller. Periodic orbits and classical quantization conditions. *Journal of Mathematical Physics*, 12(3):343–358, 1971.

[46] J. Hafner. Ab-initio simulations of materials using vasp: Density-functional theory and beyond. *Journal of Computational Chemistry*, 29(13):2044–2078, 2008.

[47] H. Haick and D. Cahen. Making contact: Connecting molecules electrically to the macroscopic world. *Progress in Surface Science*, 83(4):217 – 261, 2008.

[48] T. Helgaker, P. Jorgensen, and J. Olsen. *Molecular electronic-structure theory*. John Wiley & Sons, 2013.

[49] E. J. Heller and S. Tomsovic. Postmodern quantum mechanics. *Physics Today*, 46:38–46, 1993.

[50] P. Hohenberg and W. Kohn. Inhomogeneous electron gas. *Phys. Rev.*, 136(3B):B864–B871, Nov 1964.

[51] K. Husimi. Some Formal Properties of the Density Matrix. *Nippon Sugaku-Buturigakkwai Kizi Dai 3 Ki*, 22(4):264–314, 1940.

[52] J. Jackson. *Classical Electrodynamics*. Wiley, 1998.

[53] H. Jeffreys and B. Jeffreys. *Methods of Mathematical Physics*. Cambridge Mathematical Library. Cambridge University Press, 1999.

[54] C. Joachim, J. Gimzewski, and A. Aviram. Electronics using hybrid-molecular and mono-molecular devices. *Nature*, 408(6812):541–548, 2000.

[55] H. Kleinert. *Path Integrals in Quantum Mechanics, Statistics, Polymer Physics, and Financial Markets*. World Scientific, 2004.

[56] W. Kohn and A. E. Mattsson. Edge electron gas. *Phys. Rev. Lett.*, 81:3487, 1998.

[57] W. Kohn and L. J. Sham. Quantum density oscillations in an inhomogeneous electron gas. *Phys. Rev.*, 137(6A):A1697–A1705, Mar 1965.

[58] H. Kramers. Wellenmechanik und halbzählige quantisierung. *Z. Phys.*, 39:828, 1926.

[59] L. Landau, E. Lifshitz, and J. Sykes. *Course of Theoretical Physics: Non-relativistic Theory. Quantum Mechanics*. Course of theoretical physics. Butterworth-Heinemann, 1965.

[60] R. Landauer. Electrical resistance of disordered one-dimensional lattices. *Phil. Mag.*, 21:172, 1970.

[61] N. P. Landsman. Between classical and quantum. *Handbook of the Philosophy of Science*, 2:417–553, 2007.

[62] R. E. Langer. On the connection formulas and the solutions of the wave equation. *Phys. Rev.*, 51:669–676, Apr 1937.

[63] S. Y. Lee and J. C. Light. Uniform semiclassical approximation to the electron density distribution. *The Journal of Chemical Physics*, 63(12):5274–5282, 1975.

[64] I. N. Levine. *Quantum chemistry*. Pearson Higher Ed, 2013.

[65] M. Levy. Universal variational functionals of electron densities, first-order density matrices, and natural spin-orbitals and solution of the v-representability problem. *Proceedings of the National Academy of Sciences of the United States of America*, 76(12):6062–6065, 1979.

[66] E. H. Lieb. Density functionals for coulomb systems. *Int. J. Quantum Chem.*, 24(3):243–277, 1983.

[67] E. H. Lieb and B. Simon. Thomas-fermi theory revisited. *Phys. Rev. Lett.*, 31:681–683, Sep 1973.

[68] J. C. Light and J. M. Yuan. Quantum path integrals and reduced fermion density matrices: One-dimensional noninteracting systems. *The Journal of Chemical Physics*, 58(2):660–671, 1973.

[69] R. Littlejohn. The van vleck formula, maslov theory, and phase space geometry. *Journal of Statistical Physics*, 68(1-2):7–50, 1992.

[70] R. G. Littlejohn and P. Wright. Semiclassical generalization of the darboux-christoffel formula. *Journal of Mathematical Physics*, 43(10):4668–4680, 2002.

[71] N. A. Logan and K. S. Yee. Note on contour integral representations for products of airy functions. *SIAM Journal on Mathematical Analysis*, 1(1):115–117, 1970.

[72] Z. Ma and M. E. Tuckerman. On the connection between proton transport, structural diffusion, and reorientation of the hydrated hydroxide ion as a function of temperature. *Chemical Physics Letters*, 511(4):177–182, 2011.

[73] C. MacLaurin. *A Treatise of Fluxions*. Number v. 1 in A Treatise of Fluxions. T. W. T. Ruddimans, 1742.

[74] N. H. March and J. S. Plaskett. The relation between the wentzel-kramers-brillouin and the thomas-fermi approximations. *Proceedings of the Royal Society of London. Series A. Mathematical and Physical Sciences*, 235(1202):419–431, 1956.

[75] R. L. McCreery, H. Yan, and A. J. Bergren. A critical perspective on molecular electronic junctions: there is plenty of room in the middle. *Phys. Chem. Chem. Phys.*, 15:1065–1081, 2013.

[76] G. Miceli, J. Hutter, and A. Pasquarello. Liquid water through density-functional molecular dynamics: Plane-wave vs atomic-orbital basis sets. *Journal of Chemical Theory and Computation*, 12(8):3456–3462, 2016. PMID: 27434607.

[77] W. H. Miller. Uniform semiclassical approximations for elastic scattering and eigenvalue problems. *The Journal of Chemical Physics*, 48(1):464–467, 1968.

[78] Y. Mishin, M. Mehl, D. Papaconstantopoulos, A. Voter, and J. Kress. Structural stability and lattice defects in copper: Ab initio, tight-binding, and embedded-atom calculations. *Physical Review B*, 63(22):224106, 2001.

[79] P. M. Morse. Diatomic molecules according to the wave mechanics. ii. vibrational levels. *Phys. Rev.*, 34:57–64, Jul 1929.

[80] B. Muralidharan, A. Ghosh, and S. Datta. Probing electronic excitations in molecular conduction. *Physical Review B*, 73(15):155410, 2006.

[81] H. Payne. Approximation of the dirac density matrix. *The Journal of Chemical Physics*, 41(11):3650–3651, 1964.

[82] D. J. Pengelley. The bridge between the continuous and the discrete via original sources. In O. B. et al, editor, *Study the Masters: The Abel-Fauvel Conference, Kristiansand*, 2002.

[83] J. P. Perdew, K. Burke, and M. Ernzerhof. Generalized gradient approximation made simple. *Phys. Rev. Lett.*, 77(18):3865–3868, Oct 1996. *ibid.* **78**, 1396(E) (1997).

[84] M. Pillai, J. Goglio, and T. G. Walker. Matrix numerov method for solving schrodinger's equation. *American Journal of Physics*, 80(11):1017–1019, 2012.

[85] G. Pöschl and E. Teller. Bemerkungen zur Quantenmechanik des anharmonischen Oszillators. *Zeitschrift fur Physik*, 83:143–151, Mar. 1933.

[86] A. Pribram-Jones, D. A. Gross, and K. Burke. Dft: A theory full of holes? *Annual Review of Physical Chemistry*, 66(1):283–304, 2015.

[87] A. Pribram-Jones, D. A. Gross, and K. Burke. Dft: A theory full of holes? *Annual Review of Physical Chemistry*, 66(1):283–304, 2015.

[88] D. Rappoport, N. R. M. Crawford, F. Furche, and K. Burke. Which functional should i choose? In E. Solomon, R. King, and R. Scott, editors, *Computational Inorganic and Bioinorganic Chemistry*. Wiley, John & Sons, Inc., 2009.

[89] M. A. Reed, C. Zhou, C. Muller, T. Burgin, and J. Tour. Conductance of a molecular junction. *Science*, 278(5336):252–254, 1997.

[90] R. F. Ribeiro and K. Burke. Uniform semiclassical approximations for one-dimensional fermionic systems. *arXiv preprint arXiv:1510.05676*, 2015.

[91] R. F. Ribeiro, D. Lee, A. Cangi, P. Elliott, and K. Burke. Corrections to thomas-fermi densities at turning points and beyond. *Phys. Rev. Lett.*, 114:050401, Feb 2015.

[92] R. F. Ribeiro, Z. Liu, J. P. Bergfield, C. A. Stafford, and K. Burke. Hard-wall quantum transport calculations: Thinking inside the box. *in prep*, 2016.

[93] J. Roccia and M. Brack. Closed-orbit theory of spatial density oscillations in finite fermion systems. *Phys. Rev. Lett.*, 100:200408, May 2008.

[94] J. Roccia, M. Brack, and A. Koch. Semiclassical theory for spatial density oscillations in fermionic systems. *Phys. Rev. E*, 81:011118, Jan 2010.

[95] A. Ruzsinszky and J. P. Perdew. Twelve outstanding problems in ground-state density functional theory: A bouquet of puzzles. *Computational and Theoretical Chemistry*, 963(1):2 – 6, 2011.

[96] H. Schaefer. *Quantum Chemistry: The Development of Ab Initio Methods in Molecular Electronic Structure Theory*. Dover Books on Chemistry. Dover Publications, 2012.

[97] E. Scheer. *Molecular Electronics: An Introduction to Theory and Experiment*. EBSCO ebook academic collection. World Scientific Publishing Company Pte Limited, 2010.

[98] L. Schulman. *Techniques and Applications of Path Integration*. A Wiley interscience publication. Wiley, 1996.

[99] K. Schwarz, E. Nusterer, P. Margl, and P. E. Blchl. Ab initio molecular dynamics calculations to study catalysis. *International Journal of Quantum Chemistry*, 61(3):369–380, 1997.

[100] M. J. Stephen and K. Zalewski. On the classical approximation involved in the thomas-fermi theory. *Proceedings of the Royal Society of London. Series A. Mathematical and Physical Sciences*, 270(1342):435–442, 1962.

[101] L. H. Thomas. The calculation of atomic fields. *Math. Proc. Camb. Phil. Soc.*, 23(05):542–548, 1927.

[102] C. T. Tri. *Semiclassical Fermion Densities*. PhD thesis, National University of Singapore, 2016.

[103] O. Vallee and M. Soares. *Airy Functions and Applications to Physics*. Imperial College Press, London, 2004.

[104] J. H. Van Vleck. The correspondence principle in the statistical interpretation of quantum mechanics. *Proceedings of the National Academy of Sciences*, 14(2):178–188, 1928.

[105] Y. A. Wang and E. A. Carter. Orbital-free kinetic-energy density functional theory. In S. D. Schwartz, editor, *Theoretical Methods in Condensed Phase Chemistry*, chapter 5, page 117. Kluwer, Dordrecht, 2000.

[106] G. Wentzel. Eine verallgemeinerung der quantenbedingungen für die zwecke der wellenmechanik. *Z. Phys.*, 38:518, 1926.

[107] E. Whittaker and G. Watson. *A Course of Modern Analysis*. A Course of Modern Analysis: An Introduction to the General Theory of Infinite Processes and of Analytic Functions, with an Account of the Principal Transcendental Functions. Cambridge University Press, 1996.

[108] E. Zeidler. *Applied Functional Analysis: Applications to Mathematical Physics*. Number v. 108 in Applied Mathematical Sciences. Springer New York, 1995.

[109] J. Zinn-Justin. *Path Integrals in Quantum Mechanics*. Oxford Graduate Texts. OUP Oxford, 2010.

[110] M. Zworski. *Semiclassical Analysis*. Graduate studies in mathematics. American Mathematical Society, 2012.